Soil Moisture Dynamics in the Cold, Arid Climate of Mongolia

(モンゴルの寒冷・乾燥気候における土壌水分動態)

By

Banzragch NANDINTSETSEG

A thesis submitted to the United Graduate School of Agricultural Sciences, Tottori University
In partial fulfillment of the requirements
for the degree of

DOCTOR OF PHILOSOPHY

In

BIOENVIRONMENTAL SCIENCE

September 2010

I hereby certify that the work embodied in this thesis is the result of original research and has not been submitted for a higher degree to any other University or Institution, and to the best of my knowledge this thesis does not contain any material previously published or written by another person, except where due reference is made in the text.

Banzragch NANDINTSETSEG

This work is dedicated

To

My family members

All of my friends

With all my love

Энэхүү диссертацийн ажлаа

Хайрт эмээ, аав, ээж

Хайрт хань болон хүүдээ

зориулж байна.

Acknowledgements

It is a pleasure to thank the many people whose contributions have made this thesis possible.

First, I extend my deepest thanks to my main supervisor, Dr. Prof. Masato Shinoda, who took care of every issue that arose from the time I applied to join the Ph.D. course at the United Graduate School of Agricultural Science, Tottori University, Japan, until finally submitting this thesis. I am highly indebted to Dr. Prof. Masato Shinoda for his guidance, expert advice, encouragement, and valuable comments, which provided me with new ideas and support for my own ideas, helping me to achieve my goals. I thank Dr. Prof. Masato Shinoda with my deepest gratitude.

I also wish to thank my co-supervisors, Dr. Kimura Reiji, Assoc. Prof. at the Arid Land Research Center, Faculty of Agriculture, Tottori University, and Dr. Ibaraki Yasuomi, Assoc. Prof. at the Faculty of Agriculture, Yamaguchi University, for their support and excellent advice during all stages of my research.

I express my sincere appreciation to the members of the Dissertation Committee at the United Graduate School of Agricultural Sciences, Tottori University, for reviewing this thesis.

I would like to acknowledge and thank Tottori University and the Arid Land Research Center (ALRC) for inspiring me during this research. I also thank the staff at ALRC for their support and assistance, and the Global Center of Excellence for Dryland Science Foundation for research support.

Very special thanks go to my colleagues at the Division of Climatology and Water Resources, ALRC, for their kind cooperation, support, comments, and help.

I am deeply indebted to colleagues at the Institute of Meteorology and Hydrology (IMH) in Mongolia; special thanks are extended to colleagues at the Agro Meteorological Section of IMH.

I am deeply grateful to the Japanese Ministry of Education, Culture, Sports, Science and Technology (Monbukagakusho) for providing the opportunity to conduct this research in Japan.

I express my sincere thanks and gratitude to all of my friends for their cooperation and sincere encouragement and help during this period, which helped me to attain my goals.

Finally, I wish to extend a special thanks to my family for their unwavering support and encouragement. I also wish thank to my parents, Banzragch and Tserendivaa, who raised me, supported me, taught me, and loved me. I would very much like to thank my mother-in-law, Chantsal, for understanding and supporting me. I also thank my brothers and sisters. Finally, I would especially like to thank my husband, Jamts, and my lovely son, Davaadalai, for their love and continued support. Thank you.

Banzragch NANDINTSETSEG
Author

CONTENTS

Acknowledgements.....i
Contents.....ii
List of Abbreviations.....v
List of Symbols.....vi
List of Figures.....vii
List of Tables.....xi

Chapter 1: General Introduction

1.1 Background.....1
1.2 Soil Moisture Dynamics in Drylands.....4
1.3 Study Area: Mongolia.....6
1.3.1 Overview of Topography and Climate.....6
1.3.2 Water Resources.....7
1.3.3 Vegetation.....7
1.3.4 Socio Economy.....9
1.3.5 Problem Facing the Mongolian Grassland.....9
1.4 Objectives.....11

Chapter 2: Seasonal Change of Soil Moisture: It's Climatology and Modeling

Abstract.....12
2.1 Introduction.....13
2.2 Materials and Methods.....14
2.2.1 Data.....14
2.2.2 Soil Moisture Modeling.....17
2.3 Results.....20
2.3.1 Seasonal Change in Soil Moisture.....20
2.3.2 Spatial Variations in Soil Moisture.....22
2.3.3 Soil Moisture Estimation.....25
2.4 Discussion and Conclusions.....27

Chapter 3: Multi-decadal Trend and Memory of Modeled Soil Moisture

Abstract.....30
3.1 Introduction.....31

3.2 Datasets and Methods....32
3.2.1 Datasets....32
3.2.2 Palmer Drought Severity Index....33
3.2.3Water Balance Model....34
3.2.4Temporal Autocorrelation....35
3.3 Results....35
3.3.1 Model Performance....35
3.3.2 Seasonal Variations in Modeled Soil Moisture....36
3.3.3 Multi-decadal Trend in Modeled Soil Moisture....38
3.3.4 Comparison between Wet and Dry Years....40
3.3.5 Temporal Scales of Soil Moisture....42
3.4 Discussion and Conclusions....42

Chapter 4: Relationship between Soil Moisture and Vegetation Activity

Abstract....45
4.1 Introduction....46
4.2 Data and Methodology....46
4.2.1 NDVI Data....46
4.2.2 Observed Data....47
4.2.3 Modeled Data....47
4.2.4 Statistical Analysis....48
4.3 Results and Discussion....49
4.3.1 Seasonal Variations in NDVI and W_m....49
4.3.2 Interannual Variations in NDVI and W_m....50
4.3.3 A Stepwise Multiple-regression Modeling....52
4.4 Conclusions....53

Chapter 5: Soil Moisture and Vegetation Memories

Abstract....55
5.1 Introduction....56
5.2 Data and Methods....57
5.2.1 Observed Soil Moisture....57
5.2.2 Modeled Soil Moisture....58
5.2.3 NDVI Data....58
5.3 Results and Discussion....58
5.3.1 Climatological Patterns....58
5.3.2 Correlation Patterns....59
5.2.3 Autocorrelations....62
5.2.4 Comparison between Wet and Dry Years....63
5.4 Conclusions....69

Chapter 6

General Conclusions and Future Tasks.....72
Summary.....76
Summary in Japanese.....79
References.....81
List of Publications.....89

LIST OF ACRONYMS

AGB	Above-ground biomass
AVHRR	Advanced Very High Resolution Radiometer
GCM	General Circulation model
GIMMS	Global Inventory Modeling and Mapping Studies
IMH	Institute of Meteorology and Hydrology of Mongolia
IPCC	Intergovernmental Panel on Climate Change
NDVI	Normalized Difference Vegetation Index
$NDVI_{max}$	Yearly-maximum NDVI
NOAA	National Oceanic and Atmospheric Administration
PDSI	Palmer Drought Severity Index
RMSE	Root mean square error
SD	Standard deviation
TDR	Time-domain Reflectometry
UNEP	United Nations Environment Programme

LIST OF SYMBOLS

Symbol	Explanation	Unit
α	Account for the variations in vegetation type (α = 6.81 for most vegetation types everywhere in the world)	
D	Deep drainage below the plant root zone	mm
E	Actual evapotranspiration	mm
h	The length of daylight	hours
I	The annual heat index (sum of the 12 monthly heat indices i).	
M	Melt of the snow (expressed as snow water equivalent) that is accumulated when air temperature is equal to or below 0°C. If air temperature is above 0°C, the accumulated snow melts)	mm
P	Precipitation	mm
PET	Potential evapotranspiration	mm
R	Surface runoff	mm
SD	Snow depth	cm
t	Time	days)
T	Air temperature	°C
T_g	Soil temperature	°C
T_m	Scale of temporal autocorrelation (decay time scale i.e. lag at which autocorrelation function equals to $1/e$)	
W	Plant-available soil moisture (the actual soil moisture minus the moisture content at the wilting point), 0–50 cm depth	mm
W_m	Modeled plant-available soil moisture(0–50 cm)	mm
W_o	Observed plant-available soil moisture (0–50 cm)	mm
W_{fc}	Soil moisture content at the field capacity (0–50 cm)	mm
W_{wp}	Soil moisture content at the wilting point(0–50 cm)	mm
W^*	Moisture storage capacity (0–50 cm)	mm
τ	Residence time or turnover period signifies the time required for a volume of water equal to the annual mean of exchangeable soil moisture to be depleted by evapotranspiration	days

LIST OF FIGURES

Figure 1.1 Schematic representation of the climate–soil–vegetation system. The grey area indicates the focus of this thesis....1

Figure 1.2 Schematic diagram illustrating land surface–atmosphere interaction during a period of drought. After Shinoda (2000)....2

Figure 1.3 Map of African and Asian drylands (UNEP, 1992) and soil freezing in cold, arid regions (Brown *et al.*, 2005). Drylands are defined based on the aridity index, which represents the ratio of mean annual precipitation (P) to mean annual potential evapotranspiration (PET)....3

Figure 1.4 A local soil moisture balance....5

Figure 1.5 Location of Mongolia (shading denotes arid regions, as defined by the aridity index; UNEP, 1992)....6

Figure 1.6 Sheep Grazing in the Mongolian Grassland....10

Figure 2.1 Locations of soil moisture measuring stations and natural zones in Mongolia....16

Figure 2.2 The climatological (1986–2005) seasonal changes of 10-day precipitation, temperature, soil moisture, and snow depth, averaged over 26 stations in Mongolia. The left and right axes of the upper panel correspond to precipitation (bars) and temperature (line) and phenological phenomena (vertical dashed lines, Em to Ss), respectively. The left axis and thick line of the bottom panel correspond to plant-available soil moisture in the 0–50-cm layer (20-year average with standard deviation), along with three soil moisture phases (I–III). The right axis and bars correspond to snow depth. The y-axis on the left (soil moisture) corresponds to that on the right (snow depth) with an assumption of snow density of 0. 20 g/cm^3 (Badarch, 1987)....21

Figure 2.3 Spatial patterns of climatological (1986–2005) temperature, precipitation and the plant-available soil moisture averaged during the warm season. The patterns of precipitation and air temperature were based on the 26 stations data during the warm season (April to October) of 1986–2005....24

Figure 2.4 The same as in Figure 2.2 with the exception for each of the natural zones: forest steppe (a), steppe (b) and Gobi Desert (c). Figure 2.4d shows a comparison of soil moisture during April–October among the three zones....25

Figure 2.5 Scatter diagram between the observed 10-day soil moisture and estimated soil moisture by the water balance model for 26 stations during 1986–2005....26

Figure 2.6 The seasonal changes of 10-day air temperature (T) and water balance variables: precipitation (P), the observed (circle) and estimated (solid line) soil moisture (W), potential (PET) and actual (E) evapotranspiration averaged over all 26 stations of Mongolia

(a) and three stations for each of the vegetation zones (b–d) during 1986–2005. Three soil moisture phases (I–III) are denoted. The daily soil moisture estimations were averaged over 10-day intervals....28

Figure 3.1 Locations of nine stations at which the soil moisture was measured, and vegetation zones in Mongolia....33

Figure 3.2 Scatter diagram between the observed 10-day soil moisture (W_o) and estimated soil moisture (W_m) by the water balance model for three vegetation zones during 1986–2005....36

Figure 3.3 Seasonal changes in 10-day precipitation (P), air temperature (T), actual evapotranspiration (E), potential evapotranspiration (PET), observed soil moisture (W_o), modeled soil moisture content (W_m), and monthly NDVI, also showing the timing of three soil moisture phases (I–III) averaged over three stations for each of three vegetation zones in Mongolia during 1986–2005. The daily soil moisture estimation was averaged over 10-day intervals....37

Figure 3.4 Interannual time series (1961–2006) of precipitation (P) and potential evapotranspiration (PET) anomalies (a), the modeled (W_m) and observed (W_o) soil moisture contents, and Palmer Drought Severity Index (PDSI) (b), and the timing of three soil moisture phases (I–III) during the warm season in the forest steppe zone (c). Circles and triangles in (Figure 3.4b) indicate years with wet and dry soils, respectively, which were used for the composite analysis in Figure 3.3....39

Figure 3.5 Seasonal changes in the precipitation (P), modeled soil moisture content (W_m), and actual evapotranspiration (E) (10-day data are plotted) showing three phases of soil moisture content (a and b), and comparison between the composites of 1989, 1990, 1993, and 1994 (wet soil years) and 1996, 2000, 2001, and 2002 (dry soil years) (see Fig. 4b), as well as their differences (c). Squares, circles, and triangles indicate differences between wet and dry years in terms of W_m, P, and E, respectively, significant at 5% level....41

Figure 3.6 Temporal autocorrelation values of the time series of the monthly modeled soil moisture (W_m) for the forest steppe zone for each month (from April (A) to the following year March (M))....43

Figure 4.1 Locations of nine stations at which soil moisture was measured and vegetation zones in Mongolia....48

Figure 4.2 Seasonal changes in 10-day (a) precipitation (P), soil moisture (W_m), the timings of snow disappearance (vertical arrows) for the three zones (F: forest steppe, S: steppe, and D: desert steppe), and (b) 10-day above-ground biomass (AGB) and monthly NDVI averaged over nine stations with their standard deviations (vertical dashed bars) in the Mongolian steppe during 1982–2005....50

Figure 4.3 Interannual (1982–2005) anomalies (a) of precipitation (P), potential evapotranspiration (PET), and (b) soil moisture (W_m) for the period June–August, and maximum NDVI ($NDVI_{max}$) averaged over nine stations in the Mongolian steppe (values are in reverse order). Triangles and circles indicate years with high and low values of $NDVI_{max}$, respectively.....51

Figure 4.4 Seasonal changes in 10-day (a) precipitation (P), modeled soil moisture (W_m), and monthly NDVI, comparing the composites for 1993, 1994, 1996, and 1998 (h-NDVI is high-$NDVI_{max}$ years) with those for 1999, 2000, 2001, and 2004 (l_NDVI is low-$NDVI_{max}$ years) (Figure 4.3), (b) as well as their differences. Triangles, circles, and squares indicate differences between high- and low-$NDVI_{max}$ years in terms of P, W_m, and NDVI, respectively, significant at the 5% level.....52

Figure 5.1 (a) Topography and climatological patterns of the following parameters: (b) summer (June-September) P (mm/month) ($P_{6\text{-}9}$); (c) late summer (August–September) W in the top 50cm-deep layer (mm) ($W_{8\text{-}9}$); and (d) NOAA-derived NDVI for the autumn (September) ($NDVI_9$). Climatological values are averaged over the period from 1986 to 2005. UB and UK indicate the locations of Ulaanbaatar and Underkhaan, respectively. The circles indicate the observational stations.....60

Figure 5.2 Maps of the following correlations: (a) between the $P_{6\text{-}9}$ and $W_{8\text{-}9}$ anomalies for the same year; (b) between the $W_{8\text{-}9}$ anomaly for one year and the $W_{4\text{-}5}$ anomaly for the following year; (c) between the $P_{6\text{-}8}$ and $NDVI_9$ anomalies for the same year; and (d) between the $NDVI_9$ anomaly for one year and the $NDVI_5$ anomaly for the following year. The correlation coefficients are expressed as values multiplied by 100. Stippling indicates values exceeding 40 at the 5 % significance level.....61

Figure 5.3 (a) Climatological (1986–2005) seasonal changes in W_o, NDVI, and SD for Underkhaan and autocorrelations of (a) W_o (only for the reference of September, circle) and W_m, and (b) NDVI using each month as references. The red line indicates autocorrelations of W_m with the reference of September. The horizontal thin lines in Figures. 5.3b and 3c denote the 5% significance level.....64

Figure 5.4 Interannual (1986–2005) time series of $W_{8\text{-}9}$ by the gravimetric and TDR methods (mm), and $NDVI_9$ for Underkhaan. Triangles and circles indicate years with three highest and lowest values of $W_{8\text{-}9}$ used for the composite analysis in Figure 5.5, respectively.....65

Figure 5.5 Seasonal changes in monthly (a) T and P, (b) W_o, NDVI, and SD for Underkhaan; comparisons between the four years with the largest (1987/1993/1998/2003) and smallest (1988/1989/1991/2004) $W_{8\text{-}9}$ values and (c) their differences. Squares, circles, and triangles indicate differences between the wet and dry years in terms of P, W_o, and NDVI, respectively, significant at 5% level. The horizontal dashed lines in Figure 5.5b are W_{fc} and W_{wp} (Chapter 1).....66

Figure 5.6 Seasonal changes in daily P, W, and T_g at the 20 cm depth for Underkhaan; comparisons between the wet (2003/04, blue) and dry (2002/03, red) soil years. W is not shown when $T_g < 0^oC$.....67

Figure 5.7 North-south cross-sections of (a) vegetation type, (b) P, (c) $W_{8\text{-}9}$, W_{fc}, and W_{wp}, (d) $NDVI_9$, (e) correlations between $W_{8\text{-}9}$ for one year and $W_{4\text{-}5}$ for the following year, and between $NDVI_9$ for one year and $NDVI_4$ for the following, and (f) the depth of soil freezing (Jambaajamts, 1989). The section includes, from the north to south, the four stations of Darkhan (DK), Underkhaan (UK), Mandalgovi (MG), and Dalanzadgad (DZ). The horizontal bars in Figure 5.7c indicate standard deviations (σs) of the $W_{8\text{-}9}$ values from 1986 to 2005.....68

LIST OF TABLES

Table 2.1 Soil moisture observation stations with information on location, elevation, soil type, wilting point (W_{wp}), and field capacity (W_{fc}) of the 0–50 cm soil layer.....15

Table 2.2 Average (AVG) and standard deviations (SD) of temperature, precipitation and soil moisture over the entire Mongolia and in three natural zones during the warm season (April–October) during 1986–2005.....24

Table 3.1 Nine soil moisture observation stations with information on location, elevation, soil type, wilting point (W_{wp}), and field capacity (W_{fc}) of the 0–50 cm soil layer. The stations are listed in order from north to south and west to east. The stations are also shown in Figure 3.1.....32

Table 3.2 Linear trend coefficients of the modeled soil moisture (W_m), precipitation (P), air temperature (T), potential evapotranspiration (PET), and three phases changes (Phases I, II, and III) of W_m per decade over three zones (forest steppe, steppe, and desert steppe) during the period of 1961–2006.....40

Table 4.1 Models that account for interannual variation in current-year maximum NDVI for the Mongolian steppe. The rows correspond to stepwise multiple regressions with different sets of variables during 1982–2005. W_m indicates soil moisture during June–August; N is yearly-maximum NDVI. The models include variables with a significant effect, in which (t), (t–1), and (t–2) indicate the current, first, and second preceding years, respectively.....53

CHAPTER 1

General Introduction

1.1 BACKGROUND

Water flow throughout the soil–plant–atmosphere continuum is regulated by a number of complex physical and biophysical processes that are mutually dependent. Important "top-down" controls on water uptake by plants include hydrologic and climate conditions, which determine the rates of potential evapotranspiration and assimilation, and ecosystem productivity. In contrast, vegetation exerts a "bottom-up" control on both regional climate and hydrologic conditions through its interactions (via water and energy) with the near-surface atmosphere. Almost all interactions within the soil–plant–atmosphere system are mediated by soil moisture (Figure 1.1), which is a key variable in terms of controlling the influence of climate, soil, and vegetation on the water balance and also in controlling the dynamic impact of the water balance on plants (e.g., Neilson, 1995; Laio *et al.*, 2001; Porporato *et al.*, 2001; Porporato and Rodriguez-Iturbe, 2002).

Soil moisture plays a central role in the global water cycle and climate system by

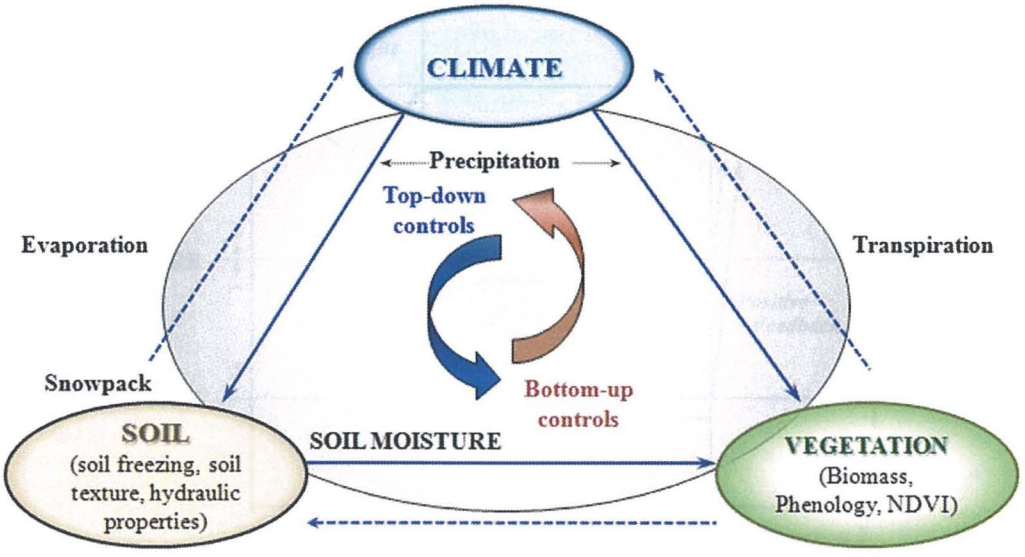

Figure 1.1 Schematic representation of the climate–soil–vegetation system. The grey area indicates the focus of this thesis.

controlling the partitioning of water and energy fluxes at the earth's surface, and may control the distribution of water upon continents via land surface–atmosphere feedback mechanisms (Koster *et al.*, 2003). Soil moisture acts as a memory of anomalies in the water cycle; consequently, it has a delayed and durable influence on the overlying atmosphere through land-surface fluxes of heat and moisture. Early general circulation model (GCM) simulations (Delwarth and Manabe, 1988, 1989) and observational evidence (Vinnikov and Yeserkepova, 1991) indicate that a continental soil-moisture anomaly shows interseasonal persistence as a climate memory due to its low potential evaporation.

Figure 1.2 schematically illustrates land surface–atmosphere interaction during periods of drought (Shinoda, 2000). A rainfall anomaly (Phenomenon 1 in the figure) results in the persistence of anomalous land-surface conditions (soil moisture and vegetation) during the cold season (Phenomenon 2), leading in turn to an anomaly of the same sign during the following warm season (Phenomenon 3). This mechanism may operate as a positive feedback system. The resulting positive feedback can increase the duration and intensity of climate extremes such as droughts, heat waves, and floods (e.g., Charney, 1975; Sud and Smith, 1985; Seneviratne *et al.*, 2006). This feedback is strongest

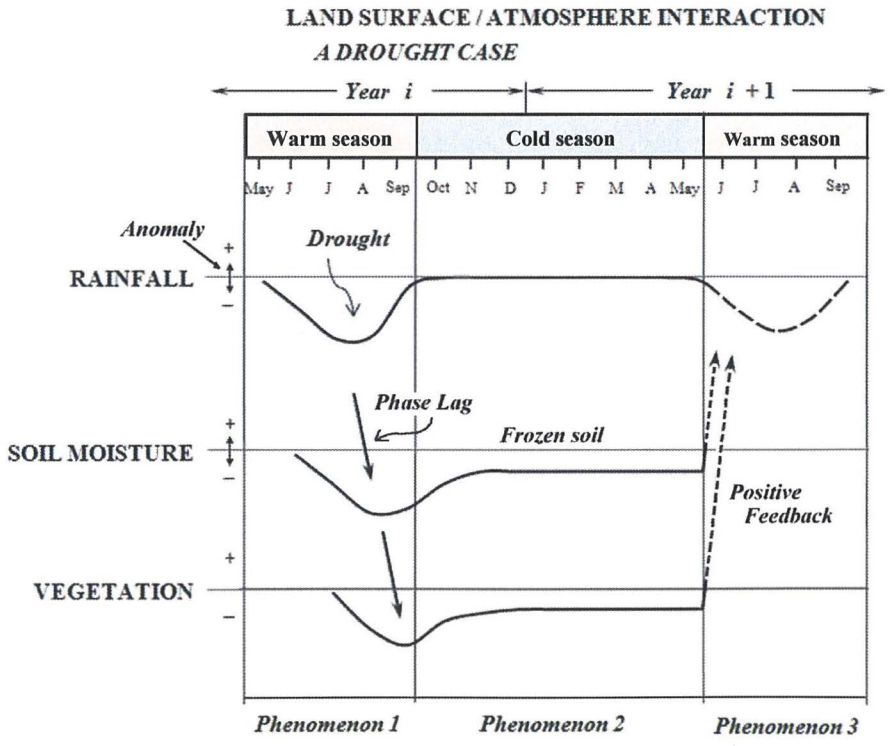

Figure 1.2 Schematic diagram illustrating land surface–atmosphere interaction during a period of drought. After Shinoda (2000).

in mid-continental regions with a transitional climate (Koster *et al.*, 2004).

Soil moisture is generally the key environmental variable in terms of analyses of vegetation dynamics. Temporal variations in the availability of soil moisture have a direct effect on plant water potential, related tissue turgor, transpiration rate, and leaf carbon assimilation by photosynthesis, which in turn influence plant growth and reproduction (e.g., Porporato *et al.*, 2001; Porporato and Rodriguez-Iturbe, 2002). This effect is most noticeable in water-controlled ecosystems such as drylands (Rodrigues-Iturbe and Proporate, 2004), where vegetation is frequently subjected to water stress.

Spatial differences in the dynamics of soil moisture availability are a key factor in the development of distinct functional vegetation types (e.g., grasslands, savannas, forests) and ecosystem structures. Many extratropical arid and semi-arid regions suffer water stress, which is controlled by temporal fluctuations in soil moisture (e.g., Smith and Griffith, 1993; Rodriguez-Iturbe *et al.* 2001). Although other sources of stress (e.g., temperature, fire, grazing, nutrient availability) are generally present, soil moisture is the most important factor controlling vegetation activity in many dryland ecosystems.

More than 40% of the continental areas worldwide are covered by drylands, which are characterized by an aridity index (UNEP, 1992; defined as the ratio of annual mean precipitation to annual potential evapotranspiration) that is generally between 0.00 and 0.65. The main dryland regions are located in continental interiors. Figure 1.3 shows the distribution of cold drylands in mid-latitude Asia and warm drylands in low-latitude

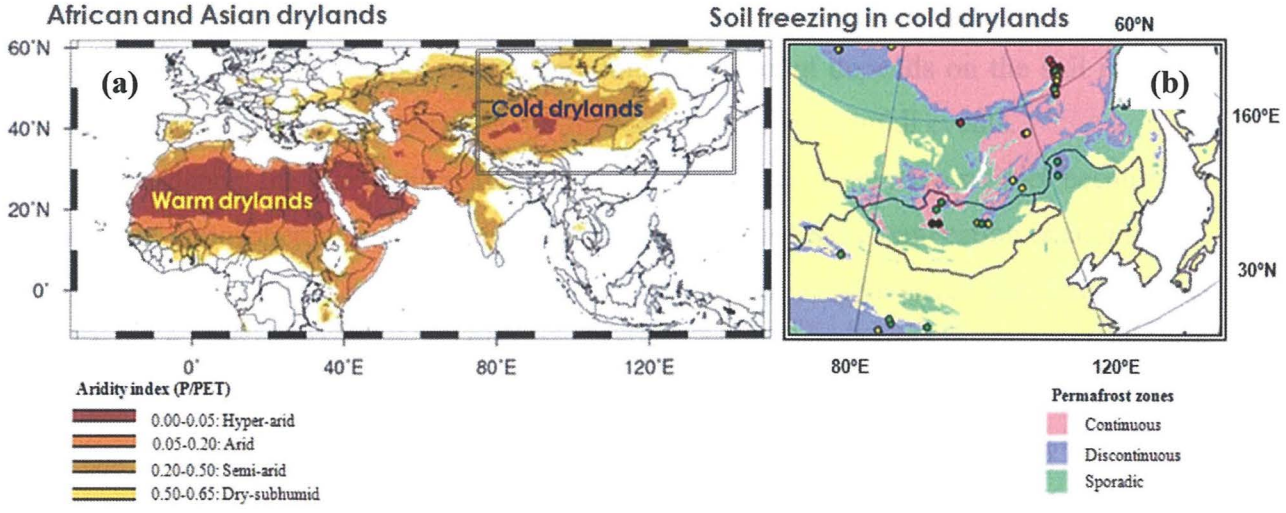

Figure 1.3 (a) Map of African and Asian drylands (UNEP, 1992) and (b) soil freezing in cold, arid regions (Brown *et al.*, 2005). Drylands are defined based on the aridity index, which represents the ratio of mean annual precipitation (*P*) to mean annual potential evapotranspiration (PET).

Africa. The mid-latitude drylands are characterized by distinct warm and cold seasons (with large seasonal amplitudes in temperature). The plant-growing season is limited by the short rainy season during the warm months, while the soil is frozen in winter. Permafrost is widespread in east Eurasia (mean annual air temperature, < 0°C), including Mongolia, where sporadic and to a lesser extent continuous permafrost predominates (Figure 1.3b).

1.2 SOIL MOISTURE DYNAMICS IN DRYLANDS

The main control exerted by hydrological processes on vegetation activity in drylands is via the soil moisture dynamic, which in turn is controlled by complex interactions among precipitation, evapotranspiration, runoff, and drainage. The soil moisture dynamic, which is complex and depends on many interactions and processes, can be expressed as follows:

$$\frac{dW}{dt} = P(t) - E(w,t) - R(w,t) - D(w,t) \qquad 1.1$$

where W is soil moisture content (mm), P is precipitation (mm), R is runoff (mm), E is evapotranspiration (mm), and D is deep drainage below the plant root zone (mm). In cold drylands, P includes water from snowmelt, as described in Chapter 2. The schematic diagram in Figure 1.4 defines water loss as water that is not stored in the root zone as deep drainage, runoff, evaporation, or transpiration; this amount depends on the soil moisture status when precipitation occurs and during periods between rainfall events.

In drylands, the global circulation prevents large-scale convective activity because the dominant atmospheric movement is downwards. In areas where convection is suppressed, cloud formation is rare, meaning that the radiation receipt is high. Given that little water is available for evaporation, most of this radiation yields sensible rather than latent heat; thus, temperatures are high and rainfall is low. The low annual precipitation in these regions is almost exactly matched by the annual evapotranspiration (e.g., Robock *et al.*, 2000). Potential evapotranspiration is high; consequently, runoff and deep drainage are negligible. Moreover, a negligible amount of deep drainage is commonly found within natural vegetation areas of arid regions where annual precipitation is less than 300 mm

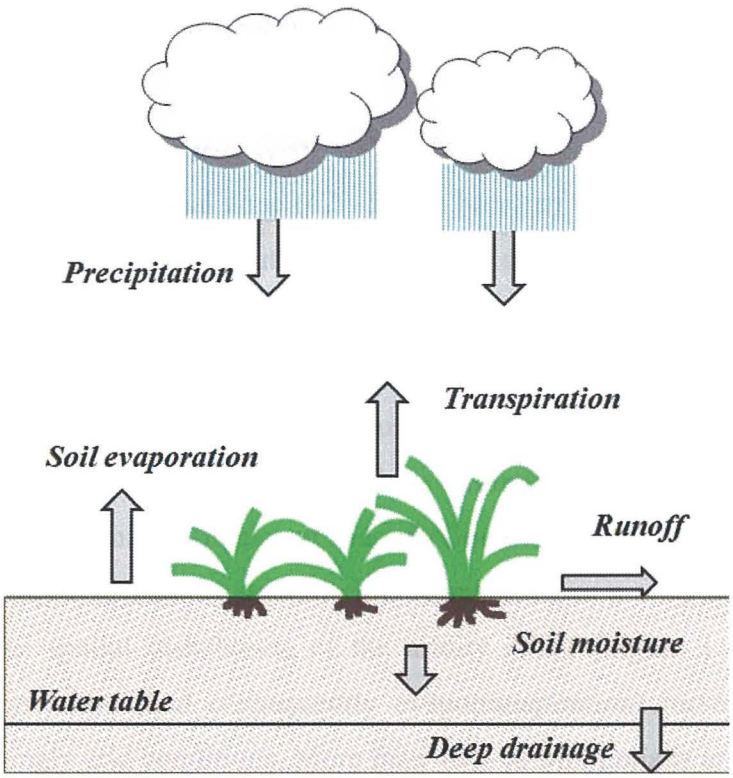

Figure 1.4 A local soil moisture balance

(e.g., Scanlon *et al.*, 1997). In such regions, the small amount of rainfall and high evaporative demand provide constraints on vegetation growth and yield.

The vegetation in drylands is generally well adapted to conditions of water stress and is divided into several major plant functional types, such as grasses, shrubs, forbs, and succulents (Sala *et al.*, 1997). Grasses are dominant in cold drylands with continental climates; i.e., in areas with increasing availability of soil moisture during the warm season. In such regions, precipitation is the main immediate source of water, meaning that the availability of soil moisture plays a crucial role in controlling vegetation patterns and the type of vegetation cover (e.g., as observed in Mongolia), and is consequently of primary importance to the ecosystems in such areas (Miyazaki *et al.*, 2004; Zhang *et al.*, 2005; Munkhtsetseg *et al.*, 2007; Bat-Oyun *et al.*, 2010; Nandintsetsetseg *et al.*, 2010; Shinoda *et al.*, 2010b).

1.3 STUDY AREA: MONGOLIA

1.3.1 Overview of Topography and Climate

Mongolia lies in a transitional zone (42°–52°N) between the boreal forests of Siberia and the Gobi Desert, spanning the southernmost border of the area of permafrost and the northernmost deserts of Central Asia. About half of Mongolia lies at an altitude of around 1400 m a.s.l, making it one of the highest countries in the world. Mongolia is separated from the ocean by large distances and high mountain chains, which is an important factor in defining its climate. The climate of Mongolia is strongly influenced by its topography and location north of the high Himalayan massif (Goulden *et al.*, 2009). Because of its geographical and topographical characteristics, Mongolia has a cold and arid climate. As indicated by the spatial distribution of the aridity index (Figure 1.5), precipitation decreases and temperature (and consequently evapotranspiration) increases southward, resulting in increasingly arid conditions. More than 40% of Mongolia is arid or hyper-arid. Mongolia typically has a long, cold, dry winter (Siberian winter) and a short, warm summer. The annual mean temperature is 0.7°C, with large seasonal differences. Average annual precipitation is 230 mm, most of which occurs in summer (June–August). In general, May to August is the period of plant growth upon the Mongolian grasslands (Shinoda *et al.*, 2007). Snowfall occurs between mid-October and the end of April, and the annual maximum snow depth (3.4 cm) occurs in January (Morinaga *et al.*, 2003).

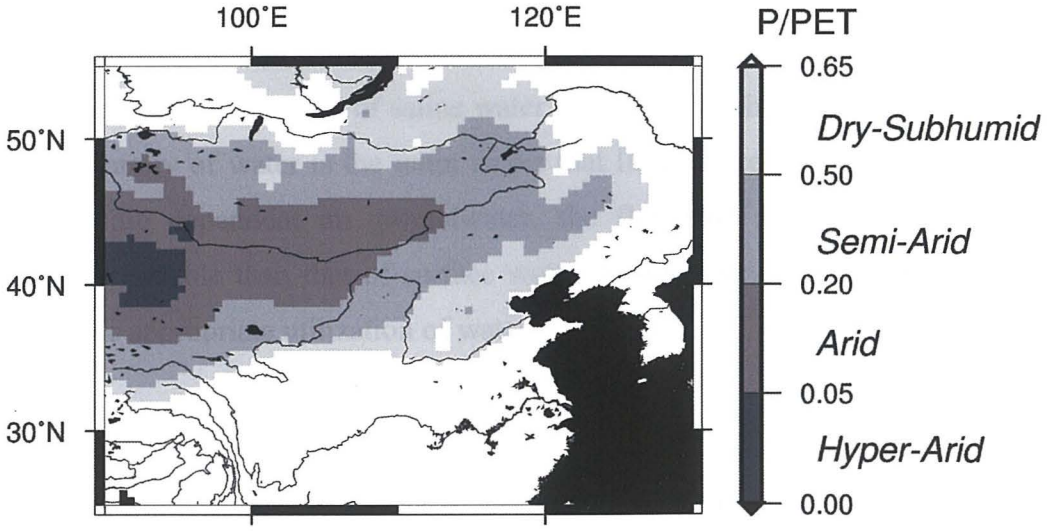

Figure 1.5 Location of Mongolia (shading denotes arid regions, as defined by the aridity index; UNEP, 1992).

Due to its cold climate, almost half (51.4%) of Mongolia is permafrost (Figure 1.2b). Northern Mongolia represents the southernmost boundary of the Siberian continuous permafrost zone (Sharkhuu, 2004), where deep soils remain frozen throughout the year. The average thickness and temperature of continuous permafrost are 50–250 m and 1–3°C, respectively. Seasonal thaw (to depths of 2–3 m in silt soils and 4–5 m in coarse soils) occurs between May and September. In non-permafrost areas, ground-soil freezing occurs between mid-October and the end of April.

Recent studies in northern Mongolia indicate that permafrost is currently showing a thawing trend (Sharkhuu *et al.*, 2007). With climate warming, the active layer or surface soil layer above the permafrost that thaws each summer is gradually increasing in depth with thawing of the near-surface layer of permafrost. A pronounced warming trend has been reported throughout Mongolia (Marcc, 2009). Related changes have also been detected, such as a decrease in the number of extremely cold days and an increase in the number of extremely warm days (Nandintsetseg *et al.*, 2007).

1.3.2 Water Resources

Mongolia contains limited water resources. The total water resources are estimated to be 599 km^3, consisting mainly of water stored in lakes (500 km^3) and in glaciers (62.9 km^3). Surface water and groundwater make up just 4% and 2% of the total water resources, respectively. However, these additional water resources play a vital role in the country's economy with regard to agriculture, forestry, and livestock production, as well as industrial and domestic supply. Salinization and poor water quality are major problems in Mongolia. The use of water resources in Mongolia is limited by problems with water quality related to the occurrence of saline water, seasonal freezing, and droughts, although the overall scarcity of water is the main factor that limits water supply. Many users and communities are dependent on groundwater, the flow and availability of which are inherently more stable than that of surface water. Sustainable development in Mongolia depends on the appropriate utilization of water resources.

1.3.3 Vegetation

Mongolia contains many different ecosystems, ranging from alpine tundra to deserts. The region's location, size, and topography have resulted in a unique assembly of natural vegetation zones. The northernmost zone consists of taiga forest and forest steppe, while

the southern region contains steppe, desert steppe, and desert. The present study focuses on the forest steppe, steppe, and desert steppe zones (Figure 2.1), which are described below.

Forest steppe: Most of Mongolia's forest is actually part of the forest–steppe transition, which is restricted to north-facing slopes; south-facing slopes are covered by steppe vegetation. The forest-steppe zone is an ecotone between the more typical taiga of Siberia and the steppe regions of Mongolia and other mid-latitude countries of the Asian continent. In the northern part of the forest–steppe transition zone, trees are found on east-, west-, and north-facing mountain slopes. Farther south, the forest is limited to northern slopes and the steppe expands onto the eastern and western slopes, ultimately leaving few, if any, trees in the steppe areas of central Mongolia. In most forest steppe areas, annual precipitation ranges from 300 to 400 mm. The soil of the forest steppe is generally dark chestnut and chestnut. In this zone, forb-grass is the most abundant vegetation (*e.g.*, *Stipa* spp., *Cleistogenes Keng-Stpa* spp., *Artemisia-Stipa* spp., *Festuca-artemisia* spp.) and the forest area is dominantly larch (*Larix sibirica*), locally mixed with Siberian pine (*Pinus sibirica).*

Steppe: Steppe ecosystems are widespread in Mongolia, with almost 80% of the land area being covered by grassland or steppe. Grasses and sedges (*e.g.*, *Poa* spp., *Stipa* spp., *Leymus* spp., and *Carex* spp.) are dominant in many areas, in combination with forbs on dryer slopes. In most steppe areas, annual precipitation ranges from 125 to 250 mm, and the main soil types are calcareous chestnut and non-calcareous chestnut. The steppe is ideal grazing land for mixed herds of sheep, cashmere goats, cows, and horses, as commonly tended by nomads.

Desert steppe: The desert steppe transition zone is drier than the steppe but receives more precipitation (100–120 mm) than desert areas. This transition zone is distinguished from semi-desert and steppified desert. Shrubs are common on the desert steppe, whereas grasses are sparse and forest patches are rare. Desert species (*Anabasis* spp., *Caragana* spp., *Ajania* spp.) become increasingly dominant within this zone, where the soil is mainly brown desert soil. This ecotone, in which camels and cashmere goats are important livestock animals, is expanding northward with increasing desertification caused by heavy grazing pressure and climate change.

1.3.4 Socio-Economy

Climate and landscape conditions are key factors in determining land use and sustainable development throughout Mongolia, where the economy is centered on agriculture and mining. Agriculture in Mongolia contributes 20.6% of annual gross domestic product and employs 42% of the labor force. However, the dominance of a cold, arid climate means that limited potential exists for further agricultural development. Of a total land area of 1,564 million km^2, less than 1% is arable, 8–10% is forested, and the remainder is pasture. Most of the population depends on livestock and other climate-dependent sectors of the economy. Animal husbandry plays a major role in the national economy, employing 40% of the total population, contributing 21.2% to agricultural gross production, and accounting for 30% of the country's exports. Climatic variability appears to be the major limiting factor in terms of expansion of the economy in Mongolia. Hence, the adoption of an environmental management strategy based on climate conditions would be important in ensuring the sustainable development of the country.

1.3.5 Problems Facing Mongolian Grasslands

Temperate grasslands occur in mid-latitude regions where the seasonal climate favors the dominance of perennial grasses (Archibold, 1995). In Mongolia, grasslands occupy 82% of the total land area (Batima and Dagvadorj, 2000), being the main source of forage for livestock farming. This vast grassland makes up 4.5% of the total area of Asia, and it has the potential to affect climate variability in adjacent areas (*e.g.,* Siberia and East Asia) and to affect the global atmosphere via land surface–atmosphere interaction. Xue (1996) showed that reduced vegetation activity over grasslands plays an important role in modifying the East Asian monsoon circulation, and in producing a rainfall anomaly over China. The author suggested that interannual variability in vegetation activity within grasslands has a significant effect not only on Mongolia, but on the climate of East Asia.

The annual mean temperature in Mongolia has increased by 2.14°C during the past 70 years, during which time precipitation showed a slight decrease (Marcc, 2009). The rising temperature and increasing uncertainty in rainfall associated with climate change are likely to result in increased variability in extreme climate events, including their frequency and magnitude (Goulden *et al.*, 2009). In Mongolia, drought frequency has increased and become widespread since the mid-1960s, affecting grasslands and creating problems in the farming sector (*e.g.*, Natsagdorj, 2003). Drought has led to the occurrence of dzud, which

is harmful to the pastoral life of nomads and to the economy overall. Dzud is a natural disaster in which unusual weather and/or land-surface conditions (involving snow/ice cover and a lack of bare pasture) result in high livestock fatalities during winter and spring (Shinoda and Morinaga, 2005).

A recent assessment found that 78.2% of Mongolia has been affected by moderate to very severe desertification, mainly identified based on soil erosion, due to overgrazing (Mandakh *et al.*, 2007). The increasing frequency of drought and increasing rate of desertification, in combination with the effects of climate change, have severely affected arid ecosystems in Mongolia, leading to degradation of grasslands. Nomadic herding families face limited access to adequate pasture resources due to a lack of wells, and the quality of much of the available pasture land has declined due to overgrazing, desertification, and drought caused by climate change. An estimated 12 million animals died during the severe droughts and dzuds that occurred between 1999 and 2002 (Batima *et al.*, 2008).

Figure 1.6 Sheep Grazing in the Mongolian Grassland.

1.4 OBJECTIVES

The present study aims at exploring soil moisture dynamics and its relationship with climate and vegetation activity in the cold, arid climate of Mongolia, with a focus on three vegetation zones: the forest steppe, steppe, and desert steppe. The study concentrated on soil moisture dynamics that act to mediate the climate–vegetation system. In this context, the specific objectives of the study were as follows:

- To explore in detail the seasonal and spatial changes in soil moisture, and the relationship among these changes, climatology, and plant phenology across Mongolia. A specific goal was to modify the water balance model for cold, arid regions by considering region-specific processes of winter soil-freezing and spring snowmelt. Twenty-year (1986–2005) soil moisture observations were used to validate the model (Chapter 2).
- To study multi-decadal trends in soil moisture and to clarify the nature of temporal fluctuations in climate forcing and its long-term changes (Chapter 3).
- To investigate the relationships between soil moisture and vegetation activity on seasonal and interannual timescales (Chapter 4).
- To understand the memory mechanism of the soil moisture–vegetation system in a cold, arid climate and its temporal timescales (Chapter 5).

The results of this dissertation are presented in six chapters. Chapter 1 provides a general introduction and describes the study area. Some of the work arising from this thesis is included in two published papers and in two manuscripts submitted for publication. The work presented in Chapter 2 has been published in the *International Journal of Climatology* (Nandintsetseg and Shinoda, 2010a), while that in Chapter 3 has been submitted to the *Journal of Arid Environment* (Nandintsetseg and Shinoda, 2010b). The content of Chapter 4 has been published in *SOLA* (Nandintsetseg *et al.*, 2010), and that of Chapter 5 presents the results of the paper submitted to the *Journal of Geophysical Research, Atmospheres* (Shinoda and Nandintsetseg, 2010). Finally, the main conclusions and future tasks are presented in Chapter 6.

CHAPTER 2

Seasonal Change of Soil Moisture: Its Climatology and Modeling*

Abstract

Mongolia has an arid and cold climate due to its geographical settings of inland and mid-latitude highlands. The soil moisture varies seasonally, depending mainly on the balance of precipitation and evapotranspiration as well as on winter soil-freezing and spring snowmelt. Soil moisture climatology (1986–2005) for Mongolia is presented with a focus on three vegetation zones; the forest steppe, steppe, and Gobi Desert. For this purpose, we used soil moisture observations based on the gravimetric method for the top 50-cm soil layer from 26 grass-covered field sites during April–October of the 20-year period. In general, there was a latitudinal gradient in soil moisture content, with the southwestern soils drier than northeastern soils. The seasonal change in soil moisture was small and the seasonal pattern was similar throughout Mongolia. The seasonality was characterized by three major phases of the warm season; the spring drying, summer recharge, and autumn drying phases, although each phase differed somewhat in timing and length between zones. In the northernmost forest steppe zone, the recharge phase was longer than in the southern steppe and Gobi Desert zones, while the two drying phases were shorter in the forest steppe zone. This difference had a significant effect on the plant phenological timings of *Stipa* spp. and earlier in the forest steppe zone and later in the Gobi Desert zone. A simple water balance model was developed to examine the observed soil moisture dynamics, which implicitly simulated snow accumulation and soil freezing. The model simulated the observed seasonal and interannual soil moisture variations reasonably well ($r = 0.75$, $p < 0.05$). The results demonstrated that the three phases of seasonal change were produced by a subtle balance between precipitation and evapotranspiration. This model will provide a useful tool for a reliable and timely monitoring of agricultural drought for decision-makers and herders in Mongolia.

*This chapter is edited version of:
Banzragch Nandintsesteg and Masato Shinoda. 2010. Seasonal change of soil moisture in Mongolia: its climatology and modeling. *International Journal of Climatology*.
DOI: 10.1002/joc.2134.

2.1 INTRODUCTION

Recent widespread and intense droughts are likely manifestations of large-scale climate change, including global warming. Droughts have become widespread in the Northern Hemisphere, including Asia, and notably in Mongolia (e.g. Dai *et al.*, 1998; Barlow *et al.*, 2002; Hoerling and Kumar, 2003; Lotsch *et al.*, 2005). In Mongolia, the trend of increasing drought frequency has become increasingly important for animal husbandry and pasturing (e.g. Natsgadorj, 2003; Batima *et al.*, 2008).

The continental arid climate in Mongolia creates an extensive area of steppe that is the main source of forage for livestock, and pastoral animal husbandry is the country's major agricultural sector. The effect of drought on Mongolian grasslands has been identified quantitatively (e.g. biomass) (Miyazaki *et al.*, 2004; Zhang *et al.*, 2005; Munkhtsetseg *et al.*, 2007; Shinoda *et al.*, 2009) and also qualitatively in aspects such as phenology (Kondoh *et al.*, 2005; Shinoda *et al.*, 2007). Soil moisture plays an important role in many complex land-surface processes and their interactions with the atmosphere, acting as a bridge between deficits in precipitation (meteorological drought) and failures of plant growth (agricultural drought). It has been found that soil moisture deficits limit the growth of pasture in Mongolia (Miyazaki *et al.*, 2004; Zhang *et al.*, 2005; Nakano *et al.*, 2008; Shinoda *et al.*, 2009). Therefore, accurate assessment and modeling of soil moisture in these pasture lands are required for reliable and timely monitoring of agricultural drought for decision-makers and herders.

Historical records of soil moisture content measured *in situ* are available for few regions in the world and often represent very short periods (Robock *et al.*, 2000); however, unique long-term, updated measurements are available for Mongolia. Several studies have investigated the time-space variability of soil moisture across Mongolia using datasets from the Global Soil Moisture Data Bank (Robock *et al.*, 2000). In Mongolia, the seasonal variations in soil moisture are small and vertical profiles are almost constant with depth (Robock *et al.*, 2000; Ni-Meister *et al.*, 2005). Thus, soil moisture in Mongolia is characterized by relatively small temporal variability. However, subtle seasonal changes can have a significant impact on vegetation dynamics, controlling plant growth and phenology (*e.g.*, Shinoda *et al.*, 2007).

With this background in mind, the present study aimed to explore the detailed seasonal changes in observed and estimated soil moisture across Mongolia, focusing on

three vegetation zones; forest steppe, steppe, and Gobi Desert. In this analysis, a unique long-term, updated dataset for 26 stations during 1986–2005 was used to present soil moisture climatology. Moreover, we produced a water balance model for extratropical regions such as Mongolia by considering region-specific processes of winter soil-freezing and spring snowmelt. The long-term continuous observations for Mongolia are useful for the validation of soil moisture modeling.

2.2. MATERIALS AND METHODS

2.2.1 Data

The soil moisture dataset used in this paper was obtained from the Institute of Meteorology and Hydrology of Mongolia (IMH). Soil moisture observations were started in Mongolia more than 20 years ago (Erdenentsetseg, 1996). We chose 26 stations in grass-covered fields for the entire period of 1986–2005 (Table 2.1), while the periods of available soil moisture data differed from station to station. To study natural conditions of soil moisture on a consistent basis, only data collected at grass-covered field sites were analyzed. In general, the dominant soil texture in the top 50-cm layer at the selected stations was sandy.

The northern part of Mongolia is covered by forested mountain ranges with a dry sub-humid climate, whereas the southern part encompasses the Gobi Desert at lower elevations with a drier climate (Batima and Dagvadorj, 2000). This climatic pattern as a function of latitude characterizes the vegetation cover in the zones. These zones form belts of vegetation at different altitudes (from mountains to plains) and latitudes (from the north to south). The locations of the soil-moisture sampling stations and distribution of the seven natural zones are shown in Figure 2.1. For the convenience of discussion, the locations of those stations are categorized, into three zones; forest steppe, steppe, and Gobi Desert. The vegetation cover of the forest steppe, steppe, and Gobi Desert is 53, 25, and 15 %, respectively (Gunin *et al.* 1999).

At all stations, soil moisture observations were conducted on the 8^{th}, 18^{th}, and 28^{th} of each month during the warm season (April–October) using the gravimetric method. Soil moisture was not measured in winter (November–March) as the soil was frozen. Soil moisture was measured in 11 vertical layers; 5-cm layers from 0–10 cm and 10-cm layers from 10–100 cm. Most of the stations had no observations beneath 50 cm depth, and thus only data for the 0–50-cm soil layer were analyzed.

Table 2.1. Soil moisture observation stations with information on location, elevation, soil type, wilting point (W_{wp}), and field capacity (W_{fc}) of the 0–50 cm soil layer.

Station name	Lat. (°N)	Long. (°E)	Elev. (m)	Natural zone	Soil type	W_{wp} (mm)	W_{fc} (mm)
Ulgii	48.97	89.97	1714	Gobi desert	Brown, sandy	6	62
Ulaangom	49.80	92.08	934	Gobi desert	Light-brown, sandy	13	70
Khovd	48.02	91.65	1405	High mountain	Light-brown, sandy	6	62
Uliastai	47.75	96.82	1751	High mountain	Dark-brown, coarse silt	15	104
Tosontsengel	48.70	98.28	1724	High mountain	Dark-brown, coarse silt	19	89
Altai	46.40	96.25	2147	High mountain	Light-brown, sandy	13	80
Tsetserleg[a]	47.45	101.47	1695	Forest steppe	Dark-brown, medium silt	19	89
Murun[a]	49.63	100.17	1288	Forest steppe	Dark-brown, medium silt	19	89
Khutag[a]	49.37	102.70	938	Forest steppe	Dark-brown, medium silt	25	129
Bulgan	48.80	103.55	1210	Forest steppe	Dark-brown, medium silt	25	129
Onon	49.12	112.70	896	Forest steppe	Dark-chestnut, coarse silt	19	89
Darkhan	49.47	105.98	709	Steppe	Dark brown, sandy	17	104
Ugtaal	48.27	105.42	1160	Steppe	Dark-brown, sandy	19	89
Zuunmod	47.72	106.95	1529	Steppe	Dark-brown, coarse silt	25	140
Maanit	47.30	107.48	1427	Steppe	Brown, sandy	19	89
Undurkhaan	47.32	110.67	1028	Steppe	Brown, sandy	19	89
Choibalsan[a]	48.07	114.60	759	Steppe	Dark-brown, sandy	15	79
Khalkhgol	47.62	118.52	688	Steppe	Dark-chestnut, coarse silt	28	104
Bayankhongor	46.13	100.68	1860	Steppe	Light-brown, sandy	16	104
Arvaikheer[a]	46.27	102.78	1831	Steppe	Brown, coarse silt	17	80
Baruun-Urt[a]	46.68	113.28	986	Steppe	Dark-brown, sandy	25	79
Mandalgobi[a]	45.77	106.28	1398	Gobi desert	Light-brown, sandy	16	79
Sainshand[a]	44.90	110.12	915	Gobi desert	Desert- brown, sandy	13	80
Saikhan	44.08	103.55	1302	Gobi desert	Desert- brwon, sandy	22	80
Dalanzadgad[a]	43.58	104.42	1469	Gobi desert	Desert- brown, sandy	13	59
Ulaangom	49.80	92.08	934	Gobi Desert	Light-brown, sandy	13	70

The stations are listed in order from north to south and west to east. The stations are also shown in Figure 2.1.
[a] selected the stations to represent each of the natural zones

This soil layer includes the major rooting zone of the grasses that dominate most of Mongolia. The data are expressed as plant-available soil moisture (mm) in the upper 0–50 cm soil layer and were calculated as the actual total soil moisture minus the moisture content at the wilting point. We also used data of soil hydraulic properties such as wilting point (W_{wp}) and field capacity (W_{fc}) (Table 2.1) from the IMH. The field measurements of W_{wp} and W_{fc} were based on the methods described by Kachinsky (1965). In addition, precipitation, air temperature snow depth data for the 26 stations from IMH were used to investigate the soil moisture dynamics. Furthermore, the phenology data of *Stipa* spp.

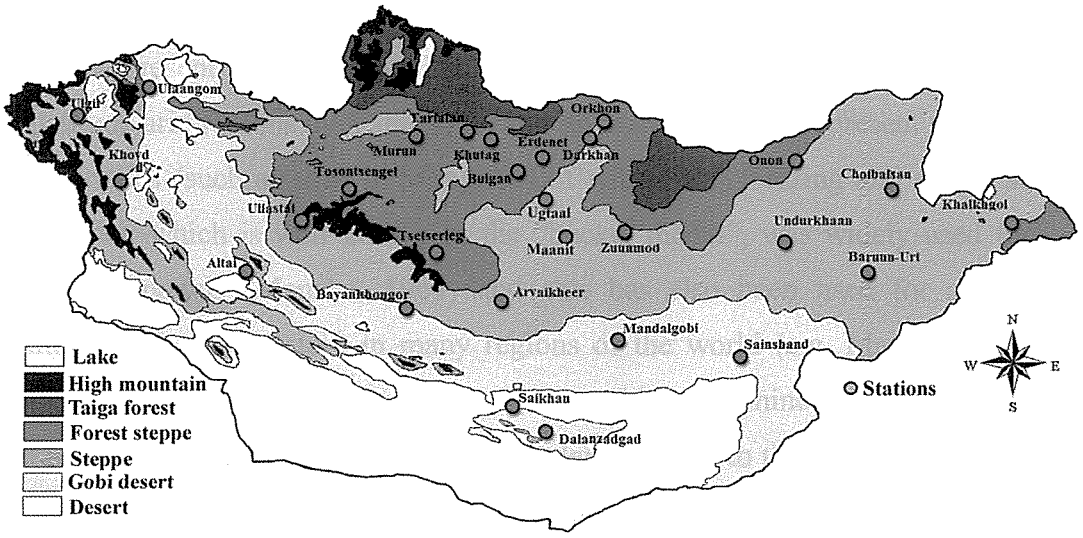

Figure 2.1 Locations of soil moisture measuring stations and natural zones in Mongolia.

were used; this is known as one of the dominant species representing the Mongolian steppe. The phenology data, which were taken with in-fence observations that had not been influenced by grazing, are useful for studying the relationship between the natural-state vegetation, climate and soil environments. In this analysis, used is the data for the phenological timing when more than half of the samples of *Stipa* spp. show a phenological phenomenon such as emergence (Em), heading (Hd), flowering (Fl), maturity (Mt), and senescence (Ss). The detailed information on the data is given in Shinoda *et al.* (2007).

Climate data (precipitation, temperature, and snow depth) underwent a series of data quality evaluation procedures at the IMH to correct or remove errors. The actual quality control (QC) included numerical formulas or visual inspections of time series that considered three basic statistical relationships: (1) relationships of data elements to themselves (e.g. outliers relative to long-term means); (2) relationships to nearby station data (e.g. neighbor checks); and (3) relationships to some other parameters e.g., sea level pressure to station pressure (Jambaajamts and Norjmaa, 1997; Richard and Masika, 2002). In the present study, QC of time-series of the observed soil moisture data was conducted to exclude outliers; we eliminated the soil moisture values having an increase that exceeded the precipitation amount during a 10-day period.

2.2.2 Soil Moisture Modeling

In the present study, we modified the one-layer water balance model developed for low-latitude arid regions by Yamaguchi and Shinoda (2002) to represent the extratropical characteristics (such as seen in Mongolia) of winter soil freezing and spring snowmelt. This model, which is well known as the "bucket model", was widely used for general circulation models (Manabe, 1969) and this has also been used for an operational monitoring of soil moisture in many regions of the world (e.g. Marengo *et al.*, 1996; Huang *et al.*, 1996; Yeung, 2005; Yamaguchi and Shinoda, 2002; Shinoda and Yamaguchi, 2003). We applied this water balance model to the 20-year (1986–2005) soil moisture observations of the top 50-cm soil layer for 26 Mongolian stations. The model calculates absolute plant available soil moisture content using only daily precipitation (P) and air temperature (T) data with a limited number of measured soil parameters, as expressed by the following equations:

$$\frac{dW_m(t)}{dt} = P_r(t) - E(t) + M(t) - R(t) \tag{2.1}$$

$$\begin{array}{lll} R = W - W_{fc} & \text{for} & W > W_{fc} \\ R = 0 & \text{for} & W \leq W_{fc} \end{array} \tag{2.2}$$

where W_m, the plant-available soil moisture, is expressed as the actual soil moisture minus the moisture content at the wilting point (mm) that exists from the surface to 50-cm depth; t is time (days); P_r is daily rainfall (mm); M is melt of the snow (expressed as snow water equivalent, mm) that is accumulated when air temperature is equal to or below 0°C. If air temperature is above 0°C, the accumulated snow melts. E is evapotranspiration (mm); and R is the combination of surface runoff and deep drainage (mm). In the model, the P_r is considered occurring when the air temperature was above 0°C. The soil is assumed to have one layer with field capacity W_{fc}. For this model, if $W > W_{fc}$, the excess is assumed to be R (Eq. 2.1). In arid regions such as Mongolia, these two factors are generally negligible as described by Yamanaka *et al.* (2007). Moreover, a negligible small amount of deep percolation was commonly found within natural vegetation areas of various arid regions where the annual precipitation was less than 300 mm (Scanlon *et al.*, 1997). In Mongolia, the annual precipitation is approximately 200 mm that is almost exactly matched by the annual evapotranspiration (Robock *et al.*, 2000). Most of the precipitated water on the grassland quickly returns to the atmosphere from

the upper layers of the soil via evapotranspiration and the fact that precipitated water never infiltrates to depths below 20-cm (Yamanaka *et al.*, 2007). Thus, we consider that although the treatment of surface runoff and deep drainage in our model is simplified, this would not cause a serious error in the soil moisture estimation. The evapotranspiration (E) varies with W such that:

$$E = \mathrm{PET}\frac{W}{W^*} = \frac{W}{\tau} \tag{2.3}$$

where τ is interpreted as a "residence time" or "turnover period" that signifies the time required for a volume of water equal to the annual mean of exchangeable soil moisture to be depleted by evapotranspiration. W^* is a moisture storage capacity of the 0–50 cm layer soil (mm). The actual value of τ is a function of soil properties, including the W_{wp}, W_{fc}, and the potential evapotranspiration rate (PET) with higher PET values resulting in lower residence times. In addition, the parameters of W_{wp} and W_{fc} used in this study were measured in the grass-covered field, thus including some information of not only soil properties but also of the root system (implicitly). Yamanaka *et al.* (2007) showed the value of τ ranges from 20 to 26 days, suggesting the precipitated water on the grassland in Mongolia quickly returns to the atmosphere via evapotranspiration. Following Serafini and Sud (1987), we calculated the value τ such that:

$$\tau = \frac{\gamma}{\lambda \mathrm{PET}} \ln \frac{\exp(\lambda W_{fc}) - 1}{\exp(\lambda W_{wp}) - 1} \tag{2.4}$$

where

$$\lambda = \frac{\alpha}{W_{fc} - W_{wp}} \tag{2.5}$$

and

$$\gamma = 1 - \exp(-\alpha) \tag{2.6}$$

In the above equation, α accounts for variations in vegetation type and Minths and Serafini (1984) determined it based on the experimental relationship between the actual and potential evapotranspiration. Serafani and Sud (1987) suggested that α should be adjusted to account for the variations in vegetation type; α = 16–20 may be suitable for a

forest, and $\alpha = 2$ may be appropriate for a desert. However, Mintz and Serafani (1984), and Serafani and Sud (1987) suggested using $\alpha = 6.81$ for most vegetation types everywhere in the world. Thus, α value of 6.81 was used in this study. The PET depends mainly on the net radiative heating on the surface. However, long-term measurements or sufficiently accurate calculations of the net radiation at the surface are inadequate or absent over large areas of Mongolia. With this background, we estimate PET from the observed air temperature and duration of sunlight using the Thornthwaite method (1948). The PET was calculated on a daily basis with the Thornthwaite (1948) formula as modified by Mintz and Walker (1993):

$$\mathrm{PET} = \begin{cases} 0 & \text{for} \quad T < 0°\mathrm{C} \\ \left[0.553\left(\frac{10T}{I}\right)^{a}\right] & \text{for} \quad 0 \le T \le 26.5\,°\mathrm{C} \\ (-13.86 + 1.075T - 0.0144T^{2})\frac{h}{12}, & \text{for} \quad T > 26.5\,°\mathrm{C} \end{cases} \tag{2.7}$$

$$I = \sum_{1}^{12} i \qquad \text{with} \qquad i = \left(\frac{T_m}{5}\right)^{1.514} \qquad \text{and} \qquad i_{min} = 0 \tag{2.8}$$

$$a = (6.75 \times 10^{-7} I^{3}) - (7.71 \times 10^{-5} I^{2}) + (1.79 \times 10^{-2} I) + 0.492 \tag{2.9}$$

where T is the daily mean air temperature (°C), T_m is the monthly mean air temperature (°C), h is the length of daylight (hours), and I is the annual heat index (sum of the 12 monthly heat indices i). Worldwide, this method has been used to calculate soil moisture indexes (Palmer, 1965, 1968) and derive global soil moisture fields (Mintz and Serafani, 1984). The wide use of this method is due to the simplicity of the calculation, using only surface air temperature. Yamaguchi and Shinoda (2002) examined the applicability of this method to the semi-arid Sahel region, demonstrating that the Thornthwaite PET coincided fairly well with the Penman PET during May–October when the daily air temperature was below 26.5°C. However, the Thornthwaite PET reached the maximum during March–May and October–November, which is the nature of this formula when the air temperature was above 26.5°C (Yamaguchi and Shinoda, 2002). In Mongolia, the air temperature was generally below 26.5°C all year around (Figure 2.6), making the Thornthwaite method a reliable choice in this country. The effectiveness of this model was validated by comparison with the 20-year soil moisture observations in Section 3.3.

2.3 RESULTS

2.3.1 Seasonal change in soil moisture

The climatological air temperature (1986–2005) in Mongolia averaged over 26 stations revealed a substantial seasonal change; approximately 11.5°C during the warm season (April–October) and approximately –13.7°C during the cold season (November–March); the annual precipitation during this period was about 200 mm (Figure 2.2, Table 2.2). About 80% of the total precipitation was during April–September, of which 50–60% was in July–August. There was snow cover from mid-October to the end of April. Over Mongolia, the yearly maximum snow depth (3.4 cm) is in January (Morinaga *et al.*, 2003). In general, the snow ablation period is March, coinciding with that observed at similar latitudes in other parts of Eurasia (Shinoda, 2001). In mid-March, snow depth decreases rapidly when the daily mean air temperature exceeded 0°C (Figure 2.2).

The climatological seasonal changes in the 10-day plant-available soil moisture in the upper 0–50 cm layer of soil during the warm season are shown in Figure 2. During winter, we assumed that soil water was frozen, thus giving a constant value as shown by the dashed line. This assumption is based on the estimations of the depth of soil freezing (1.6–1.7 m for the Gobi Desert and 3.2–3.5 m for the forest steppe) during the mid October–early April (Jambaajamts, 1989). The increase in spring soil moisture was related not only to the melting of frozen water stored in the soil in the preceding autumn, but also to the snowpack accumulated over winter. Soil moisture appeared to increase slightly during early spring (early April) relatively to that at the time of soil freezing in autumn (late October). This increase (7.0 mm) coincided generally with the snowmelt water (9.0 mm), if we assumed the Mongolian average snow-density was 0.20 g/cm^3 (Badarch, 1987). These two factors (frozen soil water and snowpack) act as a soil moisture 'memory' during the cold season and when they thaw the retained soil moisture forms an initial condition for the following warm season (Shinoda, 2001; Shinoda, 2005). Subsequently, the soil moisture was directly affected by rainfall and evaporation during the warm season. The seasonal soil moisture change was small ($\approx$ 10 mm), although the interannual variation was large as shown by the standard deviation (Figure 2.2). There were three seasonal phases of soil moisture: the spring drying (Phase I), the summer recharge (Phase II), and autumn drying (Phase III). The physical processes that govern the soil moisture changes at each phase are examined in the following.

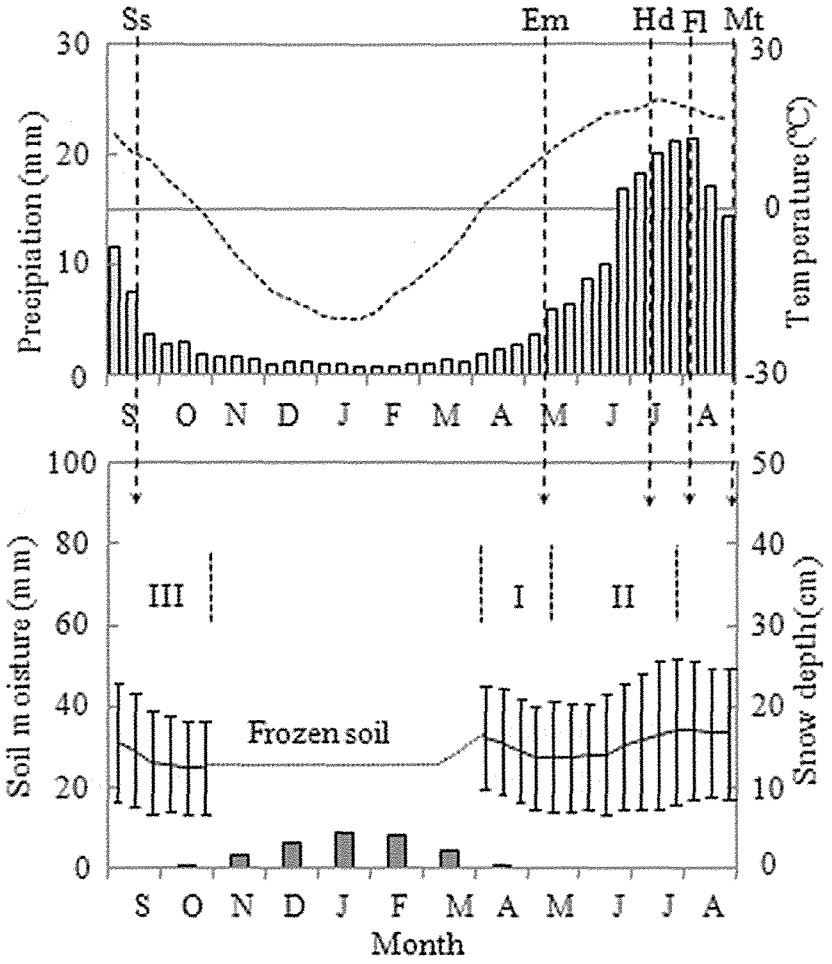

Figure 2.2 The climatological (1986–2005) seasonal changes of 10-day precipitation, temperature, soil moisture, and snow depth, averaged over 26 stations in Mongolia. The left and right axes of the upper panel correspond to precipitation (bars) and temperature (line) and phenological phenomena (vertical dashed lines, Em to Ss), respectively. The left axis and thick line of the bottom panel correspond to plant-available soil moisture in the 0–50-cm layer (20-year average with standard deviation), along with three soil moisture phases (I–III). The right axis and bars correspond to snow depth. The y-axis on the left (soil moisture) corresponds to that on the right (snow depth) with an assumption of snow density of 0.20 g/cm^3 (Badarch, 1987).

Phase I was between April (when daily air temperature was > 0°C) and May, and this trend continued until the onset of the rainy season. During this period, increased temperature leads to enhanced evaporation and hence depletion of soil moisture. This decrease in soil moisture will be further examined by using the soil moisture modeling (Section 2.3.3). Phase II occurred between late May and late July. This phase coincided with the replenished soil moisture from summer precipitation, with the seasonal maximum of soil moisture in late July. It was clear that in summer the variability of soil moisture was about twice (SD ≈ 20 mm) that during the other seasons (SD ≈ 12 mm at

the beginning of April, and SD ≈ 10 mm at the end of October). Shinoda *et al.* (2007) showed that the break of rainy season caused a similar reduction in soil moisture around mid-July in Mongolia. However, this was not clearly shown on a country-wide scale, probably because the averaging procedure over 20 years and 26 stations masked a clear timing of the break as seen in the zone scale (Section 2.3.2). Phase III was in August–October (prior to soil freezing), and was characterized by decreased soil moisture due to decreased precipitation.

In general, the beginning of plant emergence and senescence occurred in early May and late September, respectively (Figures 2.2 and 2.4). Phase I corresponds to the pre-growth period of *Stipa* spp. The emergence stage of *Stipa* spp. occurred during the transition from Phases I to II, that is, the emergence coincided with the change in trend of soil moisture from decrease to increase with a background of an increasing temperature trend (Figure 2.2). This is consistent with the findings of Shinoda *et al.* (2007), who highlighted the role of the onset of the rainy season in the emergence. The heading occurred at the end of Phase II, when the available soil moisture reached a value near the yearly-maximum due to the increased precipitation. As explained by Shinoda *et al.* (2007), the occurrence of the break or end of the rainy season may trigger a switch of the phenological phase from the vegetative growth to reproductive phase (i.e., seed production). The plant maturity and senescence occurred during Phase III when the soil moisture declined.

2.3.2 Spatial variations in soil moisture

The climatological (1986–2005) distributions of temperature, precipitation and soil moisture based on the 26 stations during the warm season are shown in Figure 2.3. There was a latitudinal gradient in soil moisture, with the southwestern (Gobi Desert) soils drier than the northeastern (forest steppe and steppe) soils. This soil moisture gradient roughly corresponded to the temperature and precipitation gradients. With the spatial patterns of precipitation/temperature and soil moisture in mind, we characterized the seasonal changes of soil moisture and their relationships to the phenological timings of *Stipa* spp. for the three zones (Figure 2.4). In this case, three stations representing climatological characteristics were selected in each zone (Table 2.1). Although the three typical phases of soil moisture were observed in all the three zones, the phases differed somewhat in timing and length between zones. There were some systematic differences in soil

moisture phases among the three zones (Figure 2.4d). Since the forest steppe zone was characterized by higher precipitation and lower evapotranspiration than the steppe and Gobi Desert zones, the Phase II was longer and the drying phases (Phases I and III) were shorter than those in the other two zones.

On a climatological basis, soil moisture values differed significantly ($p < 0.05$) between the three zones, as the result of the significant difference in precipitation and temperature (Table 2.2). Soil moisture in the forest steppe zone (46 mm and 48% of W_{fc}) was higher than the Mongolian mean (30 mm and 33% of W_{fc}); however, in the steppe zone, soil moisture was very near to the Mongolian mean. In the Gobi Desert zone, soil moisture (16 mm and 22% of W_{fc}) was below the Mongolian mean and close to the wilting point (water stressed conditions for plants) throughout the year. The soil moisture (and its standard deviation) in the forest steppe was greater than that in the steppe and Gobi Desert zones (Figure 2.4). Over the three zones, the soil moisture content at the yearly maximum in July depended strongly upon the summer precipitation, whereas the secondary maximum in early April depended on the yearly maximum snow depth in January. The early spring increases in soil moisture (7.0, 5.0, and 3.0 mm) were almost equal to the respective snowmelt water amounts (8.0, 6.0, and 4.0 mm) when a snow density of 0.20 g/cm^3 (Badarch, 1987) was assumed. As shown in Figure 2.4, in conjunction with the seasonal evolution of Phase II (earlier in the forest steppe), the occurrences of each phenological stage in the steppe and Gobi Desert zones lagged behind that in the forest steppe zone by approximately 5 and 10 days, respectively. This southward time lag in the timings is related to the phenological phenomenon that the lengths of two periods from emergence to heading (approximately 61 days), and from the emergence to the maturity (approximately 108 days) coincide roughly with each other. This may be a common physiological and phenological feature of the same genus. The emergence tends to occur around the transition from Phase I to II in all the zones (earlier in the forest steppe and later in the Gobi Desert). On the other hand, the timings of the heading exhibit a southward shift from the end of Phase I to the transition from Phase I to II. Going into the details for the steppe and the Gobi Desert zones, it is possible that *Stipa* spp. has naturally adapted to such a rainy season's pattern by completing the vegetative growth in the rainy season near its break around mid-July, and shifting to the reproductive phase as pointed out by Shinoda *et al.* (2007). The rain break, climatologically phase-locked around mid-July over Mongolia, is associated with a barotropic ridge embedded in the stationary Rossby wave of the westerlies (Iwasaki and

Nii, 2006). This break was not found in the forest steppe zone probably due to the procedure of averaging the three stations for each zone.

Table 2.2. Average (AVG) and standard deviations (SD) of temperature, precipitation and soil moisture over the entire Mongolia and in three natural zones during the warm season (April–October) during 1986–2005.

Zone (no. of stations)	Temperature (°C)		Precipitation (mm)		Soil moisture (mm)	
	AVG	SD	AVG	SD	AVG	SD
Over Mongolia (26)	11.4	6.6	200	7	29.8	3.2
Forest steppe (3)	10.3	6.1	271	10	45.8	5.7
Steppe (3)	12	6.7	199	8	25.7	3.5
Desert steppe (3)	14.2	6.7	118	4	16.1	2.9

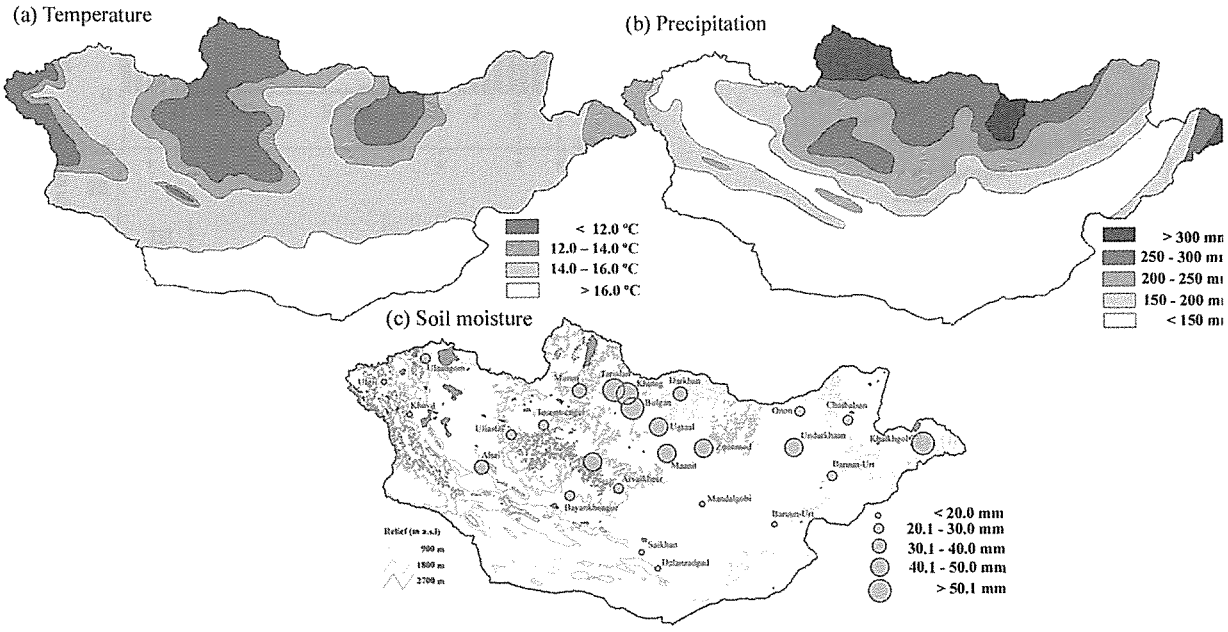

Figure 2.3 Spatial patterns of climatological (1986–2005) temperature, precipitation and the plant-available soil moisture averaged during the warm season. The patterns of precipitation and air temperature were based on the 26 stations data during the warm season (April to October) of 1986–2005.

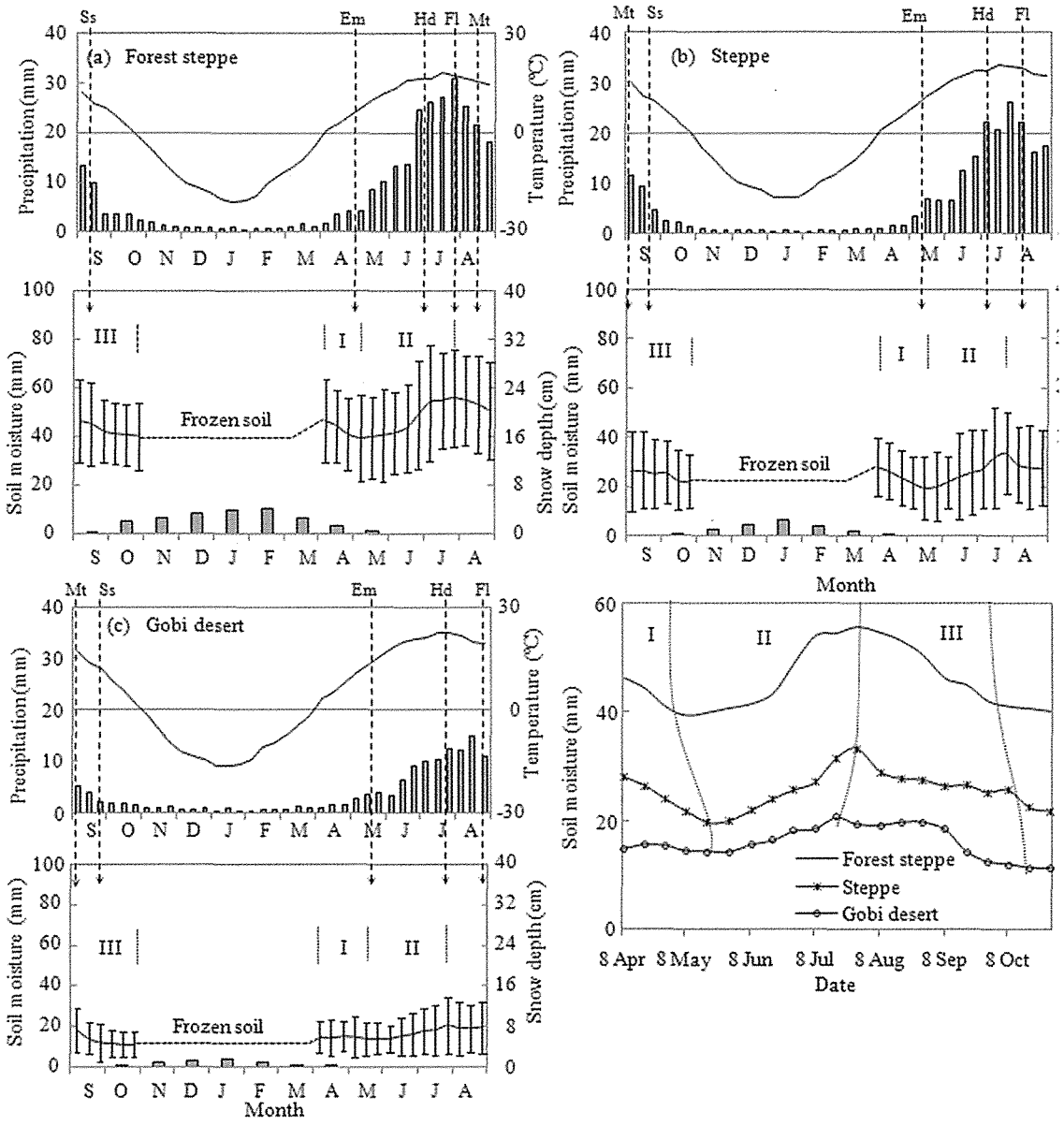

Figure 2.4 The same as in Figure 2.2 with the exception for each of the natural zones: forest steppe (a), steppe (b) and Gobi Desert (c). Figure 2.4d shows a comparison of soil moisture during April–October among the three zones.

2.3.3 Soil moisture estimation

In general, the soil moisture model performed reasonably well in simulating the seasonal and interseasonal variations in soil moisture. The correlation coefficient between the estimated and observed soil moisture was 0.75, and was statistically significant ($p <$ 0.05), with the root-mean-square error (RMSE) of 2.4 mm (Figure 2.5).

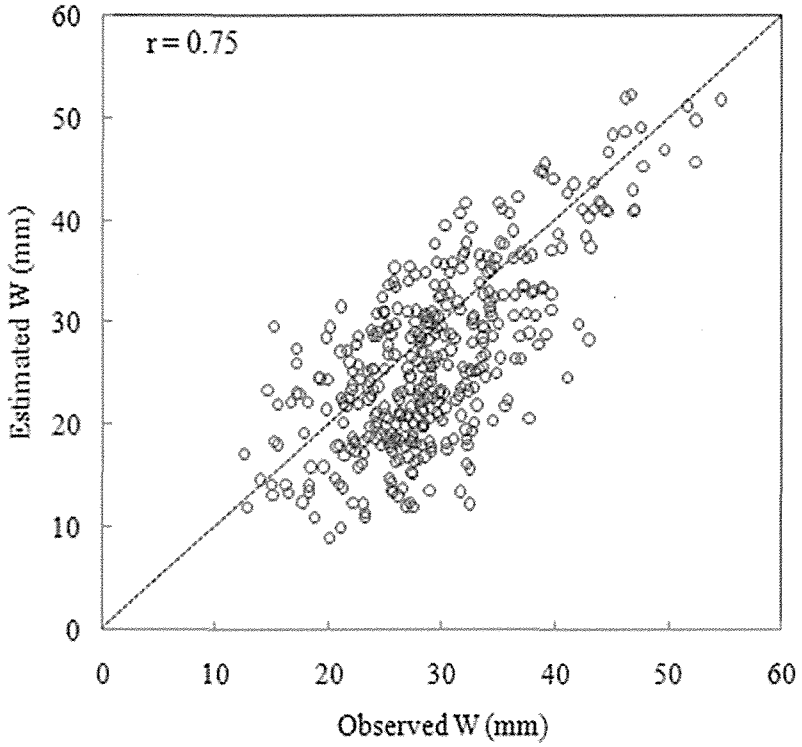

Figure 2.5 Scatter diagram between the observed 10-day soil moisture and estimated soil moisture by the water balance model for 26 stations during 1986–2005.

The seasonal cycles of temperature and each water balance variable, i.e. precipitation, observed and estimated soil moisture, potential and actual evapotranspiration, for the entire Mongolia and three vegetation zones are presented in Figure 2.6. Three stations were selected for each of the three zones (Table 2.1). In Section 2.1, we identified the three seasonal phases of soil moisture during the warm season; these three phases were clearly simulated (Figure 2.6). Generally, the annual precipitation (215 mm) was almost exactly matched by the annual evapotranspiration (208 mm) in Mongolia, about 95% of the total water was evapotransporated from the 0–50 cm soil layer which is consistent with the studies of Robock *et al.* (2000), Zhang *et al.* (2005) and Li *et al.* (2006). That is, precipitation in the warm season is likely to evaporate quickly due to the high evaporative potential. The estimated soil moisture slightly increased in early spring (early April) due to spring snowmelt when daily maximum temperature was > 0°C. The snow depth in Mongolia was small (Figure 2.2), and had a minor influence on the spring increase in soil moisture (4.0 mm). During Phase I, the estimated soil moisture decreased rapidly until the onset of the rainy season (late May) because evapotranspiration exceeded precipitation. During Phase II (from early June), soil moisture continued to increase and reached a peak

between late July and early August because precipitation exceeded evapotranspiration. Phase III occurred when precipitation was smaller than evapotranspiration from late August to mid-October. After mid-October, soil moisture was assumed constant when the daily mean temperature was < 0°C. The correlation coefficients between the observed and estimated soil moisture were for the forest steppe 0.59, for the steppe 0.81, and for the Gobi Desert 0.73, respectively, with their RMSEs of 4.8 mm, 2.2 mm, and 2.0 mm. The model simulated the observed soil moisture variations reasonably well for the steppe and Gobi Desert zones. As for the forest steppe zone, a densely vegetated area, there were some underestimates and overestimates by the model depending on the seasonal phases; the underestimates were found from the end of Phase I to Phase II, whereas the overestimates were seen in Phase III. This probably resulted from the model formulation that did not explicitly include the vegetation effect on soil moisture.

2.4 DISCUSSION AND CONCLUSIONS

In the present study, we comprehensively analyzed climatological seasonal changes in root-zone plant available soil moisture for the entire Mongolia and three vegetation zones. The long-term, quality-controlled soil moisture data enabled us to document three phase of soil moisture during the warm season; spring drying, summer recharge, and autumn drying. Moreover, to examine the underlying mechanisms that created the three phases, we modified a simple water balance model for arid and cold region such as Mongolia by considering the soil freezing and snow melting. In general, there was a latitudinal gradient in soil moisture, with the southwestern soils drier than northeastern soils. The seasonal change in soil moisture was small (≈ 10 mm), which is consistent with the studies of Robock *et al.* (2000) and Ni-Meister *et al.* (2005).

The seasonal pattern was similar throughout Mongolia. Moreover, we documented three distinct phases and their relationships to plant phenological phenomena of *Stipa* spp. that represents the dominant species in the Mongolian steppe. The three phases were simulated by soil moisture modeling during the warm season; these phases of the seasonal change were produced by a subtle precipitation–evapotranspiration balance, although each phase differed somewhat in timing and length between zones. In the northernmost forest steppe zone, the recharge phase was longer than in the southern

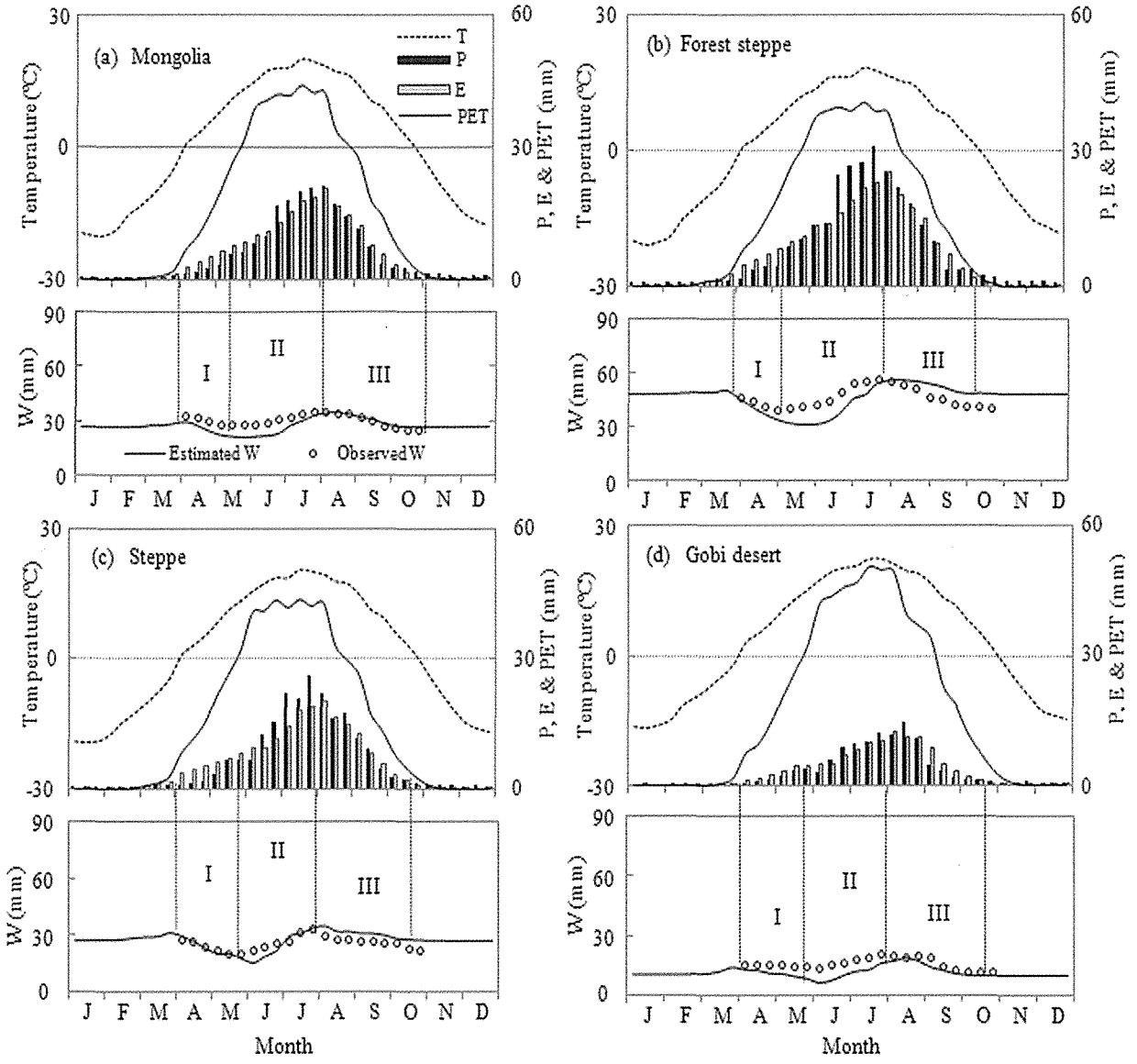

Figure 2.6 The seasonal changes of 10-day air temperature (*T*) and water balance variables: precipitation (*P*), the observed (circle) and estimated (solid line) soil moisture (*W*), potential (PET) and actual (*E*) evapotranspiration averaged over all 26 stations of Mongolia (a) and three stations for each of the vegetation zones (b–d) during 1986–2005. Three soil moisture phases (I–III) are denoted. The daily soil moisture estimations were averaged over 10-day intervals.

steppe and Gobi Desert zones, whereas the two drying phases were shorter in the forest steppe. Over Mongolia, the available soil moisture was about 30% of the soil field capacity during the warm season, while in the Gobi Desert zone, the available soil moisture was close to the wilting point throughout the year. This difference is likely to have a significant effect on the vegetation cover between the three zones as mentioned below. It has been found that soil moisture condition in the early growth stage impacts

critically on the plant phenology in Mongolia (Shinoda *et al.*, 2007). In the present study, we showed that the plant (*Stipa* spp.) emergence and heading timings occurred around the transition from Phase I to II and the end of Phase II, respectively. That is, the emergence coincided with the change in trend of soil moisture from decrease to increase with a background of an increasing trend in temperature. The heading occurred at the end of Phase II, when the available soil moisture reached a value near the yearly-maximum due to the increased precipitation. The yearly-maximum vegetation cover, observed at the end of the growing season (Phase III) ranges from 15% (for the Gobi Desert) to 53% (for the forest steppe) (Gunin *et al.*, 1999). Zhang *et al.* (2005) estimated that the partition of transpiration in evapotraspiration was 22% in the Mongolian grassland with vegetation cover ranging from 38–60% during the grass growth. This result implies that the evaporation from the soil is likely a determinant factor contributing to the total evapotranspiration and the influence of transpiration is relatively small in this sparsely vegetated area.

In general, our model simulated the seasonal and interannual variations in the observed soil moisture reasonably well ($r = 0.75$, $p < 0.05$), providing a basic method for the agricultural drought monitoring in Mongolia. The advantage of the model proposed in this study is a simple calculation that uses daily data (such as precipitation and temperature) observed operationally for long-term spans. Future studies should investigate interannual variations of soil moisture using the water balance model in this region.

CHAPTER 3

Multi-decadal Trend and Memory of Modeled Soil Moisture*

Abstract

Drought has become widespread since the middle 1950s throughout the Northern Hemisphere, affecting the Mongolian steppe and pastureland used for livestock. This situation has motivated us to assess multi-decadal trends and memory of soil moisture in Mongolia, which plays a crucial role in determine vegetation activity. We estimated daily soil moisture during 1961–2006 for three vegetation zones (forest steppe, steppe, and desert steppe) using a water balance model. The model performed reasonably well in simulating seasonal and interannual variations in observed soil moisture; and on an interannual basis, the modeled soil moisture was more strongly correlated with the observed soil moisture ($r = 0.91$, $p < 0.05$) than the Palmer Drought Severity Index ($r = 0.65$, $p < 0.05$). All three vegetation zones showed a decreasing trend in soil moisture during 1961–2006 due to decreased precipitation and increased potential evapotranspiration, although the drying trend was significant ($p < 0.05$) only in the forest steppe. In conjunction with this trend, the summer phase of recharging soil moisture was shortened in all zones during the analysis period, whereas the spring and autumn drying phases were prolonged. A comparison between years with wet and dry soil revealed that soil moisture anomalies were most manifested during June–August due to large precipitation and evapotranspiration anomalies, which were maintained throughout the freezing of winter into spring. In addition, autocorrelation analysis of W_m for the forest steppe zone showed that during the autumn and winter, the temporal scales was 6–7 months, larger than during spring and summer (1.8–3 months). These findings indicate that in cold, arid regions such as Mongolia, W_m acts as an efficient memory of P anomalies via freezing of the soil.

*This chapter is edited version of:
Nandintsesteg B and Shinoda M. 2010. Multi-decadal trend and memory of modeled soil moisture in Mongolia. submitted to *Journal of Arid Environments*.

3.1 INTRODUCTION

A strong drying trend has been observed over land areas in the Northern Hemisphere since the middle 1950s, especially over northern Africa, Canada, Alaska, and Eurasia, including Mongolia (Dai *et al.*, 2004; IPCC, 2007). Traditional Mongolian animal husbandry is closely associated with a nomadic pastoralism with seasonal migrations dependent on natural climate conditions. In Mongolia, the increased frequency of drought has led to problems in the farming of livestock and pasturing (*e.g.*, Natsagdorj, 2003). The arid continental climate in Mongolia has led to the development of an extensive area of pastureland that is the main source of forage for livestock. The livestock industry has always been affected by climatic variability, such as summertime drought and severe winters (Natsagdorj, 2003).

Soil moisture plays an important role in many complex land-surface processes and their interactions with the atmosphere, acting as a bridge between deficits in precipitation (meteorological drought) and failures of plant growth (agricultural drought). The amount of soil moisture in the root zone is a governing factor of vegetative growth via the availability of water for transpiration; thus, it could be used as a direct indicator of agricultural and pasture drought (Keyantash and Dracup, 2002). A deficit in soil moisture limits plant growth in arid regions such as Mongolia, where drought originates from persistent large-scale circulation anomalies and resulting below-average precipitation. Meteorological drought (a deficit in precipitation) may lead to soil moisture deficiency in the root zone and ultimately to plant (physiological) drought (Shinoda and Morinaga, 2005). The effects of drought on Mongolian grasslands have been both quantitative, such as decreases in phytomass (e.g., Miyazaki *et al.*, 2004), and qualitative, such as changes in phenology (Shinoda *et al.*, 2007) and species composition (Shinoda et al., 2010). Therefore, it is vital to provide timely and reliable assessments of soil moisture in Mongolia to assist in pasture management.

Drought can be classified based on its severity, frequency, duration, and spatial extent in terms of a region- or application-specific index. Although a number of drought indices have been proposed and applied in various parts of the world (Wilhite *et al.*, 2000), few studies have used ground-observed soil moisture as an indicator of drought, due to a lack of relevant observation data (Robock *et al.*, 2000). Given this background, we investigated the multi-decadal trend in modeled soil moisture in Mongolia during

1961–2006, as validated using 20-year (1986–2005) observations. These unique long-term observations available for Mongolia proved to be invaluable in the present analysis. We modified a water balance model proposed for arid and cold regions such as Mongolia by taking into account soil freezing and snowmelt. The model is designed to simulate daily soil moisture content based on widely available daily meteorological data. The analysis focused on three vegetation zones in Mongolia; forest steppe, steppe, and desert steppe.

3.2 DATA AND METHODS

3.2.1 Datasets

The soil moisture dataset used in this study was obtained from the Institute of Meteorology and Hydrology of Mongolia (IMH). We analyzed data collected at nine stations distributed widely across the Mongolian steppe, including within the major vegetation zones of forest steppe, steppe, and desert steppe (Figure 3.1 and Table 3.1). At each station, observations of soil moisture (W_o) were conducted on the 8th, 18th, and 28th of each month during the warm season (April–October) using the gravimetric method. Soil moisture was not measured in winter (November–March) because the soil was frozen. Soil moisture data were collected from the upper 50-cm of the soil layer in fenced, ungrazed pastures. This soil layer includes the major rooting zone of the grasses that dominate grasslands in Mongolia.

Table 3.1 Nine soil moisture observation stations with information on location, elevation, soil type, wilting point (W_{wp}), and field capacity (W_{fc}) of the 0–50 cm soil layer. The stations are listed in order from north to south and west to east. The stations are also shown in Figure 3.1.

Station	Lat. (°N)	Long. (°E)	Elev. (m)	Natural zone	Soil type	W_{wp} (mm)	W_{fc} (mm)
Tsetserleg	47.45	101.47	1695	Forest steppe	Dark-brown, medium silt	19	89
Murun	49.63	100.17	1288	Forest steppe	Dark-brown, medium silt	19	89
Khutag	49.37	102.70	938	Forest steppe	Dark-brown, medium silt	25	129
Choibalsan	48.07	114.60	759	Steppe	Dark-brown, sandy	15	79
Arvaikheer	46.27	102.78	1831	Steppe	Brown, coarse silt	17	80
Baruun-Urt	46.68	113.28	986	Steppe	Dark-brown, sandy	25	79
Mandalgobi	45.77	106.28	1398	Desert steppe	Light-brown, sandy	16	79
Sainshand	44.90	110.12	915	Desert steppe	Desert- brown, sandy	13	80
Dalanzadgad	43.58	104.42	1469	Desert steppe	Desert- brown, sandy	13	59

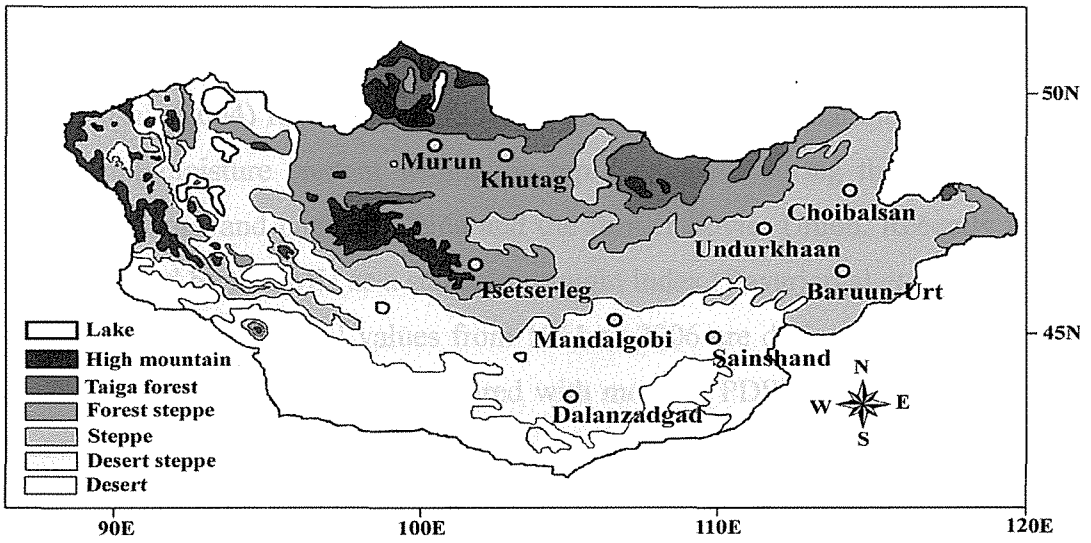

Figure 3.1 Locations of nine stations at which the soil moisture was measured, and vegetation zones in Mongolia.

The soil texture at the stations is characterized by medium silt and sandy soil (Table 3.1). We also used wilting point and field capacity data, as provided by the IMH. The W_0 is expressed as plant-available soil moisture (mm) in the upper 50-cm soil layer and was calculated as the actual total soil moisture minus the moisture content at the wilting point. Daily precipitation (P) and air temperature (T) data provided by the IMH were used to calculate the soil moisture content and PDSI. In addition, we used a 25-year (1981–2005) monthly 1° × 1° grid of NDVI data from the semi-monthly 8-km-resolution Global Inventory Modeling and Mapping Studies dataset (GIMMS) produced by Tucker *et al.* (2005). The GIMMS NDVI data sets were generated from the National Oceanic and Atmospheric Administration/Advanced Very High Resolution Radiometer (NOAA/AVHRR), which includes corrections for NDVI variations arising from calibration, view geometry, volcanic aerosols, and other factors unrelated to vegetation change (Pinzon *et al.*, 2002; Tucker *et al.*, 2005).

3.2.2 Palmer Drought Severity Index

In recent years, the PDSI has been one of the most widely used drought indices (Palmer, 1965; Alley, 1984). The PDSI is derived based on the supply-and-demand concept of the water balance equation using monthly P and T and as well as the available soil moisture content. The monthly index values range between –4 and +4. Negative

(positive) PDSI values indicate dry (wet) conditions, while a value of zero indicates a state close to the average.

Dai *et al.* (2004) found that PDSI shows a significant correlation (r =0.5–0.7) with observed soil moisture content within the top 1-m depth during the warm season in Mongolia, Illinois, and parts of China and the former Soviet Union. Recently the PDSI has been applied by the IMH as a standard drought index (Bayarjargal *et al.*, 2006). In the present study, monthly PDSI values from 1961 to 2006 are derived using P and T data. W_m values, calculated daily, are compared with monthly PDSI values during this period to examine the efficiency of the two indices.

3.2.3 Water Balance Model

We modified an existing one-layer water balance model developed for low-latitude arid regions (Yamaguchi and Shinoda, 2002) to represent the extratropical characteristics of winter soil freezing and spring snowmelt in Mongolia (Chapter 2). This type of water balance model has been widely used for drought monitoring and climate change studies in many regions of the world (e.g., Kunkel, 1990; Robock *et al.*, 1995; Poncea and Shetty, 1995; Huang *et al.*, 1996; Shinoda and Yamaguchi, 2002; Dai *et al.*, 2004). Our model calculates absolute plant-available soil moisture content using only P and T data with a limited number of measured soil parameters (e.g., soil wilting point and soil moisture storage capacity), as expressed by the following equation:

$$\frac{dW_m(t)}{dt} = P_r(t) - E(t) + M(t) - R(t) \tag{3.1}$$

where W_m is plant-available soil moisture in the upper 50-cm soil layer, t is time (days), P_r is daily rainfall (mm), M is snowmelt (mm) when air temperature is below 0°C (i.e., the snow water equivalent to an accumulated until time t), E is evapotranspiration (mm), and R is runoff (mm). In this study, we applied the model in calculating daily W_m during the period of 1961–2006. W_m values, calculated daily using the one-layer water balance model, are compared with monthly PDSI values during the period of 1961–2006 to examine the efficiency of these two indices.

3.2.4 Temporal Autocorrelation

The temporal autocorrelation function of soil moisture was employed to examine the soil moisture memory using monthly W_m anomaly time-series during 1961–2006. Delworth and Manabe (1988) developed a theory that soil moisture temporal variations correspond to the combination of a first-order Markov process signal and additive white noise by analyzing results from the Geophysical Fluid Dynamics Laboratory GCM. They assumed that the autocorrelation coefficient r_a has an exponential form:

$$r_a(t) = exp\left(-\frac{t}{T_m}\right) \tag{3.2}$$

where t is time lag and T_m is scale of temporal autocorrelation, decay time scale (i.e. lag at which autocorrelation function equal to $1/e$). The theory was successfully applied for analyzing the temporal scales of observed soil moisture by Vinnikov and Yeserkepova, (1990), Vinnikov *et al.*, (1996), and Entin *et al.*, (2000). In this study, the climatological seasonal cycles of soil moisture were first subtracted from the monthly values to create interannual anomalies, with which the autocorrelation functions were calculated for each month.

3.3 RESULTS

3.3.1 Model performance

The water balance model was run using daily meteorological data from the nine stations during 1961–2006. Model performance was validated using 10-day soil moisture observations during April to October for the period of 1986–2005 (20-year), for which continuous observation data are available. The model performed reasonably well in simulating seasonal and interannual variations in soil moisture over the three zones of interest (Chapter 1). In general, the soil moisture model performed reasonably well in simulating the seasonal ($r = 0.75, p < 0.05$) and interannual variations ($r = 0.91, p < 0.05$) in soil moisture with the root-mean-square error (RMSE) of 2.8 and 2.1 mm, respectively. The correlation coefficients between the W_m and W_o were for the forest steppe 0.71, for the steppe 0.81, and for the desert steppe 0.73, with their RMSEs of 3.8 mm, 2.2 mm, and 2.0 mm (Figure 3.2), respectively. The model simulated the observed soil moisture

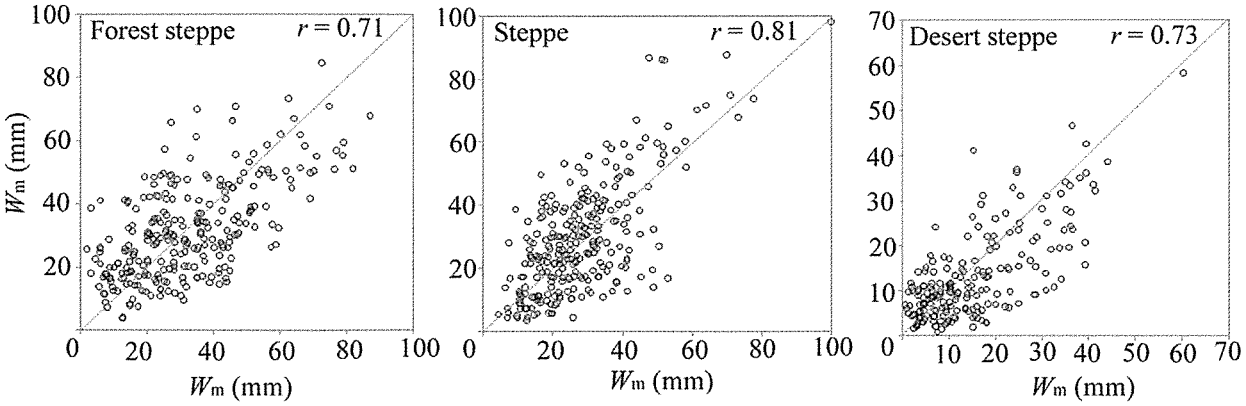

Figure 2.2 Scatter diagram between the observed 10-day soil moisture (W_o) and estimated soil moisture (W_m) by the water balance model for three vegetation zones during 1986–2005.

variations reasonably well for the steppe and desert steppe zones. As for the forest steppe zone, a densely vegetated area, there were some underestimates and overestimates by the model depending on the seasonal changes; the underestimates were found during spring, whereas the overestimates were seen in autumn. This probably resulted from the model formulation that did not explicitly include the vegetation effect on soil moisture.

3.3.2 Seasonal variations in modeled soil moisture

The seasonal cycles of temperature and each water balance variable, i.e. P, W_o and W_m, PET and E, and monthly NDVI for the three vegetation zones are presented in Fig. 3. The climatological air temperature (1986–2005) averaged over the nine stations revealed a substantial seasonal change, from approximately 12.0°C during the warm season to approximately –12.5°C during the cold season. The average annual precipitation is about 200 mm. About 80% of the total precipitation occurs during April–September. There is snow cover from mid-October until the end of April. Over Mongolia, the yearly maximum snow depth (3.4 cm) is seen in January (Morinaga et al., 2003) and snow ablation occurs during March, coinciding with that observed at similar latitudes in other parts of Eurasia (Shinoda, 2001). On a climatological basis, soil moisture values differed significantly ($p < 0.05$) between the three zones. The soil moisture in the forest steppe was greater than that in the steppe and desert steppe zones. We identified three seasonal phases of W_m; spring drying (Phase I), summer recharging (Phase II), and autumn drying (Phase III) (Chapter 1). W_m showed a slight increase in early spring (early April)

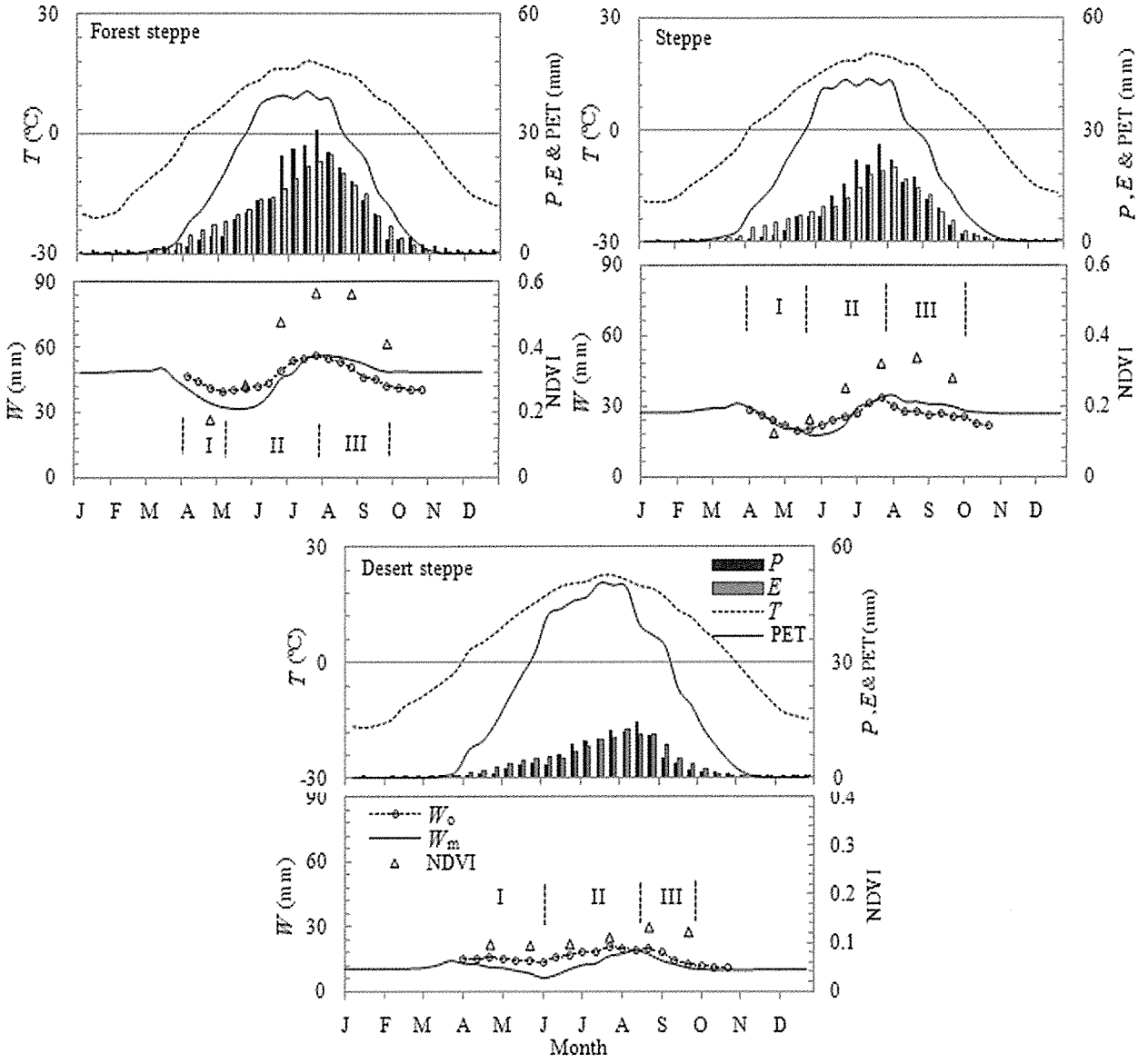

Figure 3.3 Seasonal changes in 10-day precipitation (P), air temperature (T), actual evapotranspiration (E), potential evapotranspiration (PET), observed soil moisture (W_o), modeled soil moisture content (W_m), and monthly NDVI, also showing the timing of three soil moisture phases (I–III) averaged over three stations for each of three vegetation zones in Mongolia during 1986–2005. The daily soil moisture estimation was averaged over 10-day intervals.

due to the spring snowmelt when daily $T > 0$°C. It is possible that the small snow depth might have had an influence on W_m. During Phase I, W_m decreased rapidly until the onset of the rainy season (late May), as E exceeded P. In spring, during the emergence stage, NDVI increased with increasing W_m due to the onset of the rainy season in late May. During Phase II (from early June), W_m continued to increase and reached a peak between late July and early August, when P exceeded E. During Phase II, NDVI continued to increase, reaching a peak in August due to the maximum in W_m. Phase III occurred during

late August to mid-October as a result of a deficit in the water balance ($P < E$). This water balance model was matched by decreasing NDVI (Figure 3.3). This result shows that W_m was generally controlled by the subtle balance between P and E. We found a stronger correlation between NDVI and W_m ($r = 0.91$, $p < 0.05$) than between NDVI and P ($r = 0.65$, $p < 0.05$). The soil moisture gradient roughly corresponded to the vegetation activity, with high NDVI in the forest steppe and low NDVI in the desert steppe (Figure 3.3). Although the three typical phases of soil moisture were observed in all the three zones, the phases differed somewhat in timing and length between zones. There were some systematic differences in soil moisture phases among the three zones (Figure 3.3). Since the forest steppe zone was characterized by higher P and lower E than the steppe and desert steppe zones, the Phase II was longer and the drying phases (Phases I and III) were shorter than those in other two zones.

3.3.3 Multi-decadal trend in modeled soil moisture

Table 3.2 lists the linear trend coefficients for W_m, P, T, PET, and three seasonal phases (I, II, and III) of W_m for the three zones of interest during the warm season in the period of 1961–2006. In general, a decreasing trend in W_m is found in the three zones, in conjunction with a decreasing trend in P and increasing trend in PET (driven by increased T). A statistically significant decreasing trend in W_m ($p < 0.05$) is observed in the forest steppe, but not in the steppe and desert steppe (Table 3.2). For all three zones, these changes in W_m are strongly correlated with both the decreasing trend in P ($r = 0.85$, $p < 0.05$) and increasing trend in PET ($r = 0.65$, $p < 0.05$). In addition, P and PET show a high correlation with each other ($r = 0.61$, $p < 0.05$), probably due in part to variations in sensible heating at the ground surface and/or the albedo effect of rain-bearing clouds. As mentioned above, the forest steppe zone experienced the most significantly ($p < 0.05$) pronounced multi-decadal trends of decreasing P, increasing PET (Table 3.2), and resultant decrease in W_m (see Figure 3.4a and 3.4b). The T trend (0.42°C/decade) is consistent with the temperature trend (0.5°C/decade) observed in northern Mongolia (the forest steppe) during the period of 1963–2002 (Nandintsetseg et al., 2007). Figure 3.4b compares a time series of W_m anomaly with that of PDSI. Although the W_m anomaly is generally in phase with PDSI on an interdecadal timescale, W_o is more strongly correlated with W_m ($r = 0.91$, $p < 0.05$) than with PDSI ($r = 0.65$, $p < 0.05$). This result clearly demonstrates the efficiency of the present model.

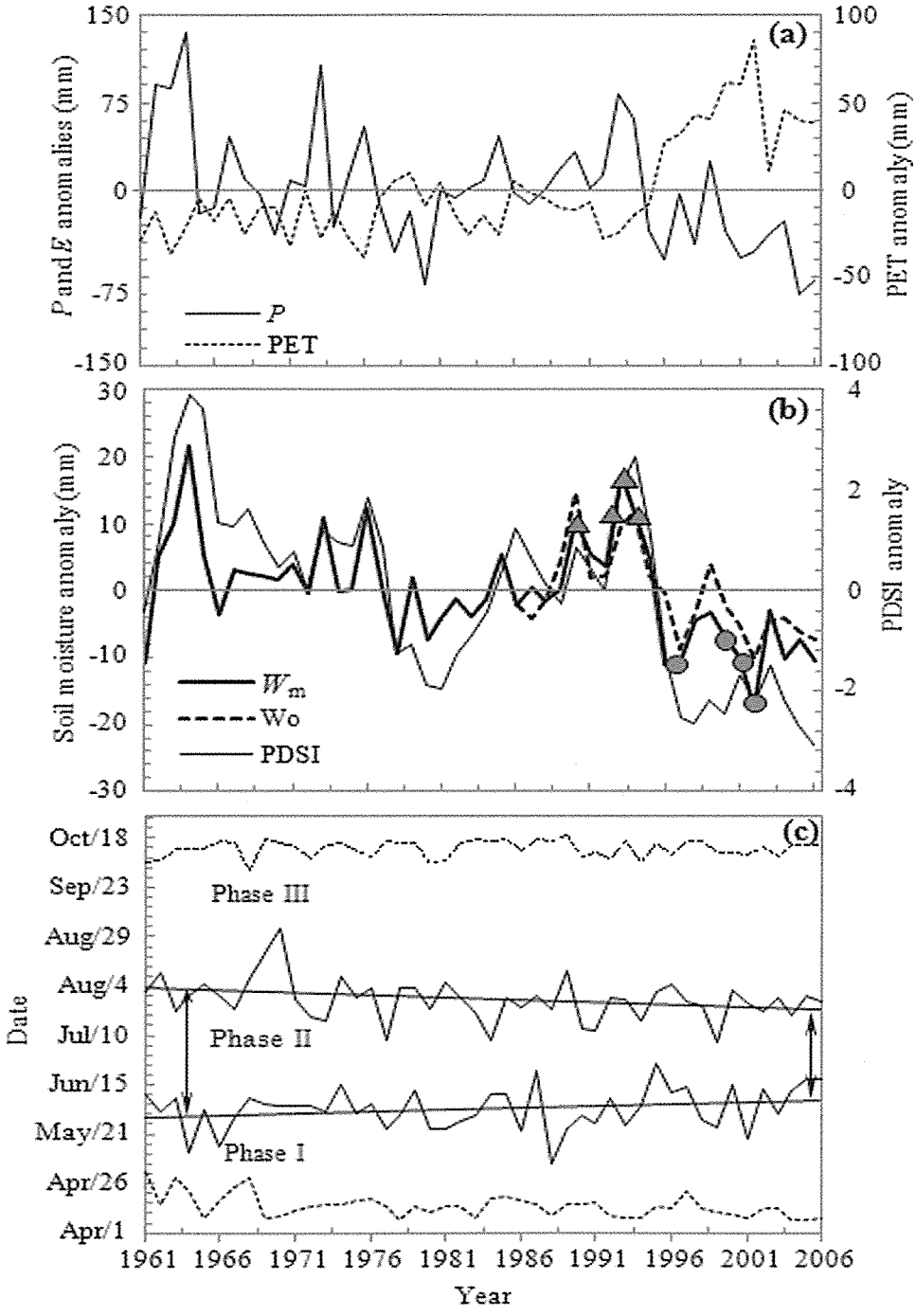

Figure 3.4 Interannual time series (1961–2006) of precipitation (P) and potential evapotranspiration (PET) anomalies (a), the modeled (W_m) and observed (W_o) soil moisture contents, and Palmer Drought Severity Index (PDSI) (b), and the timing of three soil moisture phases (I–III) during the warm season in the forest steppe zone (c). Circles and triangles in (Figure 3.4b) indicate years with wet and dry soils, respectively, which were used for the composite analysis in Figure 3.3.

Table 3.2 Linear trend coefficients of the modeled soil moisture (W_m), precipitation (P), air temperature (T), potential evapotranspiration (PET), and three phases changes (Phases I, II, and III) of W_m per decade over three zones (forest steppe, steppe, and desert steppe) during the period of 1961–2006.

Zone	W_m (mm)	P (mm)	T (°C)	PET (mm)	Phase I (days)	Phase II (days)	Phase III (days)
Forest steppe	–2.5*	–13.5*	0.42*	–11.1*	+4*	–4*	+3*
Steppe	–1.2	–7.3	0.3*	–10.0*	+1	–4	+1
Desert steppe	–0.6	–4.4	0.3*	–10.0*	+3*	–1	+1

*Significant at 5% level

Climatologically, three seasonal phases of soil moisture are identified in Mongolia (Figure 3.4c). On the multi-decadal scale, Phase II was shortened over time in all three zones and Phases I and III were prolonged (Table 3.2). Figure 3.4c shows the interannual time series of the three phases of W_m for the forest steppe. Phase II showed a significant ($p < 0.05$) shortening of 4 days per decade, while Phases I and III showed a significant ($p < 0.05$) lengthening of 4 and 3 days per decade, respectively. PET showed a significant increase during Phase II, particularly after 1995, as P decreased (data not shown). The combined effects of these two trends may account for the rapid shortening of Phase II during recent decades.

3.3.4 Comparison between wet and dry years

Interestingly, an interdecadal fluctuation is superimposed on the multi-decadal trend during 1961–2006 (Figure 3.4b); that is, wet conditions occurred during 1961–1975 and 1980–1995, while dry conditions occurred during 1976–1980 and 1996–2006. To examine the mechanism of W_m anomaly that occurs on an interdecadal scale and that is formed and maintained during the course of season, we analyzed wet and dry years upon the forest steppe, where the dominant trends were observed (Figure 3.4b). The wet and dry years were selected so as to be concentrated during the periods of 1980–1995 and 1996–2006, respectively, for examining interdecadal changes.

Figure 3.5 compares 10-day W_m, P, and E between years with wet and dry soils for the forest steppe zone. Based on Figure 3.4b, the wet years and dry years of the past two decades were selected to enable an interdecadal comparison between the extreme years. Phase II was longer during wet years than during dry years, whereas Phases I and III were shorter during wet years. It should be noted that differences in W_m between years with

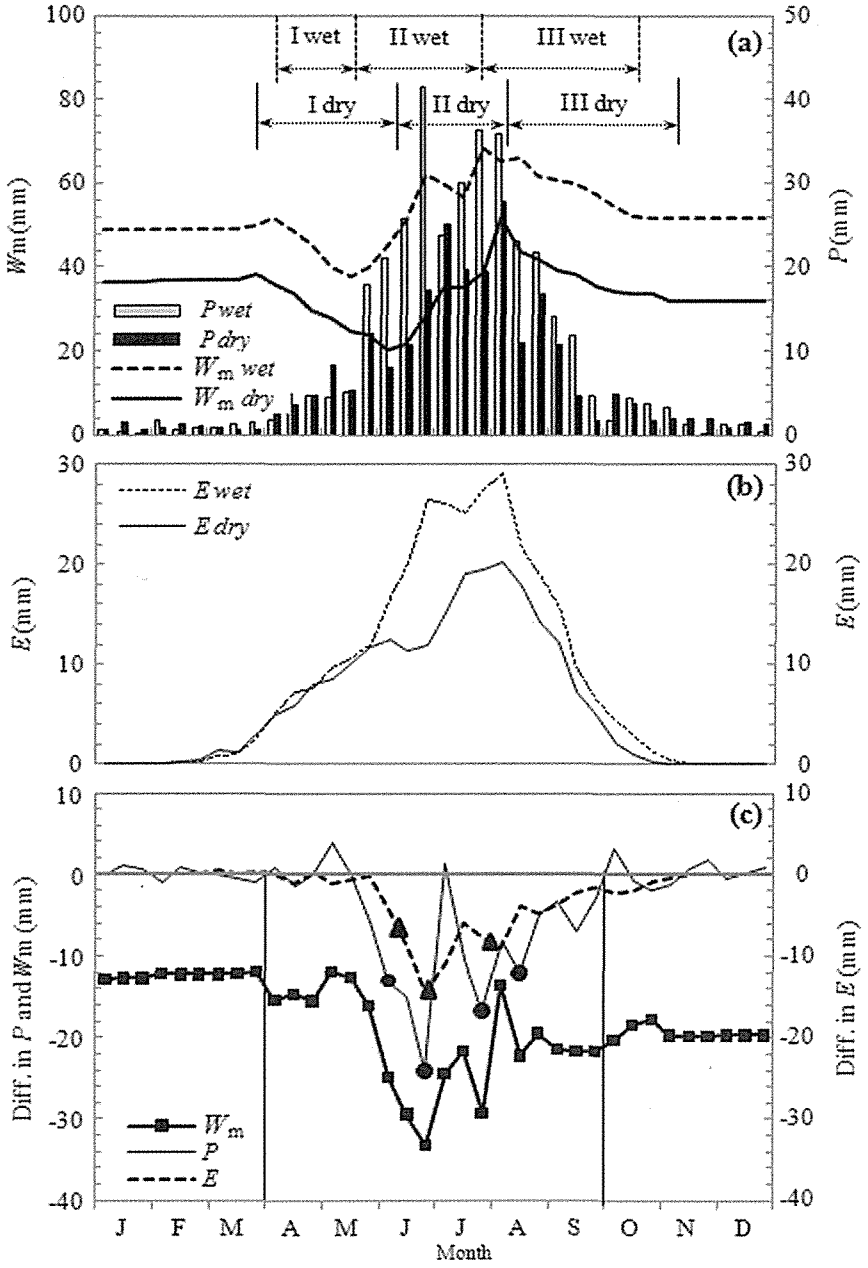

Figure 3.5 Seasonal changes in the precipitation (P), modeled soil moisture content (W_m), and actual evapotranspiration (E) (10-day data are plotted) showing three phases of soil moisture content (a and b), and comparison between the composites of 1989, 1990, 1993, and 1994 (wet soil years) and 1996, 2000, 2001, and 2002 (dry soil years) (see Figure 3.4b), as well as their differences (c). Squares, circles, and triangles indicate differences between wet and dry years in terms of W_m, P, and E, respectively, significant at 5% level.

wet and dry soils are significant throughout the year (Figure 3.5a and 3.5c). These differences were enhanced in conjunction with a significant increase in the differences between P and E during June–August. In terms of the calendar year, the last substantial difference in P occurred in mid-September, whereas the difference in W_m remained from this time until the following spring.

3.3.5 Temporal scales of soil moisture

The temporal autocorrelation function of soil moisture was employed to examine the soil moisture memory using monthly W_m anomaly time-series during 1961–2006. Figure 3.6 presented the autocorrelation functions of the W_m time series for the forest steppe zone. There are two major barriers in September and July where the interseasonal memory was interrupted. During the spring (March–May) and summer (June–August), the temporal scales are small (3 and 1.8 months), respectively, depending on a disturbance by P and PET. During the autumn (September–November) and winter (December–February), the scales are larger (6 and 7 months) due to the soil freezing (Jambaajamts, 1989) and also due to the drop in the potential evapotranspiration. This strongly suggests that W_m in the root zone retained as a memory of the P anomaly via soil freezing and as an initial moisture condition for the subsequent summer land-surface. Furthermore, a difference in W_m (between years with wet and dry soil) existed prior to the warm rainy season; this difference became more pronounced during and after the rainy season. These findings indicate that the soil moisture memory was accumulated over multiple years.

3.4 DISCUSSION AND CONCLUSIONS

In the present study, we modified an existing, simple soil-moisture model for application in cold, arid regions such as Mongolia, by considering soil freezing and snow melting. Model performance was validated by comparison with long-term observations available for Mongolia, thereby demonstrating its efficiency compared with the widely used PDSI. Moreover, the present model has an advantage in identifying abrupt changes on a shorter timescale in response to P (such as the onset of the rainy season).

We estimated daily W_m during the period of 1961–2006 for three vegetation zones: forest steppe, steppe, and desert steppe. Vegetation activity (NDVI) was more strongly

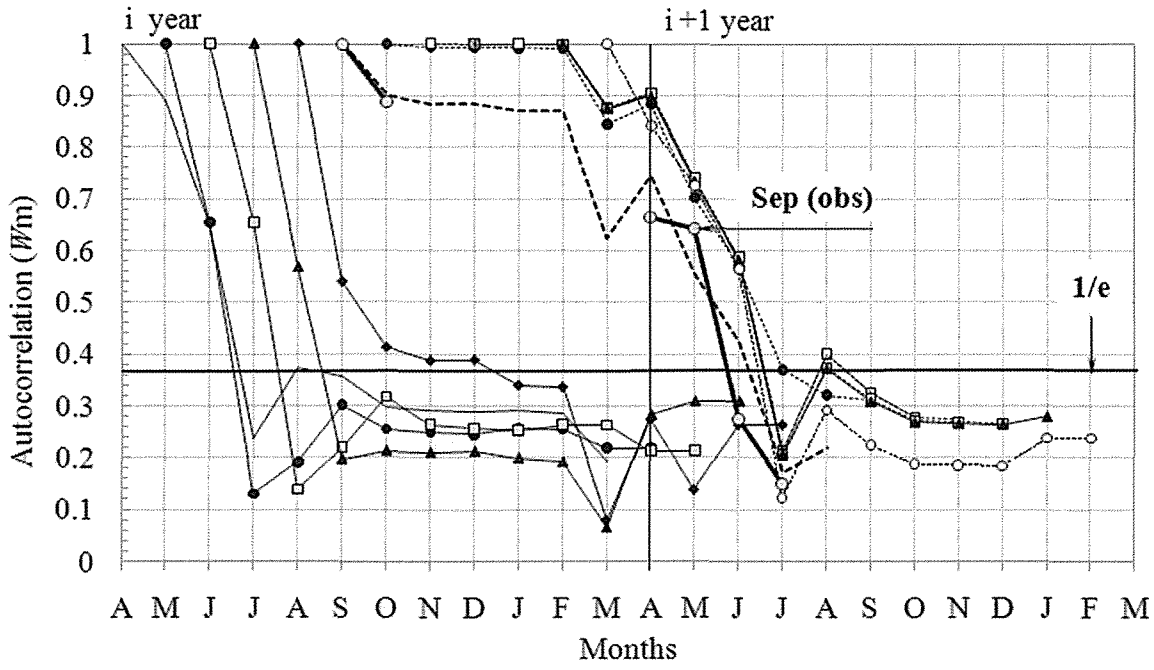

Figure 3.6 Temporal autocorrelation values of the time series of the monthly modeled soil moisture (W_m) for the forest steppe zone for each month (from April (A) to the following year March (M)).

correlated with soil moisture than with precipitation, suggesting that soil moisture plays an important and immediate role in controlling vegetation activity. For all three zones, we found a decreasing trend in W_m during 1961–2006 due to decreasing P and increasing PET; and this drying trend was only statistically significant upon the forest steppe. In conjunction with this trend, the summer phase of recharging soil moisture was shortened in all zones.

A comparison between wet and dry decades revealed that soil moisture anomalies were most manifested during June–August due to large P and E anomalies, and were subsequently maintained throughout the freezing winter until spring. Autocorrelation analysis of W_m for the forest steppe zone showed that during the autumn and winter, the soil moisture memory scales (6–7 months) are longer than during the spring and summer (3–1.8 months). These findings indicate that in cold, arid regions such as Mongolia, soil moisture retains as a memory of P anomalies during the freezing season and as an initial moisture condition for the subsequent summer land-surface.

The memory during the spring (3 months) is longer than that seen in the cold, arid region of central Eurasia, which is located at latitudes similar to the present study area, but has deeper snowpack and shallower soil freezing (Shinoda, 2001). The drying-up period after rainy season is much longer in Mongolia (6 months) than that for soil

moisture in the root zone seen in the tropical semiarid Sahel (1.5 months) (Shinoda and Yamaguchi, 2003) and the general decay timescale of 2–3 months (related to atmospheric forcing) for soil moisture in the top 1 m reported in the extratropics (Vinnikov *et al.*, 1996; Entin *et al.*, 2000). Thus, it is evident that soil freezing in Mongolia acts to prolong the timescale of soil moisture memory. In this context, further research is required on land–atmosphere interactions to explore the mechanisms by which root-zone soil moisture directly affects the multi-year persistence of drought in Mongolia (as evident in the 2000s) via soil moisture content/precipitation recycling. Furthermore, the soil moisture memory may be accompanied by a vegetation memory, as reported for this area by Shinoda *et al.* (2010). This represents another interesting topic for future study.

In terms of practical applications, the present model is a useful tool for a reliable and timely monitoring of pasture drought, thereby providing valuable information for decision-makers and herders. The advantage of this model is the use of a simple calculation that derives daily soil moisture from operationally observed daily data and its wide applicability to cold, arid regions throughout the world.

CHAPTER 4

Relationship between Soil Moisture and Vegetation Activity*

Abstract

Drought has become widespread throughout the Northern Hemisphere since the mid-1950s, affecting the Mongolian steppe and pastureland used for livestock. Given this background, we investigated the relationship between modeled root-zone soil moisture (W_m) and vegetation activity based on Normalized Difference Vegetation Index (NDVI) data for the Mongolian steppe during the period 1982–2005. In general, interannual change in NDVI coincided with that in W_m. NDVI showed a stronger correlation with W_m (r = 0.91) than with precipitation (P) (r = 0.65). A strong positive correlation was found between seasonal changes in NDVI and above-ground biomass (r = 0.94).

A comparison between years with high and low NDVI revealed that the significant difference in P led to a significant time-lagged (about a half month) difference in W_m and finally to that in NDVI with time lags of about one month. In addition, the yearly-maximum NDVI ($NDVI_{max}$) value of a given year was correlated with the W_m value for the current year (r^2 = 0.53), and was more strongly correlated with the combination of the current year W_m and the preceding year $NDVI_{max}$ of (r^2 = 0.55). This result suggests that on the interannual basis, the vegetation activity is primarily controlled by the current year soil moisture and slightly affected by underground structures stored in the root system.

*This chapter is edited version of:

Nandintsetseg B, Shinoda M, Kimura R, and Ibaraki Y. 2010. Relationship between soil moisture and vegetation activity in the Mongolian steppe. *SOLA*, **6**: 062–032.

4.1 INTRODUCTION

A strong drying trend has been observed over land areas in the Northern Hemisphere since the mid-1950s, especially over northern Eurasia, including Mongolia (Dai *et al.*, 2004). The arid continental climate in Mongolia has created an extensive area of pastureland that is the main source of forage for livestock farming, which is a major industry in the country's economy. In the Mongolian steppe, the increasing frequency of drought has led to problems in the farming of livestock and pasturing (*e.g.*, Natsagdorj, 2003). This situation motivated us to assess the temporal trend in vegetation conditions in the Mongolian steppe.

Soil moisture deficit is commonly the most important stress factor for vegetation activity, especially in arid and semi-arid regions. Soil moisture deficits limit the growth of pasture in Mongolia (Miyazaki *et al.*, 2004; Zhang *et al.*, 2005; Nakano *et al.*, 2008; Shinoda *et al.*, 2010). Previous studies have examined the relationships between seasonal and interannual climate parameters and vegetation activity, especially between precipitation and the remotely sensed Normalized Difference Vegetation Index (NDVI), which generally increases with increasing precipitation (*e.g.*, Shinoda, 1995; Suzuki *et al.*, 2003; Iwasaki, 2006). However, a limited numbers of studies have examined the relationship between soil moisture and NDVI for various vegetation types (Farrar *et al.*, 1994; Yang *et al.*, 1997; Adegoke and Carlenton, 2002; Mendez-Barroso *et al.*, 2009). Soil moisture is widely recognized as a key parameter that links precipitation and vegetation. In the present study, we investigated the effect of modeled root-zone soil moisture on vegetation activity in the Mongolian steppe, based on remotely sensed NDVI data for seasonal and interannual periods during 1982–2005.

4.2 DATA AND METHODOLOGY

4.2.1 NDVI data

We investigated seasonal and interannual variations in monthly NDVI data and assessed their relationships with root-zone soil moisture. We used a 21-year (1982–2002) monthly 1° × 1° grid of NDVI data from the semi-monthly 8-km-resolution Global Inventory Modeling and Mapping Studies dataset (GIMMS) produced by Tucker *et al.*

(2005). The GIMMS NDVI data sets were generated from the National Oceanic and Atmospheric Administration/Advanced Very High Resolution Radiometer (NOAA/AVHRR), which includes corrections for NDVI variations arising from calibration, view geometry, volcanic aerosols, and other factors unrelated to vegetation change (Pinzon, 2002; Tucker *et al.*, 2005). For the period 2003–2005, we derived monthly 1° × 1° grids of NDVI data from the semimonthly 8-km-resolution data; namely, the monthly data were composited by choosing the higher NDVI between two 15-day datasets for each month. These NDVI data are used in climate models and biogeochemical models to calculate the photosynthesis, exchange of CO_2 between the atmosphere and the land surface, land–surface evapotranspiration, and the absorption and release of energy by the land surface.

4.2.2 Observed data

We analyzed data collected at nine stations distributed widely across the Mongolian steppe, including within the major vegetation zones of forest steppe, steppe, and desert steppe (Figure 4.1). Above-ground biomass (AGB) data for the period 1986–2005 were obtained from the Institute of Meteorology and Hydrology of Mongolia (IMH). At the nine stations, AGB observations of a fenced pasture, representing the naturally occurring species above ground, were conducted on the 4th, 14th, and 24th of each month during the growing season (May–September). During these observations, the canopy height of the pasture exceeded 1 cm. The pasture AGB, which is considered an available source for livestock in this area, was not influenced by grazing.

4.2.3 Modeled data

To represent the extratropical characteristics of winter soil freezing and spring snowmelt in Mongolia, we used daily model-estimated soil moisture (W_m) data (Nandintsetseg and Shinoda, 2010a). This model is a version of the one-layer water balance model developed by Yamaguchi and Shinoda (2002) for low-latitude arid regions. This kind of water balance model has been widely used for operational monitoring of soil moisture in many regions of the world (*e.g.*, Huang *et al.*, 1996; Dai *et al.*, 2004). This model calculates absolute plant-available W_m based on precipitation (P) and air temperature (T) data with a limited number of measured soil parameters (*e.g.*, soil wilting

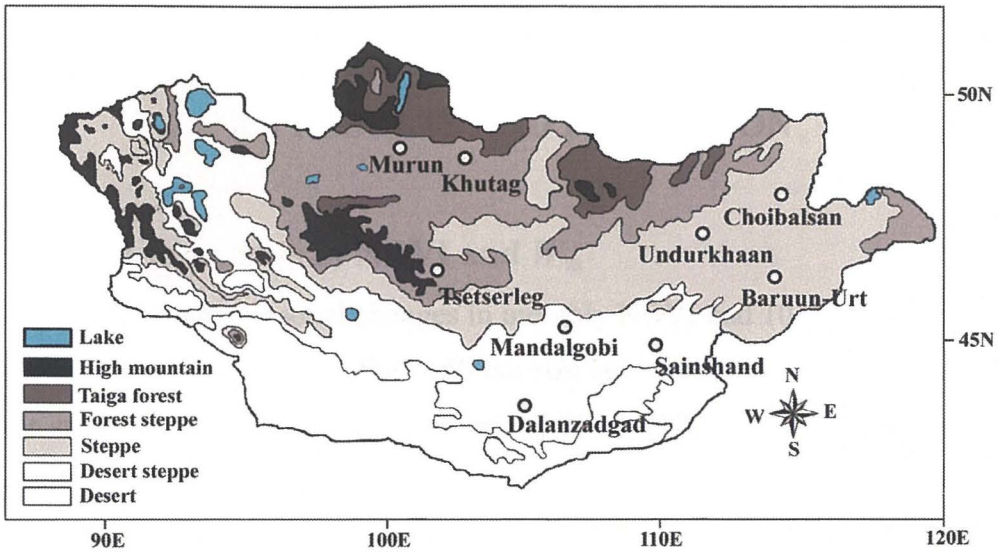

Figure 4.1 Locations of nine stations at which soil moisture was measured and vegetation zones in Mongolia.

point and field capacity). Potential evapotranspiration (PET) was calculated with the method proposed by Thornthwaite (1948).

Model performance was validated using soil moisture (10-day observations) ($r = 0.91$, $p < 0.05$) during April to October for the period 1986–2005, as measured at the nine stations (Chapters 2 and 3). The data was expressed as plant-available soil moisture (mm) in the upper 50 cm soil layer and were calculated as the actual total soil moisture minus the moisture content at the wilting point. This soil layer represents the major rooting zone of the grasses that dominate most of the Mongolian steppe. It is important to note that our aim was to explore the general relationships between vegetation activity and soil moisture at a regional scale (over the Mongolian steppe); therefore, the parameters considered in this study were averaged (P, W_m, AGB, and NDVI) over the nine stations.

4.2.4 Statistical analysis

To study interannual variations in NDVI, we considered up to five variables as parameters to explain the residuals of the temporal relationship between the current-year maximum NDVI ($NDVI_{max}$) and summer W_m (June–August). A Stepwise multiple-regression model was run by using 24-year data sets (1982–2005) of $NDVI_{max}$ and W_m (Table 4.1). The five variables, which were used in this analysis, are W_m of the current year, W_m and $NDVI_{max}$ of the first and second preceding years. At first, the current year W_m and then following the preceding year $NDVI_{max}$ during 1982–2005 were considered,

and then followed by the association effect of W_m for the first and second preceding years. Finally, we applied all five variables, including $NDVI_{max}$ of the two preceding years.

4.3 RESULTS AND DISCUSSION

4.3.1 Seasonal variations in NDVI and W_m

Figure 4.2 shows seasonal changes in monthly NDVI and 10-day AGB during the growing season, and P and W_m in the 0–50 cm soil layer averaged over the nine stations with their standard deviations during the period 1982–2005. In the previous study, we found a latitudinal gradient in W_m, with soil being drier in the southeast. This gradient is approximately consistent with the distribution of vegetation cover in the Mongolian steppe (Chapter 1). W_m and NDVI revealed a large spatial variance compared to that of P during the study period. In early spring, W_m showed a slight increase (about 5 mm) due to the spring snowmelt when daily $T > 0$°C. The timings of snow disappearance over the three zones were found within a 10-day period, likely having a minor influence on the timings of snowmelt-derived increase in W_m. The changes in W_m may have in turn affected on the vegetation activity in the Mongolian steppe. It has been reported that the beginning of plant emergence and senescence of *Stipa* spp. generally occur in early May and late September, respectively, in the Mongolian steppe (Shinoda *et al.*, 2007). In spring, during the emergence stage, NDVI increased with increasing W_m due to the snowmelt and mostly as a result of the onset of the rainy season in late May. NDVI continued to increase, reaching a peak in August, which is the plant maturity stage (and which coincides with the maximum (36 mm) in W_m). Subsequently, NDVI decreased during the senescence stage in autumn (September), matching by the decrease in W_m. After mid-October, soil moisture was assumed constant (as soil water was frozen) when the daily mean temperature was < 0°C. The dormancy season of NDVI occurs in winter (October–April). The present results reveal a strong correlation between seasonal changes in NDVI and those in AGB ($r = 0.94$, $p < 0.05$) during the growing season. Thus, NDVI was selected as a vegetation activity parameter in analyzing the relationship between soil moisture and vegetation activity. We also found a stronger correlation between NDVI and W_m ($r = 0.91$, $p < 0.05$) than between NDVI and P ($r = 0.65$, $p < 0.05$). An additional analysis showed that W_m and NDVI for each of the three zones exhibited significant correlation as mentioned above (at a regional scale).

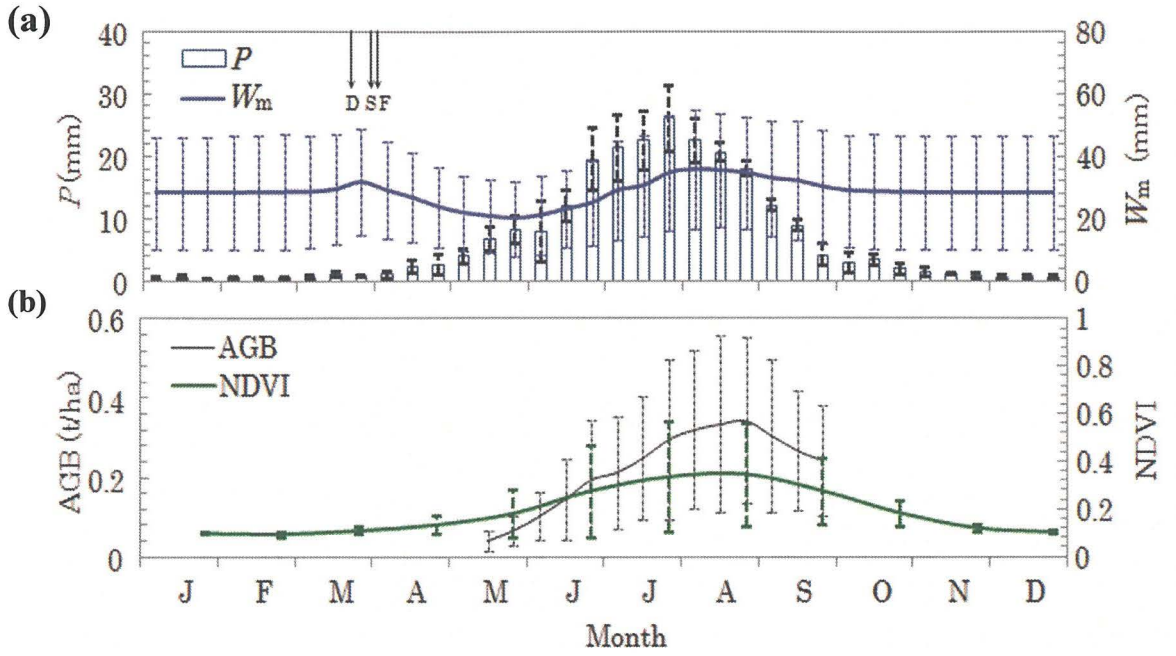

Figure 4.2 Seasonal changes in 10-day (a) precipitation (P), soil moisture (W_m), the timings of snow disappearance (vertical arrows) for the three zones (F: forest steppe, S: steppe, and D: desert steppe), and (b) 10-day above-ground biomass (AGB) and monthly NDVI averaged over nine stations with their standard deviations (vertical dashed bars) in the Mongolian steppe during 1982–2005.

4.3.2 Interannual variations in NDVI and W_m

Figure 4.3 shows the $NDVI_{max}$ and summer W_m anomalies averaged over the nine stations for the period 1982–2005. $NDVI_{max}$ showed a stronger correlation with summer (June–August) W_m ($r = 0.76$, $p < 0.05$) than with summer P ($r = 0.69$, $p < 0.05$). In general, a slight decreasing trend in $NDVI_{max}$ was found, in conjunction with the decreasing trend in W_m and it was significantly ($p < 0.05$) decreased particularly after 1995, reflecting a significant decreasing trend in W_m and an increasing trend in PET. The combined effects of these two latter trends may account for the rapid decreasing trend in $NDVI_{max}$ during recent decades. To examine the mechanism of the $NDVI_{max}$ anomaly that occurs on an interdecadal scale and that is formed and maintained during the course of the year, we analyzed years with high and low $NDVI_{max}$ values over the Mongolian steppe (Figure 4.3). Figure 4.4 shows 10-day W_m, P, and monthly NDVI for years characterized by high and low $NDVI_{max}$ values.

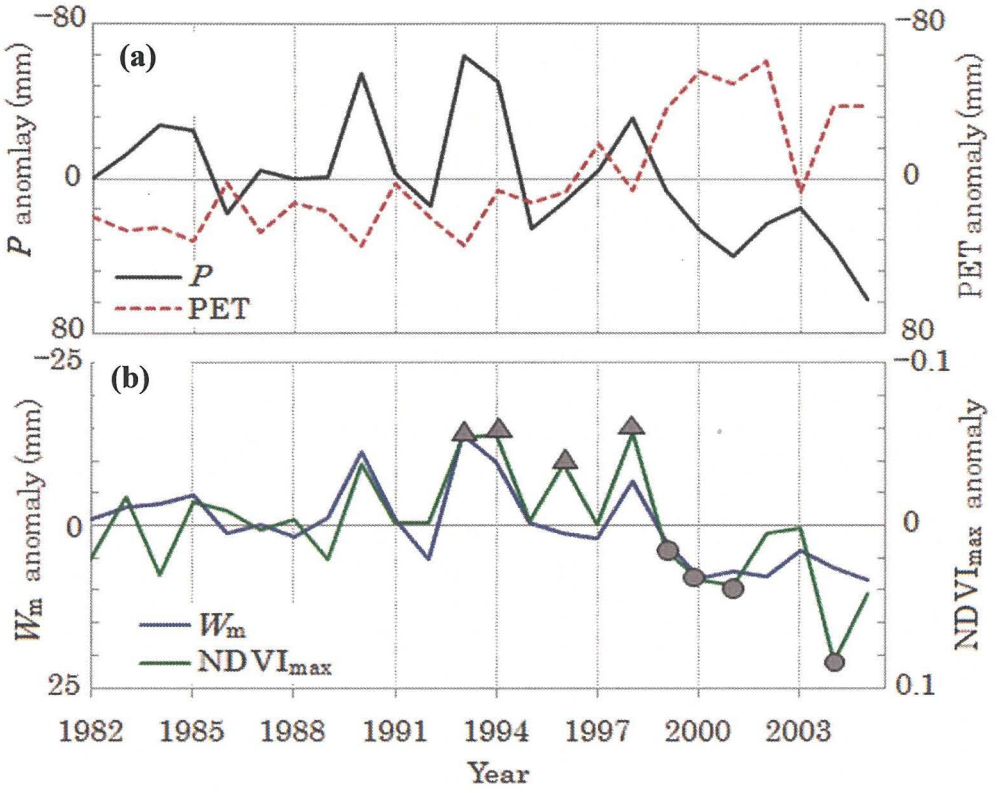

Figure 4.3 Interannual (1982–2005) anomalies (a) of precipitation (P), potential evapotranspiration (PET), and (b) soil moisture (W_m) for the period June–August, and maximum NDVI ($NDVI_{max}$) averaged over nine stations in the Mongolian steppe (values are in reverse order). Triangles and circles indicate years with high and low values of $NDVI_{max}$, respectively.

Based on Figure 4.3, two composites for years with high and low $NDVI_{max}$ over the past two decades were selected for an interdecadal comparison of extreme years. As shown in Figure 4.4, seasonal changes in NDVI consistently followed those in W_m during years with both high and low $NDVI_{max}$ values. We found no significant difference between high and low $NDVI_{max}$ years in terms of NDVI during the early growth period (May–June). However, a clear difference in NDVI was observed in July, reflecting a difference in W_m; differences between the two composites are observed in August and September. These differences resulted from the leading significant differences in P and W_m from July to August. This result shows that the significant difference in P led to a time-lagged (about a half month) significant difference in W_m, finally to that in NDVI with time lags of approximately one month. The substantial difference in W_m, which occurred in September, was maintained during winter. This indicates that W_m acted as a memory of the P anomaly via soil freezing and as an initial moisture condition for vegetation activity in the subsequent year.

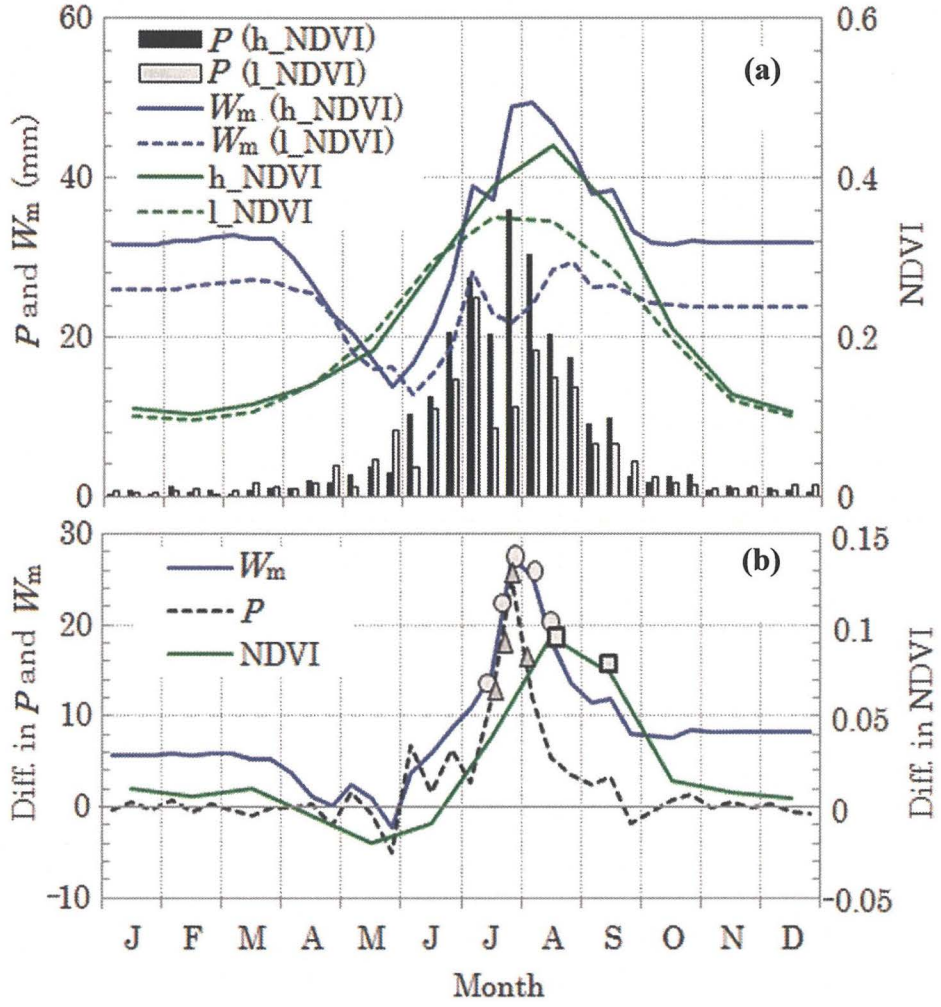

Figure 4.4 Seasonal changes in 10-day (a) precipitation (P), modeled soil moisture (W_m), and monthly NDVI, comparing the composites for 1993, 1994, 1996, and 1998 (h-NDVI is high-$NDVI_{max}$ years) with those for 1999, 2000, 2001, and 2004 (l_NDVI is low-$NDVI_{max}$ years) (Figure 4.3), (b) as well as their differences. Triangles, circles, and squares indicate differences between high- and low-$NDVI_{max}$ years in terms of P, W_m, and NDVI, respectively, significant at the 5% level.

4.3.3 A Stepwise multiple-regression modeling

To gain a better understanding of interannual variations in $NDVI_{max}$, we proposed five parameters; W_m of the current, the first and second preceding years, and $NDVI_{max}$ of the first and second preceding years as predictive variables during 1982–2005 (Table 4.1). The coefficient (r^2) of determination for $NDVI_{max}$ with W_m of the current year was 0.53. The addition of $NDVI_{max}$ for the first preceding year resulted in a slight increase in the proportion of explained variance, from 0.53 to 0.55 with the same level of statistical

Table 4.1 Models that account for interannual variation in current-year maximum NDVI for the Mongolian steppe. The rows correspond to stepwise multiple regressions with different sets of variables during 1982–2005. W_m indicates soil moisture during June–August; N is yearly-maximum NDVI. The models include variables with a significant effect, in which (t), (t–1), and (t–2) indicate the current, first, and second preceding years, respectively.

n	Possible variables	Model	r^2	p
1	$W_{m\,(t)}$	$N_{(t)}=.27 + .004\ W_{m(t)}$	0.53	<0.001
2	$W_{m\,(t)}$, $N_{(t-1)}$	$N_{(t)}=.3 + .004W_{m(t)}+.06N_{(t-1)}$	0.55	<0.001
3	$W_{m\,(t)}$, $W_{m\,(t-1)}$, $W_{m\,(t-2)}$,	$N_{(t)}=.26+ .004W_{m(t)}+.0003W_{m(t-1)}+$ $+.0009W_{m(t-2)}$	0.57	<0.005
4	$W_{m\,(t)}$, $W_{m\,(t-1)}$, $N_{(t-1)}$, $W_{m\,(t-2)}$, $N_{(t-2)}$	$N_{(t)}=.23+.004W_{m(t)}+.0004W_{m(t-1)}+$ $+.14N_{(t-1)}+.0002W_{m(t-2)}+.19\ N_{(t-2)}$	0.60	<0.008

significance ($p < 0.001$), whereas an addition of the other variables resulted in a reduction of the significance level.

4.4 CONCLUSIONS

We investigated the relationship between modeled root-zone soil moisture and vegetation activity based on remotely sensed NDVI data, focusing on the Mongolian steppe during 1982–2005. On both seasonal and interannual time-scales, NDVI was more strongly correlated with soil moisture than with precipitation, suggesting that soil moisture plays an important and immediate role in controlling vegetation activity. This result is consistent with the findings of Yang *et al.* (1997), Adegoke and Carlenton (2002), and Mendez-Barroso *et al.* (2009).

A comparison between years with high and low NDVI revealed that a significant difference in P led to a half-monthly time-lagged significant difference in W_m, finally a difference in vegetation activity, with time lags of about one month. Soil moisture anomalies were maintained throughout the following freezing winter. This implies that soil moisture acted as a memory via soil freezing and as an initial soil moisture condition

for the vegetation activity in the subsequent year. This coincides with the results of Shinoda. (2005).

Interannual fluctuations in NDVI were strongly dependent on W_m of the current year and even more strongly dependent on a combination of the current year W_m and NDVI of the preceding year. This result suggests that vegetation anomalies were likely stored as underground structures in the root system. To the best of our knowledge, this is the first study in Mongolia to point to the combination of soil moisture and root memories as predictor of vegetation. Several previous studies have reported that the current and preceding year's precipitation have a strong influence on NDVI of the current year in Africa (Martiny *et al.*, 2009) and North America (Wang *et al.*, 2003). Iwasaki (2006) examined the potential of predicting NDVI using the leading winter and spring precipitation and air temperature in Mongolia, revealing that NDVI is influenced by June precipitation with the additional influence of December precipitation. This relationship can be explained by the status of soil moisture content in the root zone as described in our study.

NDVI for a given year showed a weak dependence on the preceding year's NDVI. Shinoda *et al.* (2010) reported that in the Mongolian steppe, manipulated soil moisture deficit resulted in a marked reduction in above-ground phytomass but did not substantially affect below-ground phytomass (which was several times greater than above-ground phytomass). The effect of snow mass memory as seen in Central Eurasia (Shinoda, 2001), was not dominant in Mongolia, because the yearly-maximum snow depth is only 3.4 cm in this region (Morinaga *et al.*, 2003). Therefore, it is likely that the large root system provided a basis for rapid recovery of above-ground phytomass, leading to a weak carry-over of vegetation anomalies, as revealed by NDVI in the present analysis. In future applications, the concepts of soil moisture and root memory presented in the present study would provide a useful basis for an early warning system of reduced pasture production during drought.

CHAPTER 5

Soil Moisture and Vegetation Memories*

Abstract

Continental climate is established as a result of a complex interplay between the atmosphere and various land-surface systems such as the biosphere, soil, hydrosphere, and cryosphere. These systems function as climate memory, allowing the maintenance of interannual atmospheric anomalies. In this paper, we present new observational evidence of an interseasonal moisture memory mechanism mediated by the land surface that is manifested in the coupled cold and arid climate of Mongolia. Interannual anomalies of soil moisture and vegetation due to rainfall during a given summer are maintained through the freezing winter months to the spring, acting as an initial condition for subsequent summer land-surface and rainfall conditions. The cold-season climate with low evapotranspiration and strong soil freezing acts to prolong the decay time scale of autumn soil moisture anomalies to 7.6 months that is among the longest in the world. The vegetation also has a memory of the similar time scale, likely because the large root system of the perennial plants dominant in the Mongolian steppe may remain alive and retain under-ground biomass anomalies during the winter.

*This chapter is edited version of:
Shinoda M and Nandintsesteg B. 2010. Moisture and Vegetation Memories in a Cold, Arid Climate. Submitted to the *Journal of Geophysical Research, Atmospheres*.

5.1 INTRODUCTION

Across the world's widest continent, Eurasia, especially at middle-to-high latitudes, soil moisture acts as an efficient memory storage device for interannual precipitation anomalies due to its low potential evapotranspiration (Delworth and Manabe, 1988; Vinnikov and Yeserkepova, 1991). The interseasonally persistent hydrological effects of melted snow, simulated in general circulation models (e.g., Barnett et al., 1989; Yasunari et al., 1991), has also been considered as a potential memory mechanism and explains the apparent correlation between Eurasian snow cover and subsequent Indian summer monsoon rainfall (e.g., Hahn and Shukla, 1976). On the other hand, subsequent observational studies have shown that the hydrological effect of melted snow is limited in region and season (Shinoda, 2001; Shinoda *et al.*, 2001; Ueda *et al.*, 2003; Iijima *et al.*, 2007). Mongolia is located over mid-latitude highlands in the far eastern continent and has a cold, arid climate with soil freezing and small snowpack in the winter (Shinoda and Morinaga, 2005; Morinaga *et al.*, 2003). These climate conditions are considered to have a specific impact on the soil moisture memory that is highlighted in the present study.

A large drying trend has been observed in a soil moisture index over land areas in the Northern Hemisphere since the middle 1950s, especially over northern Africa, Canada, Alaska, and Eurasia, including Mongolia (Dai *et al.*, 2004). In particular, below-normal precipitation in the Northern Hemisphere during 1999–2002 appears to have led to extensive decreases in vegetation activity over Eurasia and North America as revealed by the satellite-estimated Normalized Difference Vegetation Index (NDVI) (Lotsch *et al.*, 2005). These facts strongly suggest that soil moisture acts as a bridge between deficits in precipitation (meteorological drought) and failures of plant growth (agricultural or vegetation drought). In fact, this phenomenon has recently been explored for Mongolia that is highlighted here (e.g., Shinoda *et al.*, 2007; Nandintsetseg *et al.*, 2010).

Historical records of soil moisture content measured in situ are available for few regions in the world and often represent very short periods (Robock *et al.*, 2000); however, a unique long-term, quality-controlled dataset has recently been established for Mongolia (Nandintsetseg and Shinoda, 2010a). Given this background, we focused on this area to explore the processes of how the interseasonal moisture memory operates in the soil-vegetation system under such markedly drying climate conditions.

5.2 DATA AND METHODS

5.2.1 Observed soil moisture

The soil moisture (W) dataset used in this paper was obtained from that produced by Nandintsetseg and Shinoda (2010a), so-called the Mongolian Soil Moisture Climatology Dataset and the original data were derived from the Institute of Meteorology and Hydrology of Mongolia (IMH). The dataset has 26 stations in grass-covered fields over Mongolia for the entire period of 1986–2005, while the periods of available soil moisture data differed from station to station. To study natural conditions of soil moisture on a consistent basis, only data collected at grass-covered field sites were included in the dataset. In general, the dominant soil texture in the top 50-cm layer at the selected stations was sandy.

At all stations, soil moisture observations were conducted on the 8, 18, and 28 of each month during the warm season (April–October) using the gravimetric method. Soil moisture was not measured in winter (November–March) as the soil was frozen. Soil moisture was measured in 11 vertical layers; 5-cm layers from 0 to 10 cm and 10-cm layers from 10 to 100 cm. Most of the stations had no observations beneath 50 cm depth, and thus only data for the 0–50 cm soil layer were included in the dataset. This soil layer includes the major rooting zone of the grasses that dominate most of the Mongolian steppe. The data are expressed as plant-available soil moisture (mm) in the upper 0–50 cm soil layer and were calculated as the actual total soil moisture minus the moisture content at the wilting point. We also used data of soil hydraulic properties such as wilting point (W_{wp}) and field capacity (W_{fc}) from the IMH. In addition, precipitation (P), air temperature (T), and snow depth (SD) data for the 26 stations from IMH were used to investigate the soil moisture dynamics. In the following analysis, the monthly anomalies were defined as the deviations from the corresponding monthly values averaged over the period from 1986 to 2005.

At the Underkhaan station in eastern Mongolia, special observations of soil moisture as well as soil temperature (T_g) were also carried out at the depths of 20, 50, 100, and 150 cm on an hourly interval from September 2002 to June 2006 by the time-domain reflectometry (TDR) method. This provided a source for a detailed analysis of the soil moisture memory.

5.2.2 Modeled soil moisture

To fill in gaps of the soil moisture observations during the winter, we used daily model-estimated soil moisture (W_m) data (Chapter 2). This model is a version of the one-layer water balance model developed by Yamaguchi and Shinoda (2002) for low-latitude arid regions and it was modified to represent the extratropical characteristics of winter soil freezing and spring snowmelt in Mongolia (Chapters 1 and 2). This kind of water balance model has been widely used for operational monitoring or climate change studies of soil moisture in many regions of the world (*e.g.*, Huang *et al.*, 1996; Shinoda and Yamaguchi, 2003, Dai *et al.*, 2004). In accordance with the observed data (W_o), this model calculates absolute plant-available W_m based on precipitation (P) and air temperature (T) data in the upper 50 cm soil layer with a limited number of measured soil parameters (*e.g.*, soil wilting point and field capacity).

5.2.3 NDVI data

We used a 21-year (1982–2002) monthly 1° × 1° grid of NDVI data from the bimonthly 8-km-resolution Global Inventory Modeling and Mapping Studies dataset (GIMMS) produced by Tucker *et al.* (2005). The GIMMS NDVI data sets were generated from the National Oceanic and Atmospheric Administration/Advanced Very High Resolution Radiometer (NOAA/AVHRR), which includes corrections for NDVI variations arising from calibration, view geometry, volcanic aerosols, and other factors unrelated to vegetation change (Pinzon, 2002; Tucker *et al.*, 2005). For the period 2003–2005, we derived monthly 1° × 1° grids of NDVI data from the semimonthly 8-km-resolution data; namely, the monthly data were composited by choosing the higher NDVI between two 15-day datasets for each month.

5.3 RESULTS AND DISCCUSSION

5.3.1 Climatological patterns

Figure 5.1 illustrates the climatological patterns of important hydrometeorological elements in Mongolia. In general, the annual P ranges from over 400 mm in the northern mountains to below 100 mm in the south (Batima and Dagvadorj, 2000), and is concentrated in the summer months from June to September (Figure 5.1b). Thus, the winter P comprises only a small portion of the annual total. The monthly T falls below

0°C from November to March. Thus, the snow depth during January, when the yearly maximum SD value is observed over most of Mongolia, ranges from over 100 mm in the northern mountains to below 10 mm in the south (Morinaga *et al.*, 2003). During the late summer and spring, W in the top 50-cm-deep layer and the NDVI both exhibit south-southwestward decreasing patterns (Figures 6.1c and 1d), similar to that observed for summer P. The absolute level of W is also the same between the two seasons, but that of the NVDI is reduced substantially in the spring, due to the beginning of the growing season (data not shown).

5.3.2 Correlation patterns

The correlations among major hydrometeorological elements were examined in a time series from the summer of one year to that of the following year (Figure 5.2). Significant correlations between summer (June–September) P ($P_{6\text{-}9}$) and time-lagged (August–September) W ($W_{8\text{-}9}$) anomalies are widespread in zones throughout the northern latitudes of Mongolia, including Underkhaan (Figure 5.2a). The period from August to September was chosen because W for this period was most highly correlated with P for the entire rainy season (June–September). Interestingly, over the central zone, the $W_{8\text{-}9}$ anomaly was most highly correlated with anomalies in spring (April–May) W ($W_{4\text{-}5}$) in the following year (Figure 5.2b). Over the entire region of Mongolia (including Underkhaan) except for its northern periphery, significant correlations were found between June–July P ($P_{6\text{-}8}$) and September NDVI ($NDVI_9$) (Figure 5.2c). A complicated pattern with a maximum axis in the latitudes near 47-49°N (including Underkhaan) is seen in the correlation between $NDVI_9$ in one year and $NDVI_5$ in the subsequent year (Figure 5.2d), although in general, positive correlations are widespread over Mongolia. The complicity manifested in the west may be owing to the existence of the Khangai and Altai Mountains in the area (Figure 5.1a) which affect climate and thus vegetation activity. It should be noted that the zone near Underkhaan exhibits high correlations in both W and NDVI between the late summer or autumn and the corresponding values in the following spring; however, SD for January has no significant correlation with the subsequent $W_{4\text{-}5}$ anomaly in Mongolia (not shown), due to low SD levels (Morinaga *et al.*, 2003). This is not the case for central Eurasia, where the yearly maximum snow depth results in sufficient melting to influence the spring W (Shinoda, 2001).

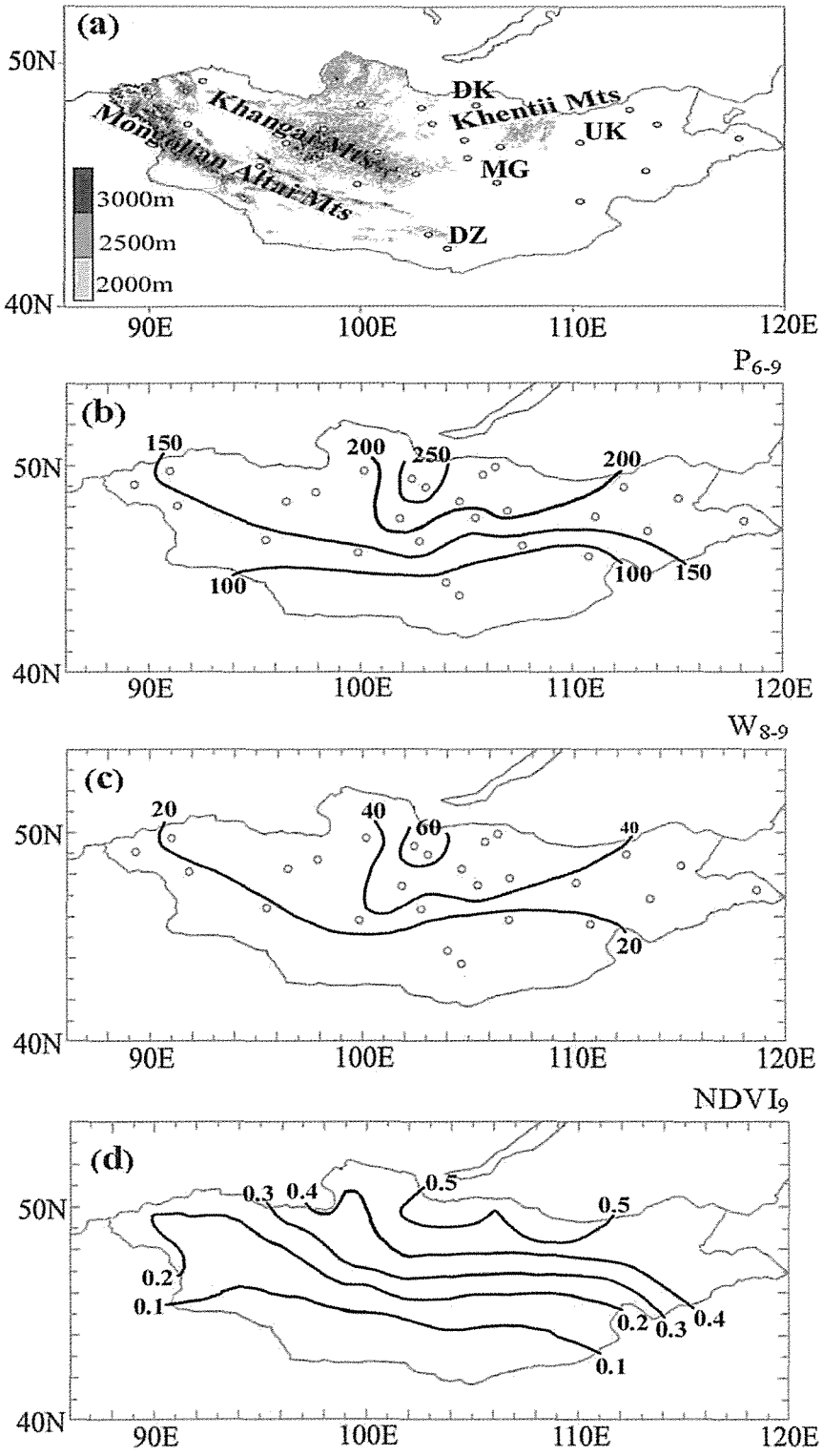

Figure 5.1 (a) Topography and climatological patterns of the following parameters: (b) summer (June–September) P (mm/month) ($P_{6\text{-}9}$); (c) late summer (August–September) W in the top 50cm-deep layer (mm) ($W_{8\text{-}9}$); and (d) NOAA-derived NDVI for the autumn (September) ($NDVI_9$). Climatological values are averaged over the period from 1986 to 2005. UB and UK indicate the locations of Ulaanbaatar and Underkhaan, respectively. The circles indicate the observational stations.

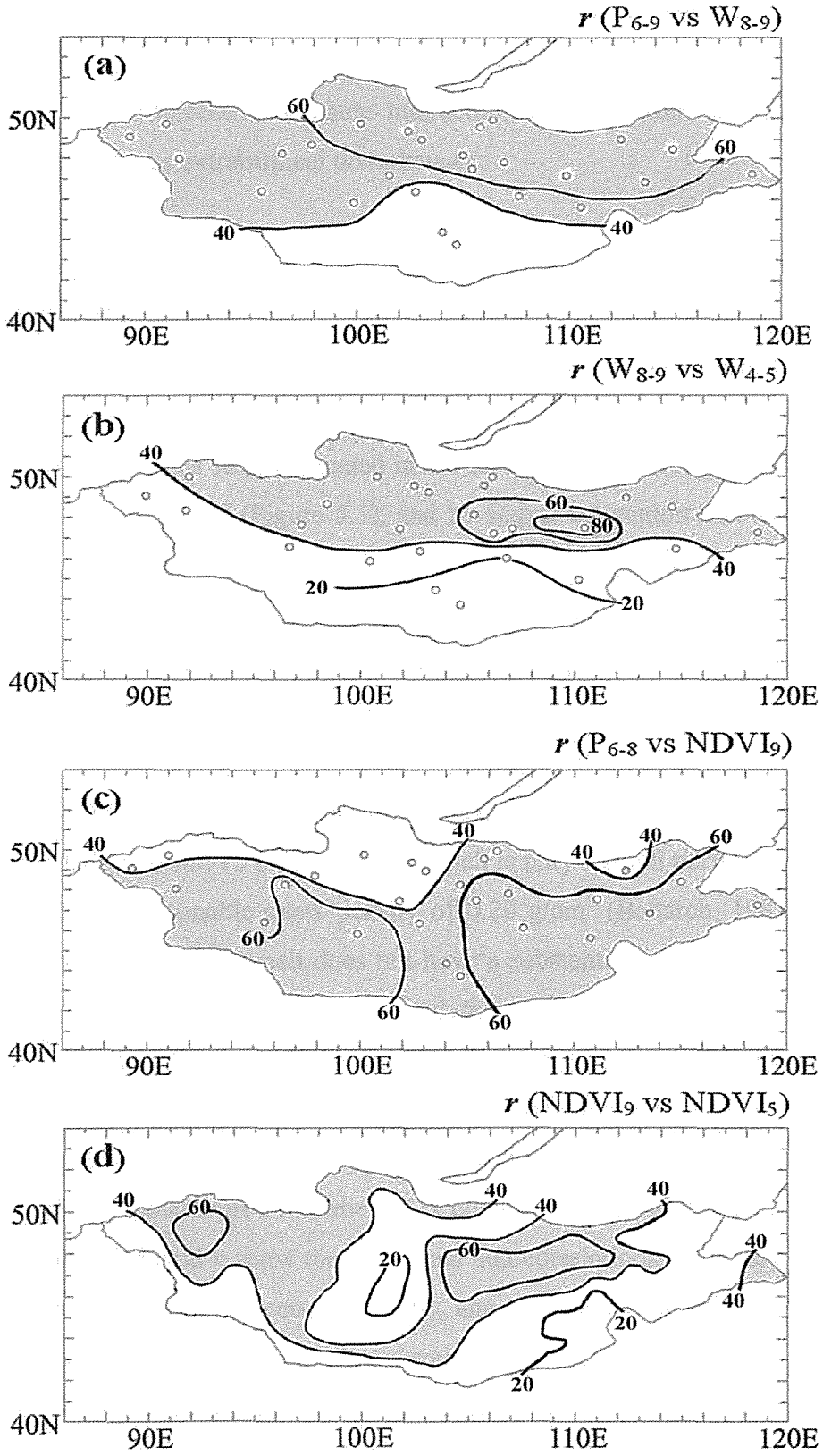

Figure 5.2 Maps of the following correlations: (a) between the $P_{6\text{-}9}$ and $W_{8\text{-}9}$ anomalies for the same year; (b) between the $W_{8\text{-}9}$ anomaly for one year and the $W_{4\text{-}5}$ anomaly for the following year; (c) between the $P_{6\text{-}8}$ and $NDVI_9$ anomalies for the same year; and (d) between the $NDVI_9$ anomaly for one year and the $NDVI_5$ anomaly for the following year. The correlation coefficients are expressed as values multiplied by 100. Stippling indicates values exceeding 40 at the 5 % significance level.

In general, $W_{4\text{-}5}$ is positively but weakly correlated with anomalies of P in the following June of the same year (P_6) (data not shown). This suggests that the P_6 anomaly may result not only from land-surface/atmosphere interaction, but also from external atmospheric forcing events, such as extratropical disturbances.

5.2.3 Autocorrelations

Based on the patterns observed in Figure 5.2, the Underkhaan station was selected for the following time series analysis, because it exhibits pronounced persistence in W and NDVI memory. This station, located in the eastern area of Mongolia, is characterized by relatively high P and W (Figure 5.1), and by steppe vegetation and brown sandy soil (Nandintsetseg and Shinoda, 2010). Figure 5.3a illustrates the seasonal changes in W_o, NDVI, and SD for Underkhaan. On a climatological basis, the W level is at a yearly maximum during the summer months, from July to August, due to the water budget that P is larger than evapotranspiration during the preceding months (Chapter 1). The April W is only slightly higher than that of October, implying the addition of snowmelt water. In addition to this, the SD reaches a yearly maximum of only 77 mm during February. This corresponds to about 15 mm of water, which is only a small portion of the normal W level, assuming a reasonable snow density of 0.20 g/cm^3 (Badarch, 1987). These facts indicate that the spring snowmelt does not have a substantial influence on the spring W due to the small amount of snowpack accumulation.

As mentioned in Section 5.2, we mainly used the modeled soil moisture instead of the observed one to fill in the gaps during the soil freezing winter months (November–March). W_m is constant during the winter because there is no addition of snowmelt water and negligible evapotranspiration when T is equal to or below 0°C as assumed in the model. Figures 5.3b and c show the individual autocorrelations of W_m and NDVI values for Underkhaan. It is clearly seen that the W_m anomaly once established in September or later is maintained until May. Similar correlations are found for the W_o, although no observation is available in the winter. In general, there are two barriers of the soil moisture memory between August and September and between June and July of the following year. On the other hand, the autocorrelation of NDVI from September (also from October) drops abruptly during the winter (Figure 5.3b), probably because snow

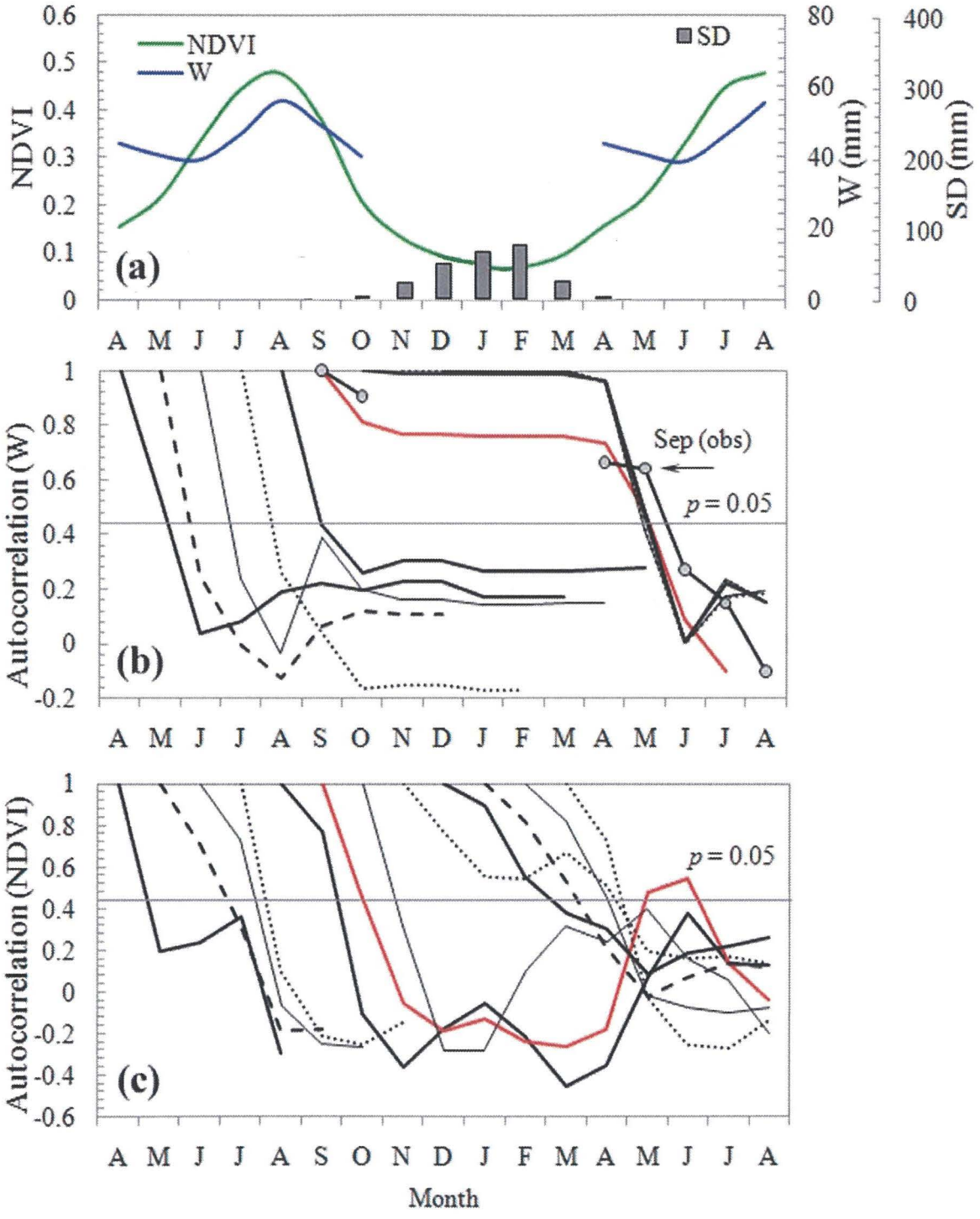

Figure 5.3 (a) Climatological (1986-2005) seasonal changes in W_o, NDVI, and SD for Underkhaan and autocorrelations of (a) W_o (only for the reference of September, circle) and W_m, and (b) NDVI using each month as references. The red line indicates autocorrelations of W_m with the reference of September. The horizontal thin lines in Figures. 5.3b and 3c denote the 5% significance level.

cover masks the anomalies (Figure 5.3a). Thus, we call this hidden memory. Then, the autocorrelation recovers during May and June of the following year, namely, the onset of the growing season, in conjunction with the snow disappearance. Such persistence was not found for the autocorrelations with references starting from October to March, likely because the NDVI reflects characteristics of snow cover without such persistence. In general, there is a barrier of the NDVI memory between July and August. In brief, the NDVI memory over the winter months suggests that the large root system of the perennial plants dominant in the Mongolian steppe may remain alive and retain as a memory of under-ground biomass anomalies under the thin snow cover and in the frozen soil, as reported by Shinoda *et al.* (2010a).

5.2.4 Comparison between wet and dry years

Figure 5.4 illustrates the year-to-year (1986-2005) time series of $W_{8\text{-}9}$ (mm) and $NDVI_9$ for Underkhaan station selected the four wettest (1987/1993/1998/2003) and driest (1988/1989/1991/2004) soil years during the observational period for a composite analysis (Figure 5.5). Water balance with a larger summer P, along with a lower summer T, namely, a possible lower E (Figure 5a), led to a higher autumn W value (Figure 5.5b and 5c), whereas a smaller summer P (Figure 5.5a) corresponded to a lower autumn W (Figure 5.5b). These W differences of the same sign were transferred from the autumn to the spring; a similar transfer was observed as an NDVI difference (Figure 5.5c). A comparison between the wet and dry composites indicates that the growth of perennial grasses (predominant in the steppe region) is substantially influenced by the amount of root-zone, plant-available soil water during the summer growing season. The above-ground biomass produced then may be transferred to underground structures in the root system during the autumn and winter, providing an initial condition for the following spring plant growth. The effect of T on the NDVI appears to be negligibly small during the initial growing season (April–May) (Figure 5.5a). Interestingly, the W_4 and $NDVI_5$ anomalies preceded P_6 anomaly in the second year, implying that the P_6 anomaly may result from land-surface/atmosphere interaction. Note that the differences (that is, anomalies) in W and NDVI persisted from the growing period through the decaying

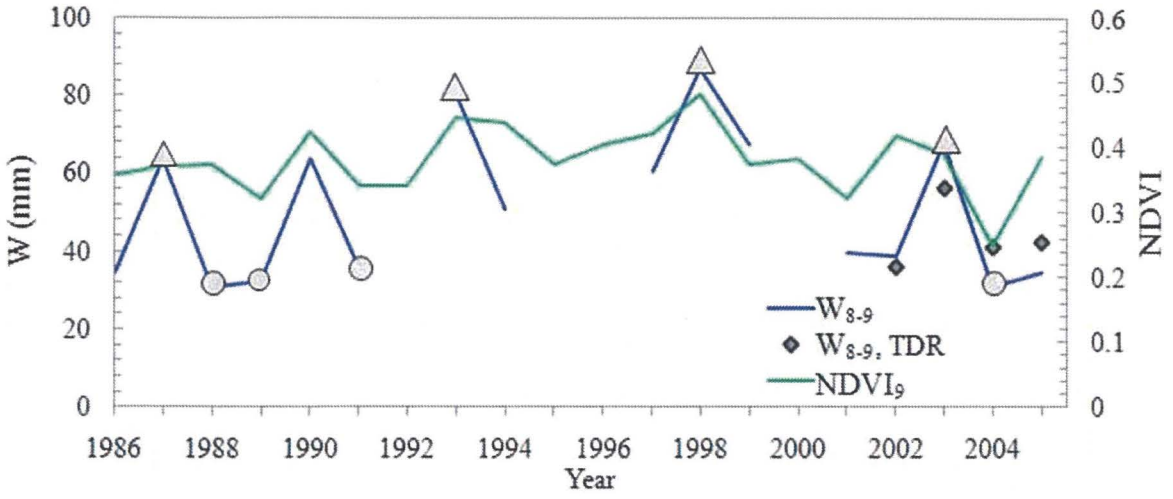

Figure 5.4 Interannual (1986-2005) time series of $W_{8\text{-}9}$ by the gravimetric and TDR methods (mm), and $NDVI_9$ for Underkhaan. Triangles and circles indicate years with three highest and lowest values of $W_{8\text{-}9}$ used for the composite analysis in Figure 5.5, respectively.

period nearly for a year. However, the sign of the anomaly was switched to the opposite in August. This mechanism remains unsolved.

The detailed W observations indicated that the levels in the springs for both the dry and wet soil years were almost the same as those in the corresponding antecedent autumns (Figure 5.6). The T_g at the 20cm depth for the winter months (November–March) was below 0°C (W not shown during this period in Figure 5.6), indicating soil freezing to this depth (even reaching a depth of 150 cm; not shown). These results strongly suggest that the wintertime carryover of W anomalies was owing to the freezing of soil water. In addition, because of the small amount of snow accumulation, the spring snowmelt was small and did not have even a small impact on the W level at the 20 cm depth (and below this) just after the snowmelt (Figure 5.6). This combination of winter soil freezing and small snow depth resulted in a strong linkage between the autumn and spring W anomalies (Figures 5.2b and 5.3b).

In contrast, the southern drier region did not show such a significant relationship. This is likely due to smaller P and W levels (Figures 5.1b and 1c, Figures 5.7b and 7c) and thus smaller their anomalies; that is, the $W_{8\text{-}9}$ level is near W_{wp}, below which it cannot fall at Mandalgovi and Dalanzadgad (desert steppe, Figure 5.7a). Also, at Darkhan (steppe), $W_{8\text{-}9}$ is relatively small, compared with Underkhaan and lowest Ws tend to bottom out at the W_{wp} level (see the range of $W_{8\text{-}9} \pm \sigma$ in Figure 5.7c); thus lower-than-

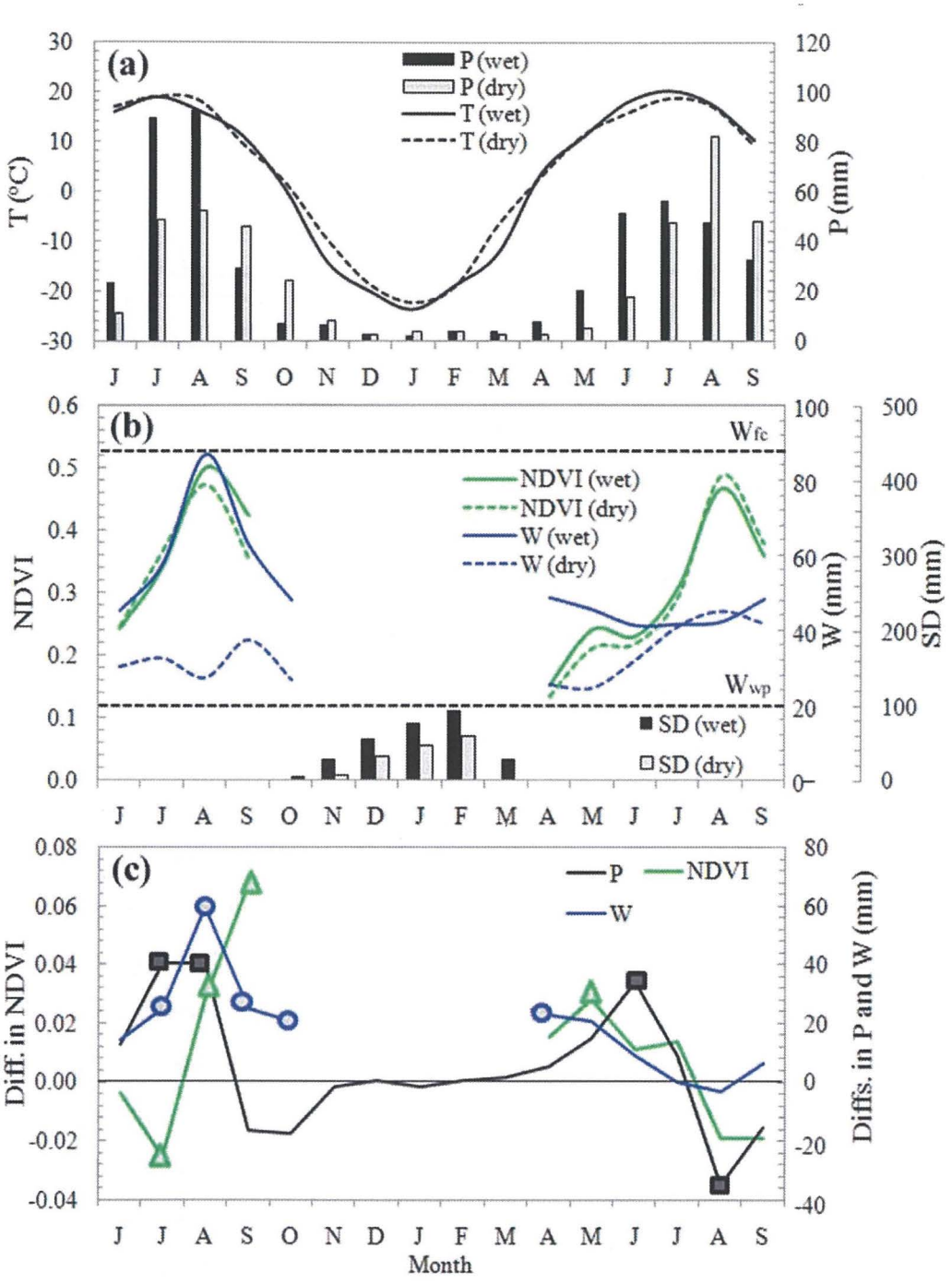

Figure 5.5 Seasonal changes in monthly (a) T and P, (b) W_o, NDVI, and SD for Underkhaan; comparisons between the four years with the largest (1987/1993/1998/2003) and smallest (1988/1989/1991/2004) $W_{8\text{-}9}$ values and (c) their differences. Squares, circles, and triangles indicate differences between the wet and dry years in terms of P, W_o, and NDVI, respectively, significant at 5% level. The horizontal dashed lines in Figure 5.5b are W_{fc} and W_{wp} (Chapter 1).

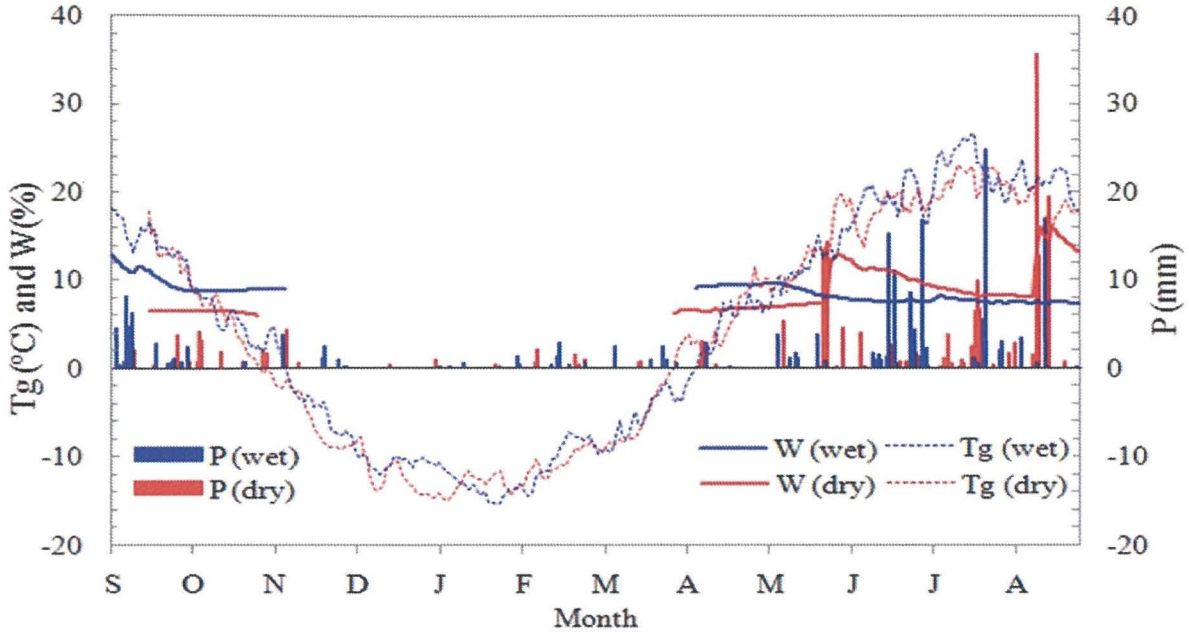

Figure 5.6 Seasonal changes in daily P, W, and T_g at the 20 cm depth for Underkhaan; comparisons between the wet (2003/04, blue) and dry (2002/03, red) soil years. W is not shown when $T_g < 0^{\circ}C$.

normal anomalies tend to be weakened. On the other hand, at Underkhaan (steppe), $W_{8\text{-}9}$ reveals a value near the center in the range between W_{wp} and W_{fc}; thus, both the lower- and higher-than-normal anomalies tend to remain. The larger W_f was established under the relatively well developed vegetation (as revealed by NDVI; Figure 5.7d). Furthermore, deeper (probably longer) soil freezing at this station is considered to allow W anomalies maintained for a longer period (Figure 5.7e). In this context, the W and NDVI anomalies of the same sign persisted through the spring, even until June (Figures 5.2b, 2d, and 5.5b), although the sign of the anomalies were switched to the opposite in August due to P anomalies of the opposite sign (Figure 5.5b).

Figure 5.8 depicts the correlations among the summer P, late summer W (or NDVI), and following spring W (or NDVI) for three Steppe stations which exhibited the marked land-surface memory. This shows that the P forcing effectively led to land-surface (i.e., W and NDVI) anomalies of the same sign and the anomalies acted as an interseasonal memory, whereas the feedback from the land-surface anomalies to summer P is too weak to produce a persistent moisture anomaly in the atmosphere-land surface system. These results strongly suggest that the summer P anomalies tend to be determined substantially by the stochastic process of rain-bearing disturbances that are activated over this area during the summer, but not by the feedback from the land-surface.

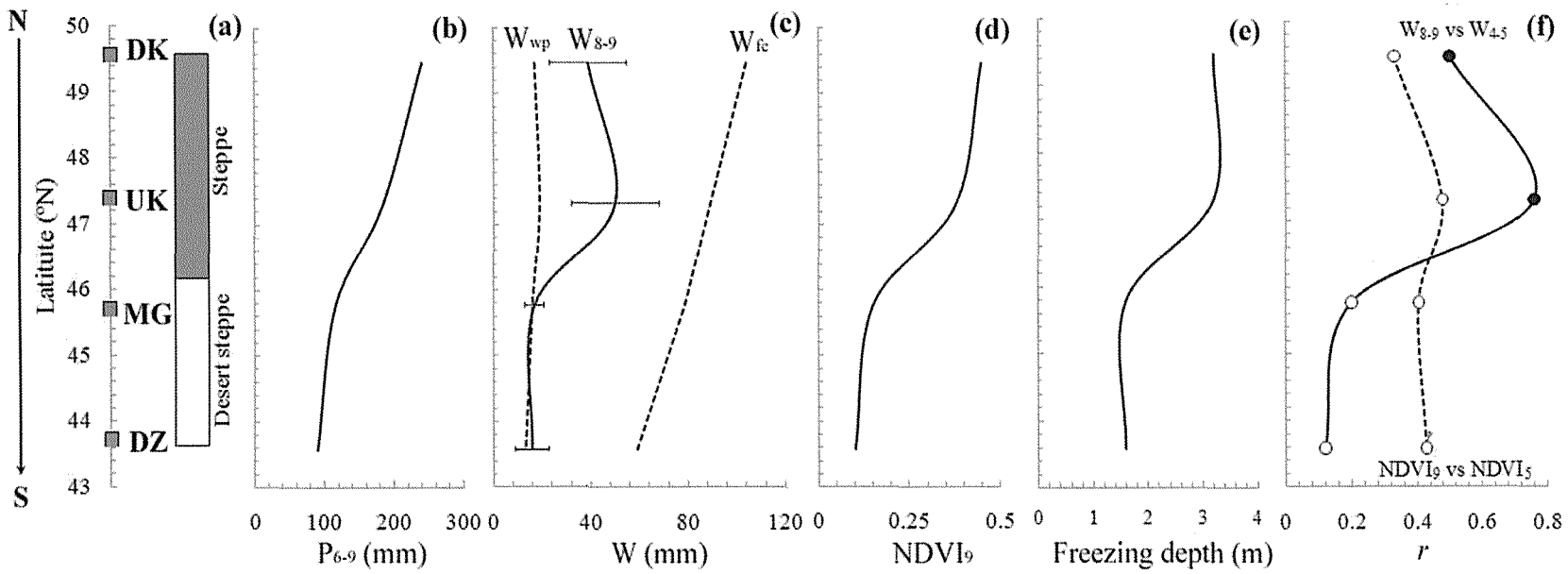

Figure 5.7 North-south cross-sections of (a) vegetation type, (b) P, (c) $W_{8\text{-}9}$, W_{fc}, and W_{wp}, (d) $NDVI_9$, (e) correlations between $W_{8\text{-}9}$ for one year and $W_{4\text{-}5}$ for the following year, and between $NDVI_9$ for one year and $NDVI_4$ for the following, and (f) the depth of soil freezing (Jambaajamts, 1989). The section includes, from the north to south, the four stations of Darkhan (DK), Underkhaan (UK), Mandalgovi (MG), and Dalanzadgad (DZ). The horizontal bars in Figure 5. 7c indicate standard deviations (σs) of the $W_{8\text{-}9}$ values from 1986 to 2005.

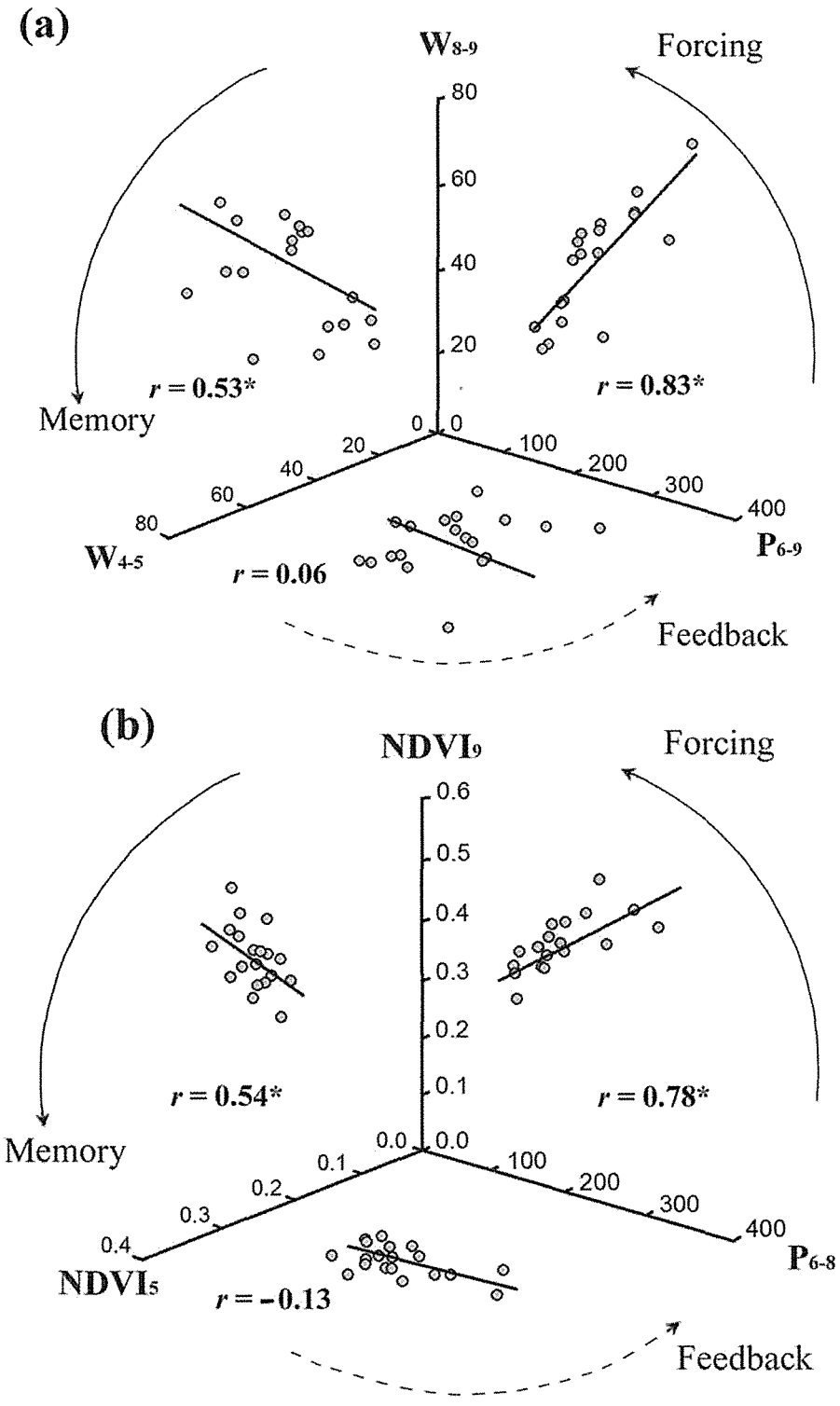

Figure 5.8. Three dimensional diagrams showing the correlations among (a) $P_{6\text{-}9}$, $W_{8\text{-}9}$, and the following $W_{4\text{-}5}$ and those among (b) $P_{6\text{-}8}$, $NDVI_9$, and the following $NDVI_5$ for three Steppe stations (Underkhaan, Zuunmod, and Darkhan). The arrows in the diagrams denote the directions of forcing, memory, and feedback in the atmosphere-land surface system. Asterisks of the correlations indicate the 5% significance.

5.4 CONCLUSIONS

In this study, we have revealed significant carryover of summer rainfall anomalies to subsequent years, mediated by the soil moisture-vegetation system. Namely, changes in rainfall led to time-lagged, directly correlated changes in W and plant production. During the following winter, anomalies in W were maintained in the frozen soil and biomass anomalies may have been stored as underground structures in the root system. Even though these land-surface anomalies are maintained through to the spring, they were shown only to have had a weak effect on early summer P. Instead, the W anomalies tended to be disturbed by large-scale atmospheric variations during the summer, producing subsequent anomalies in P, T, and E. The biomass anomalies may also have been disturbed by a similar mechanism, causing a change in plant-available W.

The autocorrelation analysis of decay time scale (i.e. lag at which autocorrelation function equals to $1/e$) showed that in the forest steppe zone, the soil moisture memory scales during the autumn and winter (6.0–7.0 months) are longer than during the spring and summer (3.0–1.8 months) (Nandintsetseg and Shinoda, 2010b). These timescales are comparable to those observed at Underkhaan that is located in the typical steppe; 7.6–6.0 months for the autumn and winter and 2.2–3.0 months for the spring and summer. The memory during the spring (2.2 months) is slightly longer than that seen in the cold, arid region of central Eurasia, which is located at latitudes similar to the present study area, but has deeper snowpack and shallower soil freezing (Shinoda, 2001). The drying-up period after rainy season is much longer in Mongolia (7.6 months) than that for soil moisture in the root zone seen in the tropical semiarid Sahel (1.5 months) (Shinoda and Yamaguchi, 2003) and the general decay timescale of 2–3 months (related to atmospheric forcing) for soil moisture in the top 1 m reported in the extratropics (Vinnikov *et al.*, 1996; Entin *et al.*, 2000). Thus, it is evident that soil freezing in Mongolia acts to prolong the timescale of soil moisture memory. It should be noted that the NDVI, as an indicator of vegetation activity, exhibited a longer memory from September of a given year to the following July (9 months) through the period of the hidden memory due to the winter snow cover (Figure 5.3c). The large root system of the perennial plants dominant in the Mongolian steppe may remain alive and retain as a memory of under-ground biomass anomalies during the winter.

In this context, further research is required on land–atmosphere interactions to explore the mechanisms by which root-zone soil-vegetation system directly affects the drying trend over Eurasia (as mentioned in the introduction) via soil moisture/precipitation recycling. Furthermore, the present study pointed to the existence of soil moisture and vegetation memories that were maintained in the Mongolian steppe from the late summer to subsequent spring when dust emission frequently occurs. The concept of the memories will enable us to predict dust emission conditions half year in advance, by monitoring and assessing the detailed time course of the soil-vegetation system on the ground and by satellite (*e.g.*, Shinoda *et al.*, 2010b; Kimura and Shinoda, 2010). This approach is challenging, but potentially very useful for the establishment of an early warning system for dust storm.

CHAPTER 6

General Conclusions and Future Tasks

The present study investigated soil moisture dynamics and modeling, its relationships with climate and vegetation activity, and soil moisture–vegetation memories in the cold, arid climate of Mongolia, with a focus on three vegetation zones: forest steppe, steppe and desert steppe. A unique long-term, quality-controlled soil moisture datasets across Mongolia have been used in this study. A simple water balance model was developed for application in the cold, arid regions such as Mongolia, by considering soil freezing and snow melting. The model was validated by comparison with long-term observations available for the region, thereby demonstrating its efficiency compared with the widely used PDSI. Moreover, the present model has an advantage in identifying abrupt changes on a shorter timescale in response to precipitation. This study is the first comprehensive analysis on soil moisture dynamics in Mongolia and moreover, it was revealed the memory processes of soil moisture and vegetation in the cold, arid climate. In terms of practical applications, the present study is essential for improving the future real-time drought monitoring system and its early warning system in Mongolia, thereby providing valuable information for decision-makers and herder. Furthermore, the advantage of this model is the use of a simple calculation that derives daily soil moisture from operationally observed daily data and its wide applicability to the cold, arid regions throughout the world.

Climatological seasonal and spatial changes in observed root-zone available soil moisture were comprehensively analyzed for the entire Mongolia in Chapter 2. The results showed that the soil moisture varies seasonally, depending not only on the balance of precipitation and evapotranspiration but also on winter soil-freezing and spring snowmelt. We documented that there were three distinct phases; spring drying, summer recharge, and autumn drying of which the plant phenological phenomena of *Stipa* spp. were related to.

Chapter 3 describes multi-decadal trend in soil moisture and memory based on estimated daily soil moisture during 1961–2006 for this region by using the water

balance model. On the interannual basis, all three vegetation zones showed a decreasing trend in soil moisture and shortening in the summer recharge phase during the study period due to decreased precipitation and increased potential evapotranspiration, although these drying and shortening trends were significant ($p < 0.05$) only in the forest steppe.

In chapter 4, the effect of root-zone soil moisture on vegetation activity was examined. Vegetation activity was more strongly correlated with soil moisture than with precipitation, suggesting that soil moisture plays an immediate role in controlling vegetation activity on seasonal and interannual timescale. A comparison between years with high and low vegetation revealed that a significant difference in precipitation led to a half-monthly time-lagged significant difference in soil moisture, finally a difference in vegetation activity, with time lags of about one month.

Soil moisture and vegetation memories were comprehensively investigated and highlighted in Chapters 4 and 5. A new observational evidence of a half year-long moisture memory mechanism mediated by the soil moisture–vegetation system was found over Mongolia. The analysis result shows that interannual anomalies of soil moisture and vegetation due to rainfall during a given summer are maintained through the freezing winter months to the spring, acting as an initial condition for subsequent summer land-surface and rainfall conditions. Vegetation anomalies were likely stored as underground structures in the root system. To the best of our knowledge, this is the first study to point to the combination of soil moisture and root memories as predictor of vegetation in Mongolia.

Several previous studies have reported that the current and preceding year's precipitation have a strong influence on NDVI of the current year in Africa (Martiny *et al.*, 2009) and North America (Wang *et al.*, 2003). Iwasaki (2006) examined the potential of predicting NDVI using the leading winter and spring precipitation and air temperature in Mongolia, revealing that NDVI is influenced by June precipitation with the additional influence of December precipitation. This relationship can be explained by the duration period of soil moisture memory remaining in the root zone as described in Chapter 4.

In the earth system, time scales of land (snow cover – 3 months, NDVI– 4 months) and ocean (sea surface temperature – 5.5 months and sea ice – 4.5 months) surface anomalies are considerably longer than those of atmospheric fluctuations (Walsh *et al.*, 1985; Shinoda and Gamo, 2000; Shinoda *et al.*, 2003). The autocorrelation analysis of decay time scale of soil moisture (i.e. lag at which autocorrelation function equals to $1/e$) presented in Chapters 4 and 5. The cold-season climate with low evapotranspiration and

strong soil freezing acts to prolong the decay time scale of autumn soil moisture anomalies to 6–7.6 months that is among the longest in the world. The memory during the spring (1.8–2.2 months) in Northern Mongolia (forest steppe and steppe zones) is slightly longer than that seen in the cold, arid region of central Eurasia, which is located at similar latitudes to the present study area, but has deeper snowpack and shallower soil freezing (Shinoda, 2001). The drying-up period after rainy season is much longer in Northern Mongolia (6–7.6 months) than that for soil moisture in the root zone seen in the tropical semiarid Sahel (1.5 months) (Shinoda and Yamaguchi, 2003) and the general decay timescale of 2–3 months (related to atmospheric forcing) for soil moisture in the top 1 m reported in the extratropics (Vinnikov *et al.*, 1996; Entin *et al.*, 2000). Thus, it is evident that soil freezing in Northern Mongolia acts to prolong the timescale of soil moisture memory.

In Chapter 4, NDVI for a given year showed a weak dependence on the preceding year's NDVI. Shinoda *et al.* (2010) reported that in the Mongolian steppe, manipulated soil moisture deficit resulted in a marked reduction in above-ground phytomass but did not substantially affect below-ground phytomass (which was several times greater than above-ground phytomass). The effect of snow mass memory as seen in Central Eurasia (Shinoda 2001), was not dominant in Mongolia, because the yearly-maximum snow depth is only 3.4 cm in this region (Morinaga *et al.*, 2003). Therefore, it is likely that the large root system provided a basis for rapid recovery of above-ground phytomass, leading to a weak carry-over of vegetation anomalies, as revealed by NDVI in the present analysis. The concepts of soil moisture and root memory presented in the present study would provide a useful basis for an early warning system of reduced pasture production during drought.

This thesis results open many routes for future research in the cold, arid region such as Mongolia. Further research is required on land–surface and atmosphere interactions, particularly on the mechanisms of land–surface (soil moisture and vegetation) feedback and its effect on drought. Our present result on extreme years suggested that such an interaction could possibly act to prolong the drought conditions. Indeed, further investigation should be made of how this interaction influences the recent drying trend in this area.

Furthermore, the present study pointed to the existence of soil moisture and vegetation memories that were maintained in the Mongolian steppe from the late summer to subsequent spring. These soil moisture and vegetation root memories are most likely to

affect dust emission. Severe dust events occur frequently during the spring in arid regions of East Asia, particularly in Mongolia and China (*e.g.*, Kurosaki and Mikami, 2005). Therefore, further research is required on the mechanisms of vegetation/soil moisture memory and aeolian processes. This approach will enable us to predict dust emission conditions half year in advance, by monitoring and assessing the detailed time course of the soil moisture and vegetation system on the ground and by satellite.

SUMMARY

Soil moisture plays a central role in the global water cycle and climate system by controlling the partitioning of water and energy between the land-surface and the atmosphere. Soil moisture acts as a memory of anomalies in the water cycle, in turn, it has a delayed and durable influence on the overlying atmosphere through land–surface fluxes of heat and moisture and plays as a bridge between meteorological drought (deficits in precipitation) and agricultural drought (failures of plant growth). A number of drought indices have been proposed and applied to quantify drought conditions, although, presently very few studies have used ground-observed soil moisture as an indicator of agricultural drought in the world. A large drying trend has been observed in a soil moisture index over land areas in the Northern Hemisphere since the middle 1950s, including Mongolia, affecting the pastureland that is used for livestock. It has been found that soil moisture deficits limit the growth of pasture in Mongolia. Hence, accurate extensive assessment and modeling of soil moisture dynamics in this pastureland is required for reliable and timely monitoring of agricultural drought. This thesis represented recent advances in the observation and modeling of soil moisture dynamics and in analyses of its relationships with climate and vegetation activity in the cold, arid climate of Mongolia with a focus on three vegetation zones; forest steppe, steppe, and desert steppe. This study is the first comprehensive analysis on soil moisture dynamics in Mongolia and moreover, it was revealed the memory processes of soil moisture and vegetation in the cold, arid climate.

Firstly, the seasonal and spatial changes of soil moisture and its climatology and modeling were demonstrated. In this analysis, a unique long-term, updated soil moisture and meteorological datasets for 26 stations during 1986–2005 were used. The results showed that the soil moisture varies seasonally, depending not only on the balance of precipitation and evapotranspiration but also on winter soil-freezing and spring snowmelt. In general, there was a latitudinal gradient in soil moisture content, with the southwestern soils drier than the northeastern soils. The seasonal change in soil moisture was small and the seasonal pattern was similar throughout Mongolia. We documented three distinct seasonal phases; the spring drying, summer recharge, and autumn drying and their

relationships to plant phenological phenomena of *Stipa* spp. that represents the dominant species in the Mongolian steppe. Over Mongolia, the available soil moisture was about 30% of the soil field capacity, while in the desert steppe; soil moisture was close to the wilting point throughout the year. A simple water balance model was developed for application in the cold, arid regions such as Mongolia, by considering soil freezing and snow melting. The model simulated the observed seasonal and interannual soil moisture variations reasonably well ($r = 0.75, p < 0.05$). This model will provide a useful tool for a reliable and timely monitoring of agricultural drought for decision-making and herding management in Mongolia.

Secondly, multi-decadal trends and memory of soil moisture were assessed in three vegetation zones using the modeled daily soil moisture during 1961–2006. On an interannual basis, the modeled soil moisture was more strongly correlated with the observed soil moisture ($r = 0.91, p < 0.05$) than the widely used Palmer Drought Severity Index ($r = 0.65, p < 0.05$). All three vegetation zones showed a decreasing trend in soil moisture and shortening in the summer recharge phase due to decreased precipitation and increased potential evapotranspiration. Although only in the forest steppe revealed significant ($p < 0.05$) drying trend due to significantly decreased precipitation. Soil moisture memory analysis showed that the decay temporal scales of soil moisture anomalies were 6–7 months in the autumn and winter, which is larger than that in spring and summer of 1.8–3 months in the forest steppe. This indicates that soil moisture acts as an efficient memory of precipitation anomalies via the soil freezing and as an initial soil moisture condition for the subsequent summer land-surface.

Thirdly, the relationship between root-zone soil moisture and vegetation activity in the Mongolian steppe was analyzed based on remotely sensed NDVI data for seasonal and interannual periods during 1982–2005. Vegetation activity was more strongly correlated with soil moisture than with precipitation, suggesting that soil moisture plays an important and immediate role in controlling vegetation activity. A comparison between years with high and low vegetation revealed that that a significant difference in precipitation led to a half-monthly time-lagged significant difference in soil moisture, finally a difference in vegetation, with time lags of about one month. Interannual fluctuations in vegetation were strongly dependent on soil moisture of the current year ($r^2 = 0.53$) and even more strongly dependent on a combination of the current year soil moisture and vegetation of the preceding year ($r^2 = 0.55$). This result suggests that vegetation anomalies are likely stored as underground structures in the root system. To

the best of our knowledge, this is the first study in Mongolia to point to the combination of soil moisture and root memories as predicting parameter for vegetation activity.

Fourthly, new observational evidence of a half year-long moisture memory mechanism mediated by the land surface that is manifested in the cold, arid climate of Mongolia was found. The analysis result showed that significant carryover of summer rainfall anomalies to subsequent years, mediated by the soil moisture–vegetation system. Namely, changes in precipitation led to time-lagged, directly correlated changes in soil moisture and plant production. During the following winter, anomalies in soil moisture were maintained in the frozen soil and biomass anomalies may have been stored as underground structures in the root system. Even though these land-surface anomalies are maintained through to the spring, they were shown only to have had a weak effect on early summer precipitation. Instead, the soil moisture anomalies tended to be disturbed by large-scale atmospheric variations during the summer, producing subsequent anomalies in precipitation, temperature, and evapotranspiration. The cold–season climate with low evapotranspiration and strong soil freezing acts to prolong the decay time scale of autumn soil moisture anomalies to 7.6 months in the steppe, which is the longest in Mongolia and among the longest in the world. In future applications, the concepts of soil moisture and vegetation memories presented in the present study would provide a useful basis for an early warning system of reduced pasture production during drought.

SUMMARY IN JAPANESE

土壌水分は、地表面と大気の間の水・エネルギーの分配を通して、世界の水循環と気候システムの形成に大きく関与している。土壌水分は、水循環の異常を保持する働き（メモリ効果）があり、熱・水の地表面フラックスを通して、時差をもって大気に持続的な影響を及ぼす。干ばつ指標の多くは干ばつ状態を定量化するため提案されてきたが、現在のところ、地上観測の土壌水分を農業干ばつの指標として用いている研究は世界でもごくわずかである。1950 年代の中頃から、北半球の広域で顕著な土壌の乾燥化が観測されており、モンゴルの放牧地にも影響を及ぼしている。この農業干ばつをタイムリーに信頼できるモニタリングをするために、放牧地の土壌水分動態の正確な広域的評価とモデリングが必要である。本論文は、モンゴルの寒冷で乾燥した気候における（とくに、3 つの植生帯に注目して）、土壌水分動態の観測・モデリングと、土壌水分と気候・植物活動との関係の解析において、新知見を提示した。本研究は、モンゴルにおいて土壌水分動態を包括的に解析した最初の研究であり、寒冷・乾燥気候下における土壌水分と植生のメモリ動態を解明している。

本論文では、第 1 に、土壌水分の季節的・地域的変化とその気候的特性を調べ、そのモデリングを行った。本解析では、他に類のない長期間の土壌水分・気象データセットを用いた。その結果、土壌水分は降水と蒸発散の微妙なバランスばかりでなく、冬の土壌凍結と春の融雪に影響を受けながら、季節的に変動していることがわかった。一般的に、土壌水分には南北経度があり、南西で小さく北東で大きい。モンゴル全域にわたって、その季節変化は小さく類似しているが、3 つの季節、すなわち、春の乾燥化季、夏の湿潤化季、春の乾燥化季に区分することがでた。また、モンゴル草原の優占種である *Stipa* spp.の植物季節との関係もみられた。モンゴルでは、圃場容水量のおよそ 30%しか土壌水分がなく、砂漠ステップでは、一年を通じてしおれ点に近い。モンゴルのような寒冷・乾燥気候に適用できる、土壌凍結と融雪を考慮した単純な土壌水分モデルを開発し、実測値の季節・経年変化をうまく再現した。このモデルは、政策

決定や家畜管理のための、農業干ばつの信頼性のあるタイムリーなモニタリングに役立つものと考えられる。

第 2 に、土壌水分モデルを用いて、3 つの植生帯における土壌水分の数十年規模の傾向（1961-2006 年）とメモリを調べた。経年変化において、モデルによる推定値は、世界で広く使われているパルマー干ばつ強度指数よりも観測値と高相関を示した。長期的傾向に関しては、3 つの植生帯ともに、降水の減少と可能蒸発散の増加により、土壌水分が減少し、夏の湿潤化季が短くなったが、土壌水分の減少傾向は森林ステップのみで有意であった。森林ステップにおいて、秋・冬の土壌水分偏差の減衰時間スケールは 6〜7 ヶ月で、春・夏の 1.8〜3 ヶ月より大きい。このように、凍結を通して土壌水分が降水偏差の有効なメモリとして働き、翌夏の土壌水分の初期状態となっている。

第 3 に、モンゴル草原における根圏の土壌水分と衛星による植生活動の季節的・経年的な関係を解析した。植生活動は降水よりも土壌水分に強い相関があり、土壌水分は降水と植生活動の変化の仲立ちをしているものと考えられる。植生の多い年と少ない年の比較から、降水偏差は土壌水分偏差に約半月遅れで影響し、植生偏差に約 1 ヶ月遅れで影響することがわかった。植生の経年変動は同年の土壌水分だけより、前年の植生との組み合わせのほうに高相関を示すが、これは根系が植生偏差を保持することを示唆している。このような土壌水分・根系メモリの組み合わせで植生活動を予測する試みは本研究が初めてである。

第 4 に、寒冷・乾燥気候下において、半年にわたる地表面（土壌水分・植生）の水分メモリについて新事実を示した。すなわち、夏の降水偏差が、時差をもって、土壌水分と植物生産の偏差を引き起こし、続く冬には、それぞれの偏差が凍結水と根系として保持された。しかし、その地表面偏差は大規模な大気擾乱で撹乱され保持されず、初夏の降水へ影響は小さい。寒候季の顕著な土壌凍結と小さい蒸発散により、草原における秋の土壌水分偏差の減衰時間スケールは 7.6 月とモンゴル国内で最も大きく、世界的にみても最も大きい部類にはいる。本研究で明らかになった土壌水分・植生メモリの概念は、将来、干ばつ時の牧草生産の減少を予測する早期警戒システムに応用することが可能であろう。

References

Alley WM. 1984. The Palmer Drought Severity Index: Limitations and assumptions. *Journal of Climate and Applied Meteorology* **23**: 1100–1109.

Archibold OW. 1995. *Temperate Grasslands, Ecology of World Vegetation.* Chapman & Hall, London. pp. 204–237.

Badarch M. 1987. *The methods of mapping snow cover distribution of territory of Mongolia by satellite and ground data* (in Russian). Ph.D. Dissertation, Mongolian Academy of Science, Institute of Geography, Ulaanbaatar.

Barlow M, Cullen H, Lyon B. 2002. Drought in Central and Southwest Asia: La Niña, the Warm Pool, and Indian Ocean Precipitation. *Journal of Climate* **15**: 697–700.

Barnett TP, Dümenil L, Schlese U, Roeckner E. 1989. The effect of Eurasian snow-cover on regional and global climate variations, *Journal of Atmosphereis Sciences* **46**: 661–685.

Batima P, Bat B, Tserendash Sh, Myagmarjav B. 2008. Adapting to drought, zud and climate change in Mongolia's rangelands. *Climate Change and Adaptation,* Neil L, Ian B, Adejuwon J, Barros V, Lasco R (eds). Earthscan. UK.

Batima P, Dagvadorj D. 2000. *Climate Change and Its Impacts in Mongolia.* JEMR Publishing, Ulaanbaatar, pp.227.

Batima P, Dagvadorj D. 2000. *Climate Change and Its Impacts in Mongolia.* NAMHEM JEMR Publishing. Ulaanbaatar.

Bat-Oyun Ts, Shinoda M, Tsubo M. 2010. Estimation of pasture productivity in Mongolian grasslands: field survey and model simulation. *Journal of Agricultural Meteorology* **66**(1): 31–39.

Bayarjargal Y, Karnieli A, Bayasgalan M, Khudulmur S, Gandush C, Tucker CJ. 2006. A comparative study of NOAA–AVHRR derived drought indices using change vector analysis. *Remote Sensing of Environment* **105**(1): 9–22.

Brown, J., Ferrians Jr OJ, Heginbottom J.A, Melnikov E.S. 1998 (revised 2001). Circum-Arctic map of permafrost and ground-ice conditions. Boulder, CO: National Snow and Ice Data Center/World Data Center for Glaciology, Digital Media.

Charney JP. 1975. Dynamics of deserts and drought in Sahel. *Quarterly Journal of Royal Meteorological Society* **101**: 193–202.

Dai A, Trenberth KE, Karl T. 1998. Global variations in droughts and wet spells: 1900–1995. *Geophysical Research Letters* **25**: 3367–3370.

Delworth TL, Manabe S. 1988. The influence of potential evaporation on the variabilities of simulated soil wetness and climate. *Journal of Climate* **1**: 523–547.

Entin JK, Robock A, Vinnikov KY, Hollinger SE, Liu S, Namkai A. 2000. Temporal and spatial scales of observed soil moisture variations in the extratropics. *Journal of Geophysical Research* **105**: 11865–11877.

Erdenentsetseg D. 1996: *Territorial distribution and modeling of Mongolian soil moisture* (in Russian). Ph.D. dissertation, Mongolian Academy of Science, Institute of Geography, Ulaanbaatar. p. 158.

Farrar TJ, Nicholson SE, Lare AR. 1994: The influences of soil type on the relationships between NDVI, rainfall, and soil moisture in semiarid Botswana. II. NDVI response to soil moisture. *Remote Sensing of Environment* **50**: 121–133.

Goulden CE, Nandintsetseg B, Ariuntsetseg L. 2009. *The Geology, Climate, and Ecology of Mongolia.* In Paula Sabloff (ed). Mapping Mongolia. University Museum, University of Pennsylvania. (in press).

Gunin PD, Vostokova EA, Dorofeyuk NI, Tarasov PE, Black CC. 1999. *Vegetation dynamics of Mongolia.* Kluwer, Dordrecht, NL. p. 25.

Hahn DG, Shukla J. 1976. An apparent relationships between Eurasian snow cover and Indian monsoon rainfall. *Journal of Atmospheric Sciences* **33**: 2461–2462.

Hoerling MP, Kumar A. 2003. The perfect ocean for drought. *Science* **299**: 691–694. DOI: 10.1126/science.1079053.

Huang J, van den Dool Georgakakos. 1996. Analysis of Model-Calculated Soil Moisture over the United States (1931–1993) and Applications in long-range Temperature Forecasts. *Journal of Climate* **9**: 1350–1362.

Iijima Y, Masuda K, Ohata T. 2007. Snow disappearance in eastern Siberia and its relationship to atmospheric influences. *International Journal of Climatology* **27**: 169–177.

IPCC, 2007. *Climate Change 2007: The Physical Science Basis. Contribution of Working Group I to the Fourth Assessment Report of the Intergovernmental Panel on Climate Change*, Solomon, S, et al., (Eds.), Cambridge Univ. Press, Cambridge.

Iwasaki H, Nii T. 2006. The break in Mongolian rainy season and the relation with the stationary Rossby wave along the Asianjet. *Journal of Climate* **19:** 3394–3405.

Jambaajamts B, Norjmaa L. 1997. *Meteorological observations manual 38: Quality control manual of meteorological observations* (in Mongolian). NAMHEM. Ulaanbaatar.

Jambaajamts B. 1989. *Climate of Mongolia* (in Mongolian). Ulsiin hevlel Publishers. Ulaanbaatar. p. 12.

Kachinsky NA. 1965. *Soil Physics: Part I* (in Russian). Kolos Publishers, Moscow. pp.7.

Kimura R, Shinoda M. 2010. Spatial distribution of threshold wind speeds for dust outbreaks in northeast Asia. *Geomorphology* **37**: 319–326.

Kondoh A, Kaihotsu I, Hirata M, Azzaya D. 2005. Interannual variation of phenology and biomass in Mongolian herbaceous vegetation. *Journal of Arid Land Studies* **14**: 209–218. (in Japanese with English abstract)

Koster RD, Guo Z, Dirmeyer PA, Bonan G, Chan E, Cox P, Davies H, Gordon CT, Yamada T. 2006. GLACE: The Global Land-Atmosphere Coupling Experiment. Part 1: Overview, *Journal of Hydrometeorology* **7**(4): 590–610.

Kunkel KE. 1990. Operational soil moisture estimation for the midwestern United States. *Journal of Applied Meteorology* **29**: 1158–1166.

Li SG, Romero-Saltos H, Tsujimura M, Sugimoto A, Sasaki L, Davaa G, Oyunbaatar D. 2007. Plant water sources in the cold semiarid ecosystem of the upper Kherlen River catchment in Mongolia: A stable isotope approach. *Journal of Hydrology* **333**: 109–117.

Lotsch A, Friedl MA, Anderson BT, Tucker CJ. 2005. Response of terrestrial ecosystems to recent Northern Hemispheric drought. *Geophysical Research Letters* **32**: L09705. DOI: 10.1029/2004GL022043.

Manabe S. 1969. Climate and the ocean circulation 1: The atmospheric circulation and the hydrology of the earth's surface. *Monthly Weather Review* **97**: 739–805

MARCC. 2009 (Mongolia Assessment Report on Climate Change 2009). 2009. The Ministry of Environment, Nature and Tourism, Mongolia. p.38.

Marengo JA, Nicholson SE, Lare AR, Monteny B, Galle S. 1996. Application of evapoclimatonomy to monthly surface water balance calculations at the HAPEX-Sahel supersites. *Journal of Applied Meteorology* **35**: 562–573.

Martiny N, Philippon N, Richard Y, Camberlin P, Reason C. 2009. Predictability of NDVI in semi-arid African regions. *Theory of Applied Climatology* 0177-798X: 1434–4483.

Méndez-Barroso LA, Vivoni ER, Watts CJ, Rodríguez JC. 2009. Seasonal and interannual relations between precipitation, surface soil moisture and vegetation dynamics in the North American monsoon region. *Journal of Hydrology* **377**: 59–70.

Mintz Y, Serafini Y. 1984. *Global fields of monthly normal soil moisture, as derived from observed precipitation and an estimated evapotranspiration. Part V.* Final Scientific Report. Under NASA Grant Nas 5–26, Department of Meteorology. University of Maryland.

Mintz Y, Walker G. 1993. Global fields of soil moisture and land surface evapotranspiration derived from observed precipitation and surface air temperature. *Journal Applied Meteorology* **32**: 1305–1334.

Miyazaki S, Yasunari T, Miyamoto T, Kaihotsu I, Davaa G, Oyunbaatar D, Natsagdorj L, Oki T. 2004. Agrometeorological conditions of grassland vegetation in central Mongolia and their impact for leaf area growth. *Journal of Geophysical Research* **109**: D22106. DOI: 10.1029/2004JD005179.

Morinaga Y, Tian S, Shinoda M. 2003. Winter snow anomaly and atmospheric circulation in Mongolia. *International Journal of Climatology* **23**: 1627–1636. DOI:10.1002/joc.961.

Munkhtsetseg E, Kimura R, Wang J, Shinoda M. 2007. Pasture yield response to precipitation and high temperature in Mongolia. *Journal of Arid Environments* **70**: 94–110.

Nakano T, Nemoto M, Shinoda M. 2008. Environmental controls on photosynthetic production and ecosystem respiration in semi-arid grasslands of Mongolia. *Agricultural and Forestry Meteorology* **148**: 1456–1466.

Nandintsetseg B, Greene JS, Goulden CE. 2007. Trends in extreme daily precipitation and temperature in the Lake Hövsgöl basin area, Mongolia. *International Journal of Climatology* **27**: 341–347.

Nandintsetseg B, Shinoda M, Kimura R, Ibaraki Y. 2010. Relationship between soil moisture and vegetation activity in the Mongolian steppe. *SOLA* **6**: 062–032.

Nandintsetseg B, Shinoda M. 2010a. Seasonal change of soil moisture and its climatology and modeling in Mongolia. *International Journal of Climatology*. DOI:10.1002/joc.2134.

Nandintsetseg B, Shinoda M. 2010b. Multi-decadal trend in modeled soil moisture and memory in Mongolia. Submitted to *Journal of Arid Environments* (under review).

Natsagdorj L. 2003. *Climate change: Pasture and animal husbandry*, (eds) P Batima. Institute of Meteorology and Hydrology of Mongolia. Ulaanbaatar. pp.31.

Ni-Meister W, Walker JP, Houser PR. 2005. Soil moisture initialization for climate prediction: Characterization of model and observation errors. *Journal of Geophysical Research* **110**: D13111. DOI: 10.1029/2004JD005745.

Palmer WC. 1965. Meteorological drought. *U.S. Weather Bureau Research Paper* **45**: 58.

Palmer WC. 1968. Keeping track of crop moisture conditions, national wide: The new crop index. *Weatherwise* **21**: 156–161.

Pinzon J. 2002. *Using HHT to successfully uncouple seasonal and interannual components in remotely sensed data.* SCI 2002 Conference Proceedings, 14–18 July 2002. Orlando, Florida. p.8.

Poncea VM, Shetty AV. 1995. A conceptual model of catchment water balance: 1. Formulation and calibration. *Journal of Hydrology* **173**: 27–40.

Porporato A, D'Odorico P, Laio F. Rodriguez-Iturbe. 2003. Hydrologie controls on soil carbon and nitrogen cycles. I. Modeling scheme. *Advances in Water Resources* **26**: 45–58.

Porporato A, Laio F, Ridolfi L, Rodriguez-Iturbe I. 2001. Plants in water controlled ecosystems: active role in hydrological processes and response to water stress. III. Vegetation water stress. *Advances in Water Resources* **24**: 725–744.

Richard S, Masika KMD. 2002. Data quality control methods. *Report of the climate information and prediction services (CLIPS)*: Training workshop for eastern and southern Africa: 9–10.

Robock A, Vinnikov KY, Schlosser CA, Speranskaya NA, Xue Y. 1995. Use of Russian soil moisture and meteorological observations to validate soil moisture simulations with biosphere and bucket models. *Journal of Climate* **8**: 15–35.

Robock A, Vinnikov KY, Srinivasan G, Entin JK, Hollinger SE, Speranskaya NA, Liu S, Namkhai A. 2000. The global soil moisture data bank. *Bulletin of the American Meteorological Society* **81**: 1281–1299.

Rodriguez-Iturbe I, Porporato A, Laio F, Ridolfi L. 2001. Plants in water-controlled ecosystems: active role in hydrologic processes and response to water stress I. Scope and general outline. *Advances in Water Resources* **24**(7): 695–705.

Rodriguez-Iturbe I, Porporato A. 2004. *Ecohydrology of water-controlled ecosystems: Soil moisture and Plant Dynamics*, Cambridge, New York.p.35.

Sala OE, Lauenroth WK, Golluscio RA. 1997. *Plant functional types in temperate semi-*

arid regions. In T.M. Smith, H.H. Shugart, and F.I. Woodward (Eds.), Plant Functional Types, International Geosphere-Biosphere Programme Book Series 1, Cambridge University Press. pp.217–233.

Scanlon BR, Tyler SW, Wierenga PJ. 1997. Hydrologic issues in arid, unsaturated systems and implications for contaminant transport. *Reviews in Geophysics* **35**: 461–490.

Serafini YV, Sud VC. 1987. The time scale of the soil hydrology using a simple water budget model. *Journal of Climate* **7**: 585–591.

Sharkhuu N, Anarmaa Sh. 2006. *Monitoring of Permafrost in Mongolia*. In proceedings of Asian Conference on Permafrost, Abstracts, Lanzhou, China, 7–9 August, 2006. pp.184–186.

Sharkhuu A, Sharkhuu N, Etzelmuller B, Flo Heggem E S, Nelson F E, Shiklomanov N I, Goulden CE, Brown J. 2007. Permafrost monitoring in the Hovsgol mountain region, Mongolia. *Journal of Geophysical Research* **112**: F02S06.

Shinoda M. 1995. Seasonal phase lag between rainfall and vegetation activity in tropical Africa as revealed by NOAA satellite data. *International Journal of Climatology* **15**: 639–656.

Shinoda M. 2000. Desertification and drought as a possible land-surface/atmosphere interaction. *Global Environmental Research* **3**(1): 9–15.

Shinoda M. 2001. Climate memory of snow mass as soil moisture over central Eurasia. *Journal of Geophysical Research* **106**(D24): 33393–33403.

Shinoda M, Ito S, Nachinshonhor GU, Erdenetsetseg D. 2007. Notes and correspondence: Phenology of Mongolian grasslands and moisture conditions. *Journal of the Meteorological Society of Japan* **85**: 359–367. DOI: 10.2151/jmsj.85.359.

Shinoda M, Kimura R, Mikami M, Tsubo M, Nishihara E, Ishizuka M, Yamada Y, Munkhtsetseg E, Jugder D, Kurosaki Y. 2010a. Characteristics of Dust Emission in the Mongolian Steppe during the 2008 DUVEX Intensive Observational Period. *SOLA* **6**: 9–12.

Shinoda M, Morinaga Y. 2005. Developing a combined drought-dzud early warning system in Mongolia. *Geographical Review of Japan* **78**: 928–950. (in Japanese with English abstract)

Shinoda M, Nachinshonhor GU, Nemoto M. 2010b. Impact of drought on vegetation dynamics of the Mongolian steppe: A field experiment. *Journal of Arid Environments* **74**: 63–69.

Shinoda M, Utsugi H, Morishima W. 2001. Spring snow-disappearance timing and its possible influence on temperature fields over central Eurasia. *Journal of Meteorological Society of Japan* **79**: 37–59.

Shinoda M, Yamaguchi Y. 2003. Influence of soil moisture anomaly on temperature in the Sahel: a comparison between wet and dry decades. *Journal of Hydrometeorology* **4**: 437–447.

Smith JAC, Griffith H. 1993. *Water Deficits: Plant Responses from Cell to Community.* Bios Scientific Publisher: Oxford.

Sud YC, Smith E. 1985. The influence of surface roughness of deserts on the July circulation (a numerical study). *Boundary Layer Meteorology* **33**: 383–398.

Suzuki R, Nomaki T, Yasunari T. 2003. West-east contrast of phenology and climate in northern Asia revealed using a remotely sensed vegetation index. *International Journal of Biometeorology* **47**(3): 126–38.

Thornthwaite CW. 1948. An approach toward a rational classification of climate. *Geographical Review* **38**: 55.

Tucker CJ, Pinzon JE, Brown ME, Slayback D, Pak E, Mahoney R, Vermote E, El Saleous N. 2005. An Extended AVHRR 8-km NDVI Data Set Compatible with MODIS and SPOT Vegetation NDVI Data. *International Journal of Remote Sensing* **26**(20): 4485–4498.

Ueda H, Shinoda M, Kamahori H. 2003. Spring northward retreat of Eurasian snow cover relevant to seasonal and interannual variations of atmospheric circulation, *Internatioal Journal of Climatology* **23**: 615–629.

UNEP. 1992. *World atlas of desertification.* Edward Arnold, London. p.69.

Vinnikov KY, Robock A, Speranskaya AN, Schlosser CA. 1996. Scales of temporal and spatial variability of midlatitude soil moisture. *Journal of Geophysical Research* **101**: 7163–7174.

Vinnikov KYa, Yeserkepova IB. 1990. Soil moisture: Empirical data and model results. *Journal of Climate* **4**: 66–78.

Wang JP. Rich M, Price KP. 2003. Temporal responses of NDVI to precipitation and temperature in the central Great Plains, USA. *International Journal of Remote Sensing* **24**: 2345–2364.

Wilhite DA, Sivakumar MVK, Wood, DA. 2000. Early warning systems for drought preparedness and drought management. Proceedings of an Expert Group Meeting. Lisbon, Portugal, 5–7 September 2000. World Meteorological Organization, Geneva.

Xue Y. 1996. The Impact of desertification in the Mongolian and the Inner Mongolian grassland on the regional climate. *Journal of Climate* **9**: 2173–2189.

Yamaguchi Y, Shinoda M. 2002. Soil moisture modeling based on multiyear observations in the Sahel. *Journal of Applied Meteorology* **41**: 1140–1146. DOI: 10.1175/1520–0450(2002)041.

Yamanaka T, Kaihotsu I, Oyunbaatar D, Ganbold T. 2007. Summertime soil hydrological cycle and surface energy balance on the Mongolian steppe. *Journal of Arid Environments* **69**: 65–79.

Yang Y, Yang L, Merchant JW. 1997. An assessment of AVHRR/NDVI–ecoclimatological relations in Nebraska USA. *International Journal of Remote Sensing* **18**: 2161–2180.

Yasunari T, Kitoh A,Tokioka T. 1991. Local and remote responses to excessive snow mass over Eurasia appearing in the Northern spring and summer climate - A study with the MRI·GCM. *Journal of Meteorological Society of Japan* **69**: 473–487.

Yeung CW. 2005. *Rainfall-runoff and water-balance models for management of the Fena Valley Reservoir.* Guam: U.S. Geological Survey Scientific Investigations Report 2004.5287: p.52.

Zhang Y, Munkhtsetseg E, Kadota T, Ohata T. 2005. An observational study of ecohydrology of sparse grassland at the edge of the Eurasian cryosphere in Mongolia. *Journal of Geophysical Research* **110**: D14103. DOI: 1029/2004JD005474.

Ueda H, Shinoda M, Kamahori H. 2003. Spring northward retreat of Eurasian snow cover relevant to seasonal and interannual variations of atmospheric circulation. *International Journal of Climatology* **23**: 615–629.

List of Publications

Banzragch Nandintsesteg and Masato Shinoda, 2010, Seasonal change of soil moisture in Mongolia: its climatology and modeling, INTERNATIONAL JOURNAL OF CLIMATOLOGY. Published online in Wiley InterScience, DOI: 10.1002/joc.2134.
(This paper covers Chapter 2 of this thesis)

B. Nandintsetseg, M. Shinoda, R. Kimura, Y. Ibaraki, 2010, Relationship between Soil Moisture and Vegetation Activity in the Mongolian Steppe. Scientific Online Letters on the Atmosphere, 2010, Vol. 6, 062–032, *doi:10.2151/sola.2010-008.*
(This paper covers Chapter 4 of this thesis)